

Dissertation zur Erlangung des Doktorgrades
der Fakultät für Chemie und Pharmazie
der Ludwig-Maximilians-Universität München

**Structure-function analyses of small-conductance,
calcium-activated potassium channels.**

Dieter D'hoedt

Oostende (Belgium)

2005

Erklärung

Diese Dissertation wurde im Sinne von § 13 Abs. 3 bzw. 4 der Promotionsordnung von 29 Januar 1998 von Professor Dr. Thomas Carell and Dr. Paola Pedarzani betreut.

Ehrenwörtliche Versicherung

Diese Dissertation wurde selbstständig, ohne Hilfe erarbeitet.

München,

Dieter D'hoedt

Dissertation eingereicht am 22 April 2005

1. Professor Dr. Thomas Carell
2. Dr. Paola Pedarzani (University College London, United Kingdom)

Mündliche Prüfung am 13 June 2005

Summary

Ion channels are integral membrane proteins present in all cells. They are highly selective and assure a high rate for transport of ions down their electrochemical gradient. In particular, small-conductance calcium-activated potassium channels (SK) are conducting potassium ions and are activated by binding of calcium ions to calmodulin, which is constitutively bound to the carboxy-terminus of each SK channel α -subunit.

Until now, only three SK channel subunits have been cloned, SK1, SK2 and SK3. Sequence alignment shows that the transmembrane and pore regions are highly conserved, while a high grade of divergence is observed in the amino- and carboxy-termini of the three subunits. In order to determine the expression of the different SK channel subtypes, pharmacological tools such as apamin and d-tubocurarine have been widely used.

In this work, I show the characterization of a novel toxin, tamapin, isolated from the scorpion *Mesobuthus tamulus*, which targets SK channels. Our experiments show that this toxin is more potent in blocking SK2 channels than apamin. Furthermore, tamapin only blocked the SK1 and SK3 channels at higher concentrations, with a higher efficiency to block SK3 than SK1. Therefore, tamapin should be a good pharmacological tool to determine the molecular composition of native SK channels underlying calcium-activated potassium currents in various tissues.

Secondly, I determined the molecular mechanism that prevents the formation of functional SK1 channels cloned from rat brain (rSK1). Until now, little information was available on the rSK1 channels. rSK1 shows a high sequence identity (84%) with the humane homologue, hSK1. hSK1 subunits form functional potassium channels that are blocked by apamin and d-tubocurarine. However, when I expressed rSK1 in HEK-293 cells no potassium currents above background were observed, although immunofluorescence experiments using a specific antibody against the rSK1 protein showed expression of the channel. I generated rSK1 core chimeras in which I exchanged the amino-and/or the carboxy-terminus with the same region of rSK2 or hSK1. Exchange of amino- and carboxy-terminus or only of the carboxy-terminus resulted in the formation of functional potassium channels. Furthermore, I used these functional chimeras to determine the toxin sensitivity of rSK1 for apamin and d-tubocurarine. Surprisingly, when these blockers were applied, no sensitivity was observed, although hSK1 and rSK1 show a complete sequence identity in the pore region, which is suggested to contain the binding site for apamin.

Finally, I characterized a novel splice variant of the calcium-activated potassium channel subunit rSK2, referred to as rSK2-860. The rSK2-860 cDNA codes for a protein which is 275 amino

acids longer at the amino-terminus when compared with the originally cloned rSK2 subunit. Transfection of rSK2-860 in different cell lines resulted in a surprising expression pattern of the protein. The protein formed small clusters around the cell nucleus, but no membrane stain could be observed. This data shows that the additional 275 amino acid-long stretch at the amino-terminus is responsible for retention and clustering of the rSK2-860 protein. In order to narrow down the region responsible for this phenotype, I generated truncated proteins. This resulted in the isolation of an 100 amino acid-long region that seems to be responsible for the retention and clustering of rSK2-860 channels. Further truncations and deletions could help us to find the exact signal which is responsible for this characteristic behavior of the rSK2-860 protein.

Contents

1. Introduction

1.1	Classification and structure of ion channels, in particular of potassium channels.....	page 1
1.2	Gating of small-conductance, calcium-activated potassium channels.....	page 3
1.3	Physiological role of SK channels.....	page 6
1.4	Pharmacology of SK channels.....	page 7
1.5	Aim of this work.....	page 9

2. Material and methods

2.1 Materials

2.1.1	<i>Equipment</i>	page 10
2.1.2	<i>Consumables</i>	page 11
2.1.3	<i>Kits</i>	page 11
2.1.4	<i>Enzymes, antibodies and proteins</i>	page 11
2.1.5	<i>Plasmids</i>	page 12
2.1.6	<i>Channel blockers and enhancers</i>	page 13
2.1.7	<i>Cell culture</i>	page 13
2.1.8	<i>Chemicals</i>	page 13
2.1.9	<i>DNA-ladders</i>	page 14
2.1.10	<i>Buffers and solutions</i>	page 14

2.2 Methods

2.2.1 Cell culture and transfection

2.2.1.1	<i>Cell types</i>	page 18
2.2.1.2	<i>Splitting cell lines</i>	page 18
2.2.1.3	<i>Frozen cultures</i>	page 19
2.2.1.4	<i>Transfection of cells</i>	page 19
2.2.1.5	<i>Testing G418</i>	page 20

2.2.2 Standard molecular biology techniques

2.2.2.1	<i>Restriction enzyme digest of plasmid DNA</i>	page 21
---------	---	---------

2.2.2.2	<i>Agarose gel electrophoresis of cDNA</i>	page 21
2.2.2.3	<i>Gel extraction of DNA fragments</i>	page 21
2.2.2.4	<i>Phenol/Chloroform extraction of DNA</i>	page 22
2.2.2.5	<i>Ethanol precipitation of DNA</i>	page 22
2.2.2.6	<i>Fill-In reaction of overhanging DNA ends</i>	page 22
2.2.2.7	<i>Hybridization of oligonucleotides</i>	page 22
2.2.2.8	<i>Ligation of DNA fragments</i>	page 23
2.2.2.9	<i>Generation of competent bacteria, DH5α</i>	page 23
2.2.2.10	<i>Transformation of competent bacteria, DH5α</i>	page 23
2.2.2.11	<i>Isolation of DNA from bacterial cultures</i>	page 24
2.2.2.12	<i>Amplification of DNA using PCR</i>	page 25
2.2.2.13	<i>Overview vectors</i>	page 25
2.2.2.14	<i>Cloning strategies</i>	page 27
2.2.2.15	<i>DNA sequencing</i>	page 43
2.2.3	<i>Immunocytochemistry</i>	
2.2.3.1	<i>Coating coverslips</i>	page 43
2.2.3.2	<i>Immunofluorescence</i>	page 44
2.2.4	<i>Electrophysiology</i>	
2.2.4.1	<i>Introduction</i>	page 44
2.2.4.2	<i>Electrophysiology recording equipment</i>	page 45
2.2.4.3	<i>Patch-clamp measurement configurations</i>	page 46
2.2.4.4	<i>Recording of cells expressing channels</i>	page 47
2.2.4.5	<i>Data analysis</i>	page 49

3. Results

3.1 Characterization of stable cell lines expressing SK channels

3.1.1 Immunocytochemistry

3.1.1.1	<i>rSK2 α-subunit expression in HEK-293 and CHO-FlpIn cells</i>	page 52
3.1.1.2	<i>rSK3 α-subunit expression in HEK-293 and CHO-FlpIn cells</i>	page 54

3.1.2 Pharmacology

3.1.2.1	<i>Characterization of the HEK-rSK2 stable cell line</i>	page 55
3.1.2.2	<i>Characterization of the HEK-rSK3 stable cell line</i>	page 57
3.1.2.3	<i>Characterization of the CHO-Flp-hSK1 stable cell line</i>	page 58

3.2 Tamapin: a venom peptide from the Indian red scorpion (*Mesobuthus tamulus*) which targets SK channels.

3.2.1	<i>Introduction</i>	page 60
3.2.2	<i>Effect of acetonitrile on SK α-subunit</i>	page 61
3.2.3	<i>Effect of tamapin on rSK2 channels stably expressed in HEK-293</i>	page 61
3.2.4	<i>Influence of external K⁺ and voltage on tamapin block</i>	page 62

3.2.5	<i>Effect of tamapin on rSK3 and hSK1 expressing cell lines.....</i>	page 63
3.2.6	<i>Effect of tamapin on IK channels stably expressed in HEK-293 cells....</i>	page 64
3.2.7	<i>Conclusion.....</i>	page 65
3.3	Domain analysis of the calcium-activated potassium channel SK1 from rat brain: Functional expression and toxin sensitivity.	
3.3.1	<i>Introduction.....</i>	page 66
3.3.2	<i>Expression of rSK1 in HEK-293 cells.....</i>	page 66
3.3.3	<i>Expression of rSK1 and rSK1 core chimeras.....</i>	page 68
3.3.4	<i>Expression of hSK1 core chimeras.....</i>	page 70
3.3.5	<i>Effect of apamin and d-tubocurarine on the chimeras.....</i>	page 72
3.3.6	<i>Conclusion.....</i>	page 74
3.4	Characterization of a novel splice variant of the calcium-activated potassium channel rSK2, rSK2-860.	
3.4.1	<i>Introduction.....</i>	page 76
3.4.2	<i>Primary sequence of the new splice variat of rSK2.....</i>	page 77
3.4.3	<i>Expression of rSK2 and rSK2-860 in HEK-293 cells.....</i>	page 77
3.4.4	<i>Expression of rSK2 and rSK2-860 in COS and CHO cells.....</i>	page 79
3.4.5	<i>Role of the rSK2-860 amino-terminus in protein trafficking: chimera... </i>	page 81
3.4.6	<i>Role of the rSK2-860 amino-terminus in protein trafficking: truncations and deletions.....</i>	page 82
3.4.7	<i>Role of rSK2-860 amino-terminus in protein trafficking: targeting of fusion proteins containing different parts of the amino-terminus of rSK2-860.....</i>	page 86
3.4.8	<i>Interaction of rSK2-860 with rSK2.....</i>	page 88
3.4.9	<i>Subcellular localization of rSK2-860.....</i>	page 89
3.4.10	<i>Role of the Golgi-apparatus in the trafficking of rSK2-860.....</i>	page 92
3.4.11	<i>Does rSK2-860 code for a misfolded or inefficiently folded membrane protein?.....</i>	page 94
3.4.12	<i>Ubiquitination, a new mechanism of protein targeting.....</i>	page 95
3.4.13	<i>Conclusion.....</i>	page 98

4. Discussion

4.1	Tamapin: a novel SK channel toxin.....	page 99
4.2	Domain analysis of the calcium-activated potassium channel SK1 from rat brain: Functional expression and toxin sensitivity.....	page 102
4.3	Characterization of a novel splice variant of the calcium-activated potassium channel rSK2.....	page 106

Abbreviations.....page 110

Appendix..... page 112

Reference table..... page 118

Acknowledgments..... page 130

Curriculum Vitae..... page 131

1 Introduction

1.1 Classification and structure of ion channels, in particular of potassium channels.

Ion channels are responsible for generating and propagating electrical signals in excitable tissues such as the brain, heart, and muscle and for setting the membrane potential of both excitable and non-excitable cells. Channels form pores that allow selective passage of millions of ions per second across the cell membrane. Upon opening of the channels, ions will flow down their electrochemical gradient generating an ionic current across the membrane. Ion channels can be divided into different classes dependent on their ion selectivity, such as Na⁺ channels, Ca²⁺ channels, Cl⁻ channels and K⁺ channels.

Potassium channels set the resting membrane potential (Adrian, 1969), and the duration of action potentials, terminate periods of intensive activity, time the inter-spike intervals during repetitive firing (Meech, 1978), and modulate the effectiveness of synaptic inputs on neurones. They can be separated into several classes based on the topology of the α -subunit, which forms the pore, thereby constituting the basis for functional channels. Depending on membrane topology and on the number of putative transmembrane (TM) spanning segments, the channels can be divided in 2TM, 6TM, 7TM and 4TM-2P (Fig 1). The first class are the 2TM proteins which include the inward rectifiers (Kir) (Bond et al., 1994, Takumi et al., 1995, Brecht et al., 1995) (Fig 1A). The amino- and carboxy-termini of these channels are located cytoplasmically, and the functional channel is formed by the tetramerization of the 2TM proteins. The second class of K⁺ channels are the 6TM proteins (Fig 1B). 6TM proteins can be further separated into voltage-gated channels, called the K_v channels, such as Shaker (Tempel et al., 1987), or into calcium-activated, voltage-independent channels, such as SK- (small-conductance, calcium-activated K⁺ channels) (Kohler et al., 1998) and IK channels (intermediate-conductance, calcium-activated K⁺ channels) (Ishii et al., 1997, Joiner et al., 1997 and Logsdon et al., 1997). Functional channels are formed by the tetrameric association of 6TM subunits (MacKinnon, 1991). The third class has 7 transmembrane domains (7TM) (Fig 1C) and encodes the large-conductance, voltage- and Ca²⁺-activated channel, BK (Marty, 1983, Atkinson et al., 1991, Adelman et al., 1992). In contrast to the 6TM and 2TM, the 7TM α -subunit has its amino-terminus located extracellularly, but the channel also functions as a tetramer. The last class of

potassium channels consist of the four transmembrane domains and 2 pores proteins (4TM-2P, Fig 1D), such as TREK and TASK (Fink et al., 1996, Duprat et al., 1997).

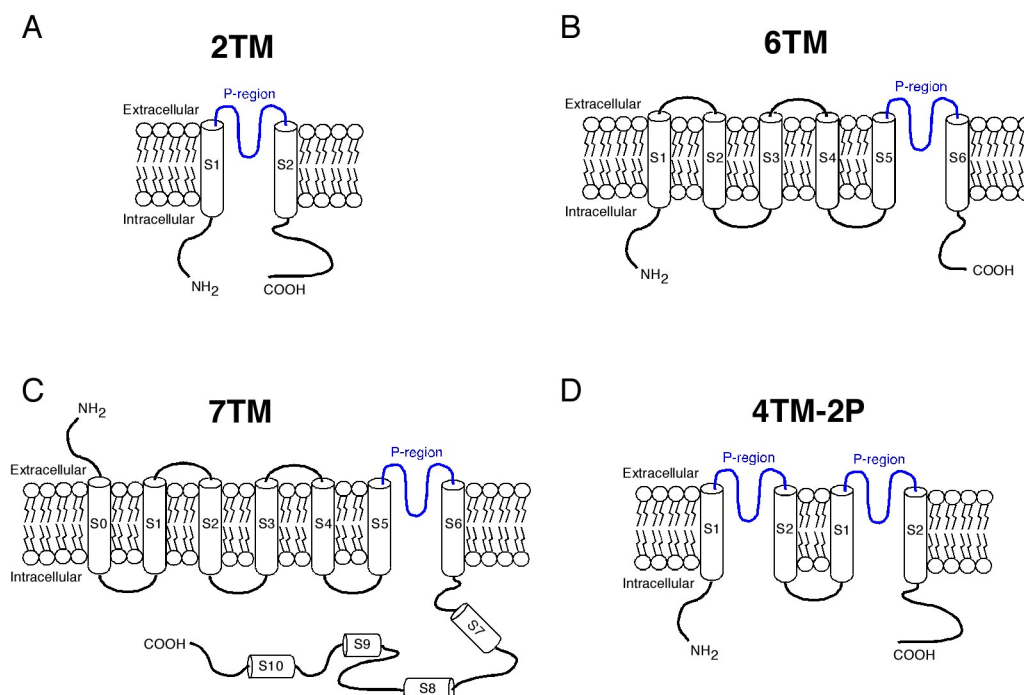


FIG 1.1. α -Subunit topology of the different classes of K⁺ channel. Functional channels are formed by tetrameris of alpha-subunits. A, Two transmembrane domain protein. B, Alpha subunit of the six transmembrane domain protein. C, Structure of the seven transmembrane domain protein. D, Four transmembrane domain subunit, most likely evolved from two 2TM proteins by gene duplication. Blue, P-region, stands for pore region, S1-S6 are the transmembrane segments.

Throughout their maturation in the ER and Golgi, α -subunits can become glycosylated (Michikawa et al., 1994, Nagaya and Papazian, 1997). Furthermore, channels can also be modulated by the interaction with accessory subunits (β -subunits). These subunits have varying structures, they may cross the lipid membrane one or more times or be entirely cytosolic. The general roles for the β -subunits identified to date include: 1) stabilization of the channel complex in the membrane, thereby enhancing channel expression and current (Fink et al., 1996, Shi et al., 1996, Trimmer J.S., 1998); 2) altering the voltage dependence of the channel (Casellino et al., 1995, Barhanin et al., 1996, Sanguinetti et al., 1996); 3) providing for, or increasing inactivation (Rettig et al., 1994, Morales et al., 1995); and 4) enabling the binding of toxins or drugs that block the channel (McManus et al., 1995, Kaczorowski et al., 1996).

Potassium channels share a distinctive feature, all of them present in the pore region (P-region) a consensus amino acid sequence “GXG”, which has been termed the K⁺ channel “signature sequence” (Heginbotham et al., 1994, Ketchum et al., 1995). These residues, GXG, repeated in the 4

α -subunits, line the selectivity filter of the potassium channel. The first insights into the tridimensional structure of the potassium channel pore came after the crystallization of the 2TM protein, KcsA, cloned from *Streptomyces lividans* (Doyle et al., 1998). The 2 membrane segments (α -helices) of each subunit span the lipid layer (Fig 2B), while the inner α -helices face the central pore of the channel (Fig 2A). The selectivity filter for potassium is located at the extracellular surface of the pore formed by a tight alignment of the 4 GXG motifs present in each subunit (Fig 2C). Although this K^+ channel contains only 2 transmembrane segments, the amino acid sequence of the pore region is very close to that of potassium channels with six transmembrane segments, for example there is more than 60% homology between KcsA and Shaker (Doyle et al., 1998, Capener et al., 2002).

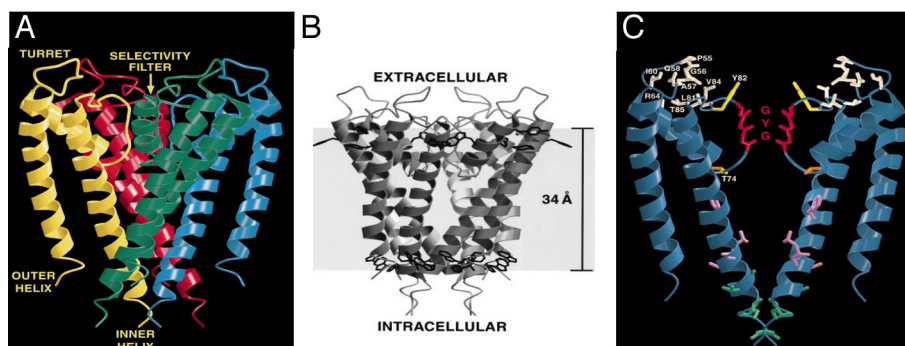


FIG 1.2. Structure of the 2TM potassium channel KcsA. A, Stereoview of the ribbon representation illustrating the 3D fold of the KcsA tetramer. B, Presentation of the channel as an integral membrane protein. C, Side view of 2 of the 4 α -subunits, showing the formation of the selectivity filter by the GYG motifs (From Doyle et al., 1998).

The 6TM calcium-activated potassium channels (K_{Ca}) represent a family of proteins that are distinct from K_V channels. They can be categorized according to their biophysical properties, the most prominent of these features is the single channel conductance. K_{Ca} are classified as small (2-25 pS) (Kohler et al., 1996) and intermediate (25-100 pS) (Ishii et al., 1997, Joiner et al., 1997, Logsdon et al., 1997) conductance K^+ channels.

1.2 Gating of small-conductance, calcium-activated potassium channels.

The 6TM K^+ -channels include channels with different mechanisms of activation. One group are the voltage gated potassium channels, K_V , which are activated by a change in the potential across the cell membrane. Another group are the calcium-dependent K^+ channels, K_{Ca} are activated by the interaction of calcium with calmodulin bound to the carboxy terminus of the K_{Ca} α -subunit.

To date, 3 members of the small-conductance, calcium-activated potassium channels (SK) family have been cloned, SK1, SK2 and SK3 (Kohler et al., 1996). Their sequences are highly conserved across the transmembrane segments, but diverge in amino acid composition and length within their amino- and carboxy-termini (see appendix 2.1). SK channels are voltage independent but are activated by submicromolar concentrations of intracellular calcium. The calcium concentration required for half maximal activation (EC_{50}) of SK channels is approximately 300 nM (Xia et al., 1998, Hirschberg et al., 1998)

In order to determine which amino acids in the SK α -subunit are responsible for the calcium binding, Xia and colleagues (Xia et al., 1998) performed several mutation studies. They found that SK channels are not gated by calcium binding directly to the channel α -subunits. Instead, SK channels are activated by binding of calcium ions to calmodulin, which is in turn constitutively bound to the carboxy-terminus of the α -subunit in a calcium-independent manner (Xia et al., 1998, Keen et al., 1999, Fanger et al., 1999, Zhang et al., 2001). This calmodulin/ α -subunit complex is located in the intracellular carboxy-terminal domain of the protein, just downstream from the S6 transmembrane segment. Their studies also revealed that the carboxy-terminal part of calmodulin (containing EF hands 3 and 4) binds to the α -subunit in a calcium independent manner, while the N-terminal part (containing EF hands 1 and 2) only interacts with the α -subunit in the presence of calcium ions. Furthermore, mutations in the EF hands 1 or 2 of calmodulin resulted in a decrease in calcium sensitivity. In contrast, mutation in EF hands 3 or 4 did not change the calcium sensitivity of SK channels. These results suggest that calcium gating of SK channels results from Ca^{2+} binding to EF hands 1 and 2 of calmodulin, and that either EF hand 1 or 2 is sufficient for channel activation (Xia et al., 1998, Keen et al., 1999).

The elucidation of the X-ray structure of the calmodulin/ α -subunit complex confirmed these findings (Schumacher et al., 2001). The crystal structure of this complex showed the presence of the calmodulin binding domain, CaMBD, in the proximal carboxy-terminal domain of each α -subunit. The interaction between the CaMBD and calmodulin (in the presence of calcium) revealed a dimeric complex. Two CaMBDs, each comprised of a short α -helix, a β -turn, and a longer extended α -helix, are arranged with the longer helices in an antiparallel configuration and do not make direct contacts. Two CaMs are symmetrically woven around the CaMBDs with each CaM making multiple contacts with the two CaMBDs. Although the crystallization was performed in the presence of calcium, only the amino-terminal EF hands (1 and 2) of CaM contain Ca^{2+} ions, while the carboxy-terminal EF

hands (3 and 4) did not, giving a view of both calcium-dependent and –independent CaM/protein interactions (Fig 3, Schumacher et al., 2001).

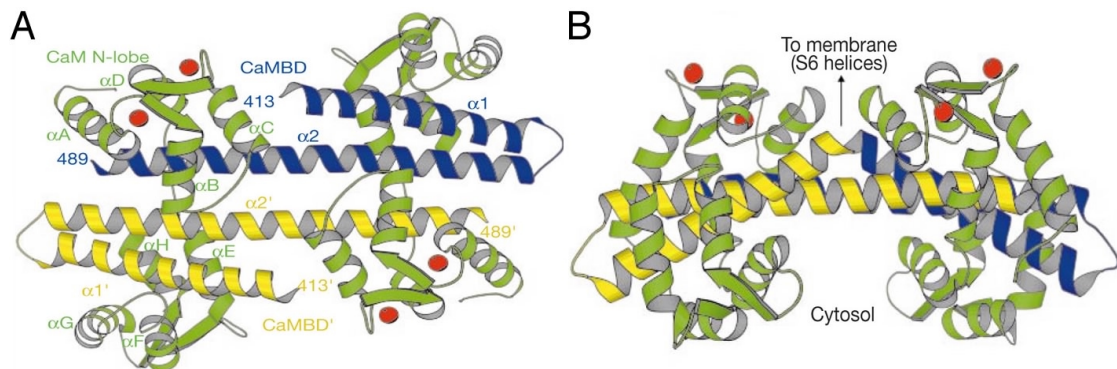


FIG 1.3. Structure of CaMBD/Ca²⁺-CaM complex. Formation of a dimeric CaMBD/Ca²⁺-CaM complex. A. Upper view of the complex. Green are the calmodulin proteins interacting with the CaMBDs, blue and yellow. amino-termini of CaM contain the calcium ions, while carboxy-termini are uncalcified. B. Site view of the same complex in A (From Schumacher et al., 2001).

The binding between CaM and CaMBD is predicted to occur, through electrostatic interactions between negatively charged residues in the CaM linker region and positively charged residues on the CaMBD, and by hydrophobic interactions (Keen et al., 1998, Wissmann et al., 2002, Lee et al., 2003). Furthermore, biochemical data showed that in the absence of calcium the CaM/CaMBD interaction is monomeric (Schumacher et al., 2001).

Taken together, the data suggest a model for Ca²⁺ gating of SK channels where CaM is bound through the C-terminus to the proximal portion of the CaMBD. Upon calcium binding to the N-lobe of CaM, a large rearrangement occurs in which the N-lobe of CaM contacts the distal domain of the CaMBD on a neighbouring subunit (Fig. 4). This rearrangement results in a conformational change of the channel and opens the ion-conducting pore (Schumacher et al., 2001).

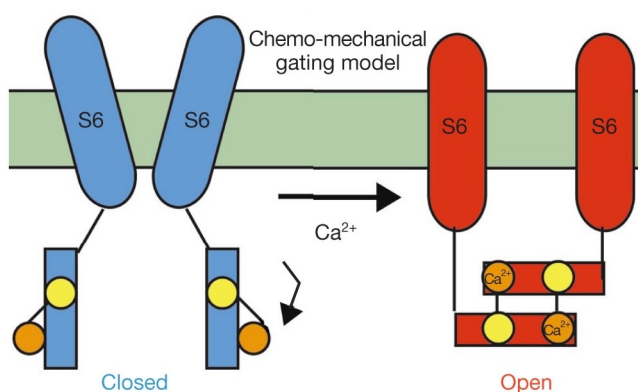


FIG 1.4. Proposed gating model for calcium-activated potassium channels. CaM is bound to the C-terminus of the α -subunit in a calcium independent manner (yellow circles). Upon interaction with calcium, CaM binds to the neighboring α -subunit, forming a dimeric complex. This movement will result in a conformational change of the channel and open the ion-conduction pore (From Schumacher et al., 2001)

Besides activation of SK channels upon binding of calcium ions, a second important role for CaM is trafficking of functional SK channel to the membrane (Joiner et al., 2001, Lee et al., 2003). Experiments which prevented or weakened binding of endogenous CaM to the α -subunits by mutating the CaMBD or by depleting the CaM pool using dominant negative proteins abolished the cell membrane expression of the SK channels. Although the α -subunits were generated, as observed by immunofluorescence and western-blot analysis, the channels were not inserted into the plasma membrane (Miller et al., 2001, Lee et al., 2003).

1.3 Physiological role of SK channels

In situ hybridization has revealed that SK channels are highly expressed in the central nervous system (Stocker and Pedarzani, 2000). These channels are present in most neurons and upon activation by calcium, due to calcium influx through voltage gated calcium channels during an action potential, they contribute to the afterhyperpolarization (AHP) following action potentials. This AHP can be dissected into two main components, the medium and the slow AHP.

The medium afterhyperpolarization (mAHP) follows a single or train of action potentials, presents a rather fast activation (≤ 5 ms), and a time course of decay in the range of hundreds of milliseconds. The Ca^{2+} -activated K^+ current that underlies part of the mAHP is described as I_{AHP} , and is voltage insensitive and blocked by the bee venom toxin apamin (Sah, 1996). mAHP limit the firing frequency of neurons by slowing the return of the membrane potential to the firing threshold, thereby prolonging the interspike interval. Given its pharmacological profile, I_{AHP} is likely to be mediated by SK channels (Villalobos et al., 2004).

The slow afterhyperpolarization (sAHP) only appears after a burst of action potentials, is characterized by a slow time course of activation (~ 500 ms), and decays in 1-4 s. The sAHP is mediated by slow calcium-activated potassium channels underlying a current known as sI_{AHP} . In contrast to I_{AHP} , the sI_{AHP} is apamin insensitive and is responsible for the late phase of spike frequency adaptation. The sAHP leads to a strong reduction or a complete cessation of action potential firing, thereby controlling the repetitive firing of neurons and limiting the numbers of action potentials generated in response to stimuli (Madison and Nicoll, 1982, Madison and Nicoll, 1984). The channels underlying the sI_{AHP} are not known yet.

Furthermore, the AHP and in particular the sAHP have been hypothesized to play a role in controlling the level of excitability of neurons and thus synaptic plasticity. As neuronal activity

plays a role in the processing of information within the central nervous system, it would not be surprising that changes in both the medium and slow AHP may be involved in aspects of learning and memory (Messier et al., 1991).

1.4 Pharmacology of SK channels

A specific toxin used to characterize different SK subtypes is apamin. Apamin is a 18 amino-acid peptide, isolated from the venom of the bee, *Apis mellifera* (Habermann et al., 1972, Habermann and Fischer, 1979). Initial studies, performed in *Xenopus* oocytes, showed that rat SK2 (rSK2) and rat SK3 (rSK3) homomeric channels were blocked by apamin, while the human SK1 (hSK1) channel was not affected by the toxin at concentrations up to 100 nM (Kohler et al., 1996, Ishii et al., 1997b, Table 1). However, further pharmacological studies in different heterologous expression systems have revealed that in mammalian cell lines also hSK1 channels are blocked by apamin (Shah and Haylett, 2000, Strobaek et al., 2000, Table 1), and one study has reported the presence of two apamin binding affinities ($IC_{50} = 0.7$ nM and 196 nM) upon hSK1 expression in *Xenopus* oocytes (Grønnet et al., 2001a, Table 1). Thus, SK channel subtypes can be distinguished on the basis of their different level of sensitivity for apamin, with hSK1 being the least sensitive (IC_{50} : 0.7-12 nM in mammalian cell lines, Table 1), SK2 channels the most sensitive (IC_{50} : 27-140 pM, Table 1), and SK3 channels presenting an intermediate sensitivity (IC_{50} : 0.6-4 nM, Table 1). In contrast, the intermediate conductance potassium channels (IK or SK4) present a distinct pharmacological profile, being insensitive to apamin, but blocked by charybdotoxin (IC_{50} : 2-28 nM, Joiner et al., 1997, Logsdon et al., 1997, Ishii et al., 1997a, Jensen et al., 1998, Table 2).

Beside apamin, other toxins from scorpion venoms target specifically SK channels and provide useful tools for their pharmacological characterization. These include scyllatoxin (Leiurotoxin I), isolated from the scorpion *Leiurus quinquestriatus* (Castle and Strong, 1986, Chicchi et al., 1988, Auguste et al., 1990) and PO5 from *Androctonus mauretanicus* (Zerrouk et al., 1993).

Table 1:

	IC ₅₀	SK1	SK2	SK3
Apamin	nM	<u>0.70</u> ^{7,a} , <u>1.3</u> ^{14,c} , <u>2.9</u> ⁴ , <u>5.1</u> ⁴ , <u>7.7</u> ⁵ , <u>8</u> ^{13,b} , <u>12.2</u> ⁵ , <u>>100</u> ^{1,2}	0.027 ⁷ , 0.063 ¹ , <u>0.07</u> ^{14,c} , 0.083 ⁴ , <u>0.14</u> ¹³	<u>0.63</u> ¹⁰ , <u>1</u> ^{14,c} , <u>1.1</u> ¹³ , <u>1.4</u> ¹¹ , <u>2</u> ² , <u>4</u> ⁷ , <u>13.2</u> ^{8,d} , <u>19.1</u> ⁸
PO5	nM			<u>25</u> ¹²
Scyllatoxin (Leurotoxin)	nM	<u>80</u> ⁴ , <u>325</u> ¹²	0.29 ⁴	<u>1.1</u> ¹² , 8.3 ¹¹

Reported are IC₅₀ values obtained from electrophysiological recordings, rubidium flux and functional fluorescence assays. Underlined values have been obtained from human SK channel clones, all other values from rat SK channel clones.

a: second component with IC₅₀ of 196 nM, b: up to 39% residual current, c: Rubidium flux measurements and d: fluorescence assays.

(1) Kohler et al., 1996; (2) Ishii et al., 1997b; (3) Khawaled et al., 1999; (4) Strobaek et al., 2000; (5) Shah and Haylett, 2000; (6) Dreixler et al., 2000; (7) Grunnet et al., 2001a; (8) Terstappen et al., 2001; (9) Fanger et al., 2001; (10) Grunnet et al., 2001b; (11) Hosseini et al., 2001; (12) Shakkottai et al., 2001; (13) Dale et al., 2002; (14) Castle et al., 2003

In addition to peptide toxins, several organic compounds, like curare, quaternary salts of bicuculline, dequalinium, UCL 1684 and UCL 1848, block all three SK channel subtypes in expression systems (Table 2).

Table 2:

	IC ₅₀	SK1	SK2	SK3
Quaternary Bicuculline salts		<u>1.4</u> ³ , <u>15.9</u> ⁴	1.1 ³ , 25 ⁴	6.6 ¹⁰
Dequalinium		<u>0.44</u> ⁴ , <u>0.48</u> ⁵	0.16 ⁴ , 0.35 ⁶	<u>30</u> ^{8,d}
d-tubocurarine		<u>23.5</u> ⁵ , <u>27</u> ⁴ , <u>76.2</u> ¹ , <u>354</u> ²	2.4 ¹ , 5.4 ² , 17 ⁴	<u>210</u> ^{8,d}
UCL 1684		<u>0.76</u> ⁴	<u>0.28</u> ⁹ , 0.36 ⁴	5.8 ¹¹ , <u>9.5</u> ⁹
UCL 1848		<u>1.1</u> ⁵	0.12 ¹¹	2.1 ¹¹

Besides SK channel blockers, also enhancers of SK channel activity have been identified. The prototypical SK channel enhancer is 1-ethyl-2-benzimidazolinone (1-EBIO), first characterized as an activator of native IK channels in colonic epithelial cells (Devor et al., 1996), and subsequently shown to enhance the activity of recombinant IK channels in transfected cultured cells (Jensen et al.,

1998, Pedersen et al., 1999). When tested on SK1 and SK2, 1-EBIO enhanced their activity by increasing their apparent Ca^{2+} sensitivity by almost an order of magnitude (Pedarzani et al., 2001). Structurally related compounds, such as the muscle relaxant chlorzoxazone and zoxazolamine, have been shown to also enhance the activity of IK and SK2 channels (Syme et al., 2000, Cao et al., 2001). The neuroprotective drug riluzole (2-amino-6-trifluoromethoxy benzothiazole), which has some structural resemblance to 1-EBIO, similarly enhances the activity of SK2 (Cao et al., 2002) and SK3 channels (Grunnet et al., 2001b).

Finally, SK channels have been shown to be the targets of a number of neuroactive drugs suppressing channel activity and including tricyclic antidepressants, Prozac (fluoxetine) and antipsychotic phenothiazines (Dreixler et al., 2000, Terstappen et al., 2001, Grunnet et al., 2001b, Terstappen et al., 2003).

1.5 Aim of this work

The aim of this work was to analyze the structure and function of the small conductance calcium-dependent potassium channels (SK). To date, three SK channels have been cloned, SK1, SK2 and SK3. I generated stable cell lines expressing the rSK2, rSK3 and hSK1 α -subunits and characterized them using immunofluorescence and/or patch-clamp techniques. The SK channels can be distinguished from each other using specific blockers. I screened for novel blockers and characterized the scorpion toxin tamapin. In contrast to rSK2, rSK3 and hSK1, which form functional homomeric channels the rat SK1 (rSK1) does not form functional channels when expressed in HEK-293 cells, although the protein is made, as shown by immunoblot analyses and immunofluorescence. I investigated the molecular determinants of rSK1 channel expression using chimeric subunits in combination with immunocytochemistry and electrophysiology. Finally, I studied the expression of a novel splice variant of rSK2, which reveals a distinct expression pattern of protein aggregates in the perinuclear region when expressed in HEK-293, CHO or COS cells. In order to assess which domain is responsible for the retention and clustering of this splice variant, I have generated truncated forms of the channel and visualized them using immunofluorescence in order to detect differences in expression pattern.

2 Material & Methods

2.1 Materials

2.1.1 Equipment

Abbott Dial-A-Flo	Emergency Medical Supply Inc. (EMS), USA
Amplifier	EPC9, HEKA Electronic
Antivibration table	Technical Manufacturing Corporation (TMC), USA
Air pressure component	MPCU-3, Lorenz
CCD camera	SPOT, Diagnostic Instruments
	QImaging, Micropublisher
Cell culture incubator	Heraeus Instruments
Centrifuge	J2-MI, Beckman
	5415 D, Eppendorf
Computer	Power Macintosh 7100/66
Electrode puller	List medical, Germany
	PP-830, Narishige, Japan
Megafuge 1.0R	Heraeus Instruments
Micromanipulator	Mini 25, Luigs & Neumann
Microscope	Axioskop2, Zeiss
Multiple Solution perfusion system	MP-6 chamber manifold, Warner Instruments corp.
PCR System 2400	GeneAmp, Applied Biosystems
Sequencer	377 DNA sequencer, ABIprism
Shaker	Innova 4230, New Brunswick Scientific, USA
Spectrophotometer	SmartSpec 3000, BIO RAD
UV-light	4W Model UVL-24, Long Wave (365 nm), 230 V, 50 Hz, UVP, Upland, USA
Vacuum pump	Dymax 30, Charles Austen pumps

2.1.2 Consumables

Cryo tube vials	Nunc
Glass coverslips 10 mm	BDH
Glass coverslip 22x22 mm	BDH
Kimax-51 capillary tubes	Kimble products, USA
Multiple well plates; 6, 12 & 96	Nunc
Petri dish, 92X19 mm	Sarstedt
Slides	76x26 mm, Menzel-Glässer
Stericup, 150 & 500 ml	Millipore
Serological pipette; 5, 10 & 25 ml	Sarstedt
Tissue culture flask; 25 & 75 cm ²	Nunc
1.5, 15 & 50 ml tubes	Sarstedt
35 mm dishes	Nunc
Syringe filters, Millex®-GP, 0.22 μm	Millipore

2.1.3 Kits

Flp-In™ System	Invitrogen
FuGENE 6	Roche
LipofectAMINE™ Reagent	Invitrogen
LipofectAMINE PLUS™ Reagent	Invitrogen
NucleoSpin Plasmid	Macherey-Nagel
Nucleospin Extract	Macherey-Nagel
Nucleobond PC 100 & PC 500	Macherey-Nagel
pGEM-T vector system	Promega
ProLong Antifade kit	Molecular Probes
Slowfade Light Antifade kit	Molecular Probes
Sequencing	BigDye™ Terminator (version 2) with AmpliTaq DNA polymerase, Applied Biosystems

2.1.4 Enzymes, antibodies and proteins

Alkaline Phosphatase	Roche
----------------------	-------

Ampicillin	Roche
anti-c-myc (clone 9E10)	Roche
anti-Ubiquitin (clone FK12)	Affiniti
anti-Vimentin (clone V9)	Sigma
Brefeldin A	Epicentre
BSA, protease free, fraction V	Sigma
Cy-3 conjugated Goat anti-rabbit	Jackson ImmunoResearch
Cy-5 conjugated Goat anti-rabbit	Jackson ImmunoResearch
FITC-conjugated Swine anti-rabbit	DAKO
Lamin A/C	sc-7292, Santa Cruz Biotechnology
Lysozyme	Roche
Pfu DNA-polymerase (2.5U/ μ l)	Stratagene
RNase A	Sigma
Taq DNA Polymerase (5U/ μ l)	Gibco-BRL
T4-DNA ligase (1U/ μ l)	Roche
T4-DNA Polymerase	Roche
Restriction enzymes were obtained from Roche, New England Biolabs and Amersham Biosciences	

2.1.5 Plasmids

Bluescript II KS ⁺ , SK ⁺	Stratagene
pcDNA3	Invitrogen
pcDNA5/FRT	Invitrogen
pEGFP-C2	Clontech
pEGFP-ENDO	Clontech
pEGFP-F	Clontech
pEYFP-ER	Clontech
pEYFP-Golgi	Clontech
pGEM-T	Promega
pOGG44 (recombinase)	Invitrogen

2.1.6 Channel blockers and enhancers

Apamin	Latoxan
1-EBIO	Tocris
d-tubocurarine chloride	Research Biochemicals Incorporated
Charybdotoxin	Latoxan

2.1.7 Cell culture

DMEM/F-12	Invitrogen
Fetal Calf Serum (FCS)	Invitrogen
Ham's F-12	Invitrogen
L-glutamine 200 mM	Invitrogen
Opti-MEM1	Invitrogen
PBS	Invitrogen
Penicillin/Streptomycin (10000U/ml)	Invitrogen
Trypsin-EDTA	Invitrogen

2.1.8 Chemicals

Acetonitrile	Sigma
Agar powder	BDH
Agarose	Ultra-Pure, Gibco-BRL
Ampicillin	Roche
Calcium chloride	Fluka
Dimethylsulfoxid (DMSO)	Sigma
EGTA	Fluka
Ethidium bromide	Sigma
G418	CalBiochem
HEPES	Fluka
Kanamycin	Sigma
Luria Broth (LB)	Gibco BRL
Paraformaldehyde (PFA)	Electron Microscopy Sciences
Poly-D-Lysine	Sigma

Potassium chloride	Merck
Sodium chloride	Merck
TAE (50X)	National diagnostics
Triton X-100	Fluka

All other chemicals have been purchased from BDH, Fluka, Merck and Sigma

2.1.9 DNA-ladders

1 kb DNA-ladder 12.216, 11.198, 10.180, 9.162, 8.144, 7.126, 6.108, 5.090, 4.072, 3.054, 2.036, 1.636, 1.018, 506, 396, 344, 298, 220, 201, 154, 134, 75 [bp]

1 Kb⁺ DNA-ladder 12.000, 11.000, 10.000, 9.000, 8.000, 7.000, 6.000, 5.000, 4.000, 3.000, 2.000, 1.650, 1.000, 850, 650, 500, 400, 300, 200, 100 [bp]

100 bp DNA-ladder 2.072, 1.500, 1.400, 1.300, 1.200, 1.100, 1.000, 900, 800, 700, 600, 500, 400, 300, 200, 100 [bp]

All DNA-ladders were obtained from Gibco BRL

2.1.10 Buffers and solutions

Buffer S1	50	mM	Tris-HCl, pH 8.0
	10	mM	EDTA
	100	μ g/ml	RNase
Buffer S2	200	mM	NaOH
	1	%	SDS
Buffer S3	2.8	mM	KAc, pH 5.1
Buffer N3	100	mM	Tris-H ₃ PO ₄ , pH 6.3
	15	%	ethanol
	1.150	mM	KCl
Buffer N5	100	mM	Tris-H ₃ PO ₄ , pH 8.5
	15	%	ethanol
	1.000	mM	KCl

Buffer NE	5	mM	Tris-Cl, pH 8.5
Blocking solution (in PBS)	10	%	FCS
	2-3	%	BSA(10% BSA stock solution)
Freezing medium	70	%	medium (with glutamate and antibiotics)
	20	%	FCS
	10	%	DMSO
G-418 (100 mg/ml)	1	ml	Hepes-NaOH (1M, pH 7.3)
	9	ml	H ₂ O
	1	g	G418
	sterile filtration, store at -20 °C		
LB-plates with Ampicillin for 1 l solution	1	l	H ₂ O
	25	g	LB
	15	g	Agar
	autoclave and cool to 50-55 °C add Ampicillin (100 µg/ml)		
LB-plates with Kanamycin for 1 l	1	l	H ₂ O
	25	g	LB
	15	g	Agar
	autoclave and cool down till 50-55 °C add Kanamycin (30 µg/ml)		
Ligation buffer (5X)	100	mM	Tris-HCl (pH 7.5)
	50	mM	MgCl ₂
	50	mM	DTT
	5	mM	ATP
Loading buffer	5	µl	deionised formamide
	1	µl	blue dextran
	1	µl	EDTA (50 mM)
	adjust pH 8.0		
One-Phor-All buffer (10X)	500	mM	KAc
	100	mM	Tris-Ac (pH 7.5)
	100	mM	MgAc
PBS (10X)	1.3	M	NaCl
	70	mM	Na ₂ HPO ₄
	30	mM	Na ₂ H ₂ PO ₄
	adjust to pH 7.3		

4% PFA	80	ml	H ₂ O
	200	μl	NaOH
	heat to 65°C and add 4g PFA, stir until dissolved		
	10	ml	10X PBS
	200	μl	HCl
adjust to pH 7.3, and store at -20°C			
Sample buffer (5X)	20	%	Ficoll 400
	100	mM	EDTA (pH 8.0)
	0.25	%	Bromphenolblau
	0.25	%	Xylencyanol
SOB-Medium for 1 l	20	g	Bacto-Trypton
	5	g	Yeast-Extract
	10	mM	NaCl
	5	mM	KCl
	10	mM	MgCl ₂
	10	mM	MgSO ₄
adjust to pH 6.8-7.0			
autoclave without Mg-salts. Sterile filter Mg-salts and add before use of medium.			
TB-medium	10	mM	MOPS, pH 6.7 with KOH
	250	mM	KCl
	15	mM	CaCl ₂
	55	mM	MnCl ₂
TE-buffer (pH 8.0)	10	mM	Tris-HCl (pH 8.0)
	1	mM	EDTA
autoclave			
STET (total volume of 50 ml)	100	mM	NaCl
	10	mM	Tris-HCl (pH 8.0)
	1	mM	EDTA
	5	%	Triton X-100
Extracellular recording solutions:			
4 mM K ⁺	4	mM	KCl
	140	mM	NaCl
	2	mM	CaCl ₂
	1	mM	MgCl ₂
	10	mM	Hepes
adjust to pH 7.4 with NaOH			

20 mM K ⁺	20	mM	KCl
	124	mM	NaCl
	2	mM	CaCl ₂
	1	mM	MgCl ₂
	10	mM	Hepes
adjust to pH 7.4 with NaOH			

144 mM K ⁺	144	mM	KCl
	2	mM	CaCl ₂
	1	mM	MgCl ₂
	10	mM	Hepes
adjust to pH 7.4 with KOH			

Intracellular recording solutions:

nominal [Ca ²⁺] free	130	mM	KCl
	10	mM	Hepes
	20	mM	BAPTA
	1.08	mM	MgCl ₂

100 nM free Ca ²⁺	130	mM	KCl
	10	mM	Hepes
	10	mM	EGTA
	1.08	mM	MgCl ₂
	4.11	mM	CaCl ₂

500 nM free Ca ²⁺	130	mM	KCl
	10	mM	Hepes
	10	mM	EGTA
	1.08	mM	MgCl ₂
	7.75	mM	CaCl ₂

1 μM free Ca ²⁺	130	mM	KCl
	10	mM	Hepes
	10	mM	EGTA
	1.08	mM	MgCl ₂
	8.75	mM	CaCl ₂

10 μM free Ca ²⁺	130	mM	KCl
	10	mM	Hepes
	10	mM	EGTA
	1.08	mM	MgCl ₂
	9.87	mM	CaCl ₂

All intracellular solutions are adjusted to pH 7.2 with KOH

Extracellular and intracellular solutions have an osmolarity of 280-300 mOsm

2.2 Methods

2.2.1 Cell culture and transfection

2.2.1.1 Cell types

HEK-293, HEK-SK2, HEK-SK3, HEK-IK and FlpIn-HEK. Human Embryonic Kidney (HEK) cells were cultured in Dulbecco's modified Eagle medium (DMEM) supplemented with 2 mM L-Glutamin; 5 ml Penicillin/Streptomycin (10.000 U/ml) and 10% FCS. Except from the wild type HEK cell (HEK-293), all other cell lines were maintained in the presence of antibiotics. Cell lines expressing SK2, SK3 and IK were grown in the presence of 400 $\mu\text{g/ml}$ G418. FlpIn-HEK cells were maintained in 100 $\mu\text{g/ml}$ Zeocin. HEK-FlpIn-rSK2 lines generated with FlpIn-HEK cells were cultured in regular medium with 100 $\mu\text{g/ml}$ Hygromycin B.

CHO-K1 and FlpIn-CHO. Chinese Hamster Ovary (CHO) cells were grown in Ham's F-12 supplemented with 5 ml Penicillin/Streptomycin (10.000 U/ml) and 10% FCS. FlpIn-CHO cells were maintained in the presence of 100 $\mu\text{g/ml}$ Zeocin. CHO-FlpIn-hSK1, CHO-FlpIn-rSK2 and CHO-FlpIn-rSK3, generated by using the FlpIn-CHO cell system, were grown in medium containing 100 $\mu\text{g/ml}$ Hygromycin.

COS-7 African green monkey kidney cells were maintained in DMEM supplemented with 2 mM L-Glutamin, 5 ml Penicillin/Streptomycin (10.000 U/ml) and 10% FCS. Cells were grown till 80-90% confluence at 37°C and 5% CO₂ before they were splitted (see 2.2.1.2)

2.2.1.2 Splitting cell lines

Cells were grown in a humidified atmosphere at 5% CO₂ and 95% air at 37°C. All cell lines were cultured in 25 cm² culture flasks until they reached 90-100% confluence. Then the medium was aspirated and the cell monolayer was washed once with 1xPBS. The washing step was followed by a brief application of 1ml Trypsin-EDTA. Trypsin-EDTA was gently added to the cell monolayer using a pipette, shaken gently for a few seconds, and then removed. Treated cells were placed for a short time in the incubator. After 1 minute the cells were resuspended in 5 ml of fresh medium. A few drops of the suspension was added to 5 ml fresh medium with or without antibiotics and transferred into a new 25 cm² culture flask. When the cells reached 80-90% confluence, they were split again.

2.2.1.3 Frozen cultures

From each cell line, wild type as well as stable cell lines, frozen cultures were made. The cells were split as described in 2.2.1.2 and counted in a “Neubauer” counting chamber, using the following formula to estimate the number of cells per μl :

$$\frac{\text{N}^{\circ} \text{ of cells}}{\mu\text{L}} = \frac{\text{N}^{\circ} \text{ of cells in 16 squares}}{16 \times 0.100 \times 0.065}$$

After counting, the cells were collected and resuspended in freezing medium. HEK and CHO cells were frozen in cryo tubes at concentrations of 3×10^6 and 2×10^6 cells/ml, respectively. For freezing, cryo tubes were placed for 24 hours at -80°C in a Cryo 1C freezing container filled with isopropanol to achieve a $-1^{\circ}\text{C}/\text{min}$ rate of cooling. Afterwards the frozen samples were transferred to a liquid nitrogen storage container.

2.2.1.4 Transfection of cells

Transient transfections of constructs for immunocytochemistry and electrophysiology. HEK-293 or CHO-K1 cells were grown to 60-70% confluency in 6 well plates or 35 mm dishes. In general, for transfection, different ratios of cDNA were transfected, although an end concentration of $2 \mu\text{g}$ DNA was always used. For co-localisation experiments $1 \mu\text{g}$ of specific channel DNA (rSK2 or rSK2-860) was incubated with $1 \mu\text{g}$ of cellular marker DNA (pEGFP-F, pEYFP-Golgi, see 2.2.2.13). Measuring of different constructs or chimeras were performed by co-transfecting the cells with $1.5 \mu\text{g}$ cDNA (see 2.2.2.14, rSK1, hSK1 and rSK2 chimeras) and $0.5 \mu\text{g}$ pEGFP-C2. In all cases the $2 \mu\text{g}$ DNA and $10.5 \mu\text{l}$ of LipofectAMINE were each incubated in $100 \mu\text{l}$ OptiMEM for 15 min at room temperature (RT). Then the LipofectAMINE was added to the DNA. This mixture was kept for 15 min at RT. After rinsing the cells once with OptiMEM, 0.8 ml of OptiMEM was added to the cells, followed by the DNA/Lipofectamine mixture. The cells were incubated for 3-5 hours at 37°C in a CO_2 incubator. At the end of the incubation, 1 ml of growth medium containing twice the normal concentration of serum was added and cells were further incubated under the same conditions as above. After 12-16 hours the cells could be split (see 2.2.1.2).

COS-7 cells were plated in regular medium (see 2.2.1.1) in 35 mm dishes at a density of 1×10^5 and incubated overnight at 37°C and 5% CO_2 . Following incubation, $3.5 \mu\text{l}$ FuGENE 6 and $1 \mu\text{l}$ DNA were mixed and stored at RT for 20 min. The mixture was added to the cells, without

replacing the medium, for 24 hours and the cells were subsequently replated for immunocytochemistry (see 2.2.3.2).

Stable transfection using LipofectAMINE. HEK-293 cells were transfected with 2 μg pcDNA3-rSK2 or pcDNA3-rSK3, as described for the transient transfections. Subsequently, 24 hours after transfection, the cells were split and divided equally over a 6 well plate and grown overnight in an incubator (5% CO₂, 37°C). The following day the cells were subjected to normal medium containing G418 (400 $\mu\text{g/ml}$). In parallel, control HEK-293 cells, not transfected, were also grown in a 35 mm dish in the presence of selection medium (contains 400 $\mu\text{g/ml}$ G418). When all control cells died, after 4-6 days, the dish containing the transfected cells was checked for surviving cell clusters. A few cell colonies were isolated, same procedure as described in 2.2.1.2, except that trypsin-EDTA (~5 μl) was locally applied to the colony. Subsequently, the colony was resuspended in selection medium and the cells were divided over a 96 well plate. Wells containing a single cell were used to grow the stable cell line. After 4-5 days the cells which survived and had divided were transferred to a 12 well plates. The stable cells were grown till 80-90% confluence. From the 12 well plate the cells were cultured in 25 cm² flasks. After reaching 90-100% confluence the stable cells were split and a part was used to make frozen cultures. The other part was transferred to a culture flask and used to check for rSK expression.

Stable transfection using the FlpIn system. FlpIn-HEK or FlpIn-CHO cells were grown in 35 mm dishes till 70% confluence. The cells were transfected using LipofectAMINE PLUS reagent. Briefly, in 100 μl OptiMEM 1 μg DNA (hSK1, rSK2-JPA or rSK3-Goe in pcDNA5/FRT, see cloning strategies) was mixed with 9 μg pOG44 and 7 μl PLUS reagent and incubated for 15 min at RT. 12 μl LipofectAMINE was mixed with 100 μl OptiMEM. Then the pre-complexed DNA and LipofectAMINE were combined and incubated for 15 min at RT. The cells were rinsed with OptiMEM and supplied with 0.8 ml of fresh OptiMEM. Now the DNA-PLUS-LipofectAMINE mixture was added drop by drop onto the cells. After a 5 hours incubation 1ml of medium containing 2X serum was added and incubated for 24 hours. After 2 days, the medium was replaced by medium containing the appropriate concentration of Hygromycin B. 3-4 days later, cells were split and maintained under selection medium. After 3-4 weeks the stable cell line was generated and cells were frozen (see 2.2.1.3).

2.2.1.5 Testing G418

In each well of a 6-well plate, 1×10^5 cells were plated and grown overnight in an incubator. Then six different G418 concentrations (from 50 – 800 $\mu\text{g/ml}$) were applied to the wells. The

concentration which killed all cells after 6 days of incubation was used to maintain stable cell lines. In general, a concentration of 400 $\mu\text{g/ml}$ was used for the maintenance of stable cell lines.

2.2.2 Standard molecular biology techniques

2.2.2.1 Restriction enzyme digest of plasmid DNA

For miniprep digestion 200-300 ng of isolated DNA, for digest of vector and fragment isolation 1 μg of DNA, was added to an eppendorf tube containing: H_2O , appropriate restriction enzyme and specific digest buffer. The total volume of the mixture was 20 μl for miniprep digestion and 40 μl for vector digestion and fragment isolation. The digest was incubated at 37°C for 1 hour or, in case of special restriction enzymes, the digest was performed according to the manufacturer's protocol. Subsequently, the cloning vector, but not DNA fragments, was subjected to dephosphorylation. The dephosphorylation mixture contained the digest mixture, 1 μl alkaline phosphatase, buffer and was incubated for 1 hour at 37°C. The digest as well as the dephosphorylation reaction was stopped by adding sample buffer to the mixtures. Afterwards the mixture was run on an agarose gel (see 2.2.2.2) and DNA fragments were isolated (see 2.2.2.3).

2.2.2.2 Agarose gel electrophoresis of cDNA

DNA was analysed on gels containing 0.7-1.5% agarose dissolved in 1xTAE and ethidium bromide (0.4 $\mu\text{g/ml}$). The running buffer was 1xTAE with 40 $\mu\text{g/ml}$ ethidium bromide. The electrophoresis was performed at 70-100 mV for 40-100 minutes. 1kb, 1kb plus and/or 100bp DNA ladders were used as markers (see 2.1.9). The bands were visualized under UV light.

2.2.2.3 Gel extraction of DNA fragments

Bands containing DNA fragments were excised from the agarose gels using a 365 nm UV light to visualize the bands and purified using the Nucleospin Extract kit. Briefly, agarose slices were melted at 56°C in buffer NT1 (300 $\mu\text{l}/100$ mg agarose), the dissolved mixture was loaded on a column. The DNA was washed two times with buffer NT3 and finally eluted from the column with buffer NE, pre-heated to 70°C to increase the yield of fragment elution.

2.2.2.4 Phenol/Chloroform extraction of DNA

Phenol/Chloroform extraction was used to remove proteins from DNA, following PCR or restriction digestion. Samples were mixed with an equal volume of phenol and some drops of chloroform (10 μ l/60 μ l), vortexed for 30 seconds and centrifuged for 2 min at maximum speed (12.000xg). The aqueous phase was transferred to a new tube and the same volume of chloroform was added. The mixture was vortexed again and centrifuged under the same conditions. The upper layer (aqueous phase) containing the DNA was transferred into a fresh reaction tube and subjected to ethanol precipitation (see 2.2.2.5).

2.2.2.5 Ethanol precipitation of DNA

DNA samples were mixed with 1/20 of the volume of 8M LiCl and 3 volumes of 100 % ethanol. Precipitation was performed at -80°C for at least 30 minutes or overnight at -20°C and collected by centrifugation (15 min., 12.000xg). The pellets were washed twice with 75% ethanol, air dried and resuspended in 30 μ l sterile water.

2.2.2.6 Fill-In reaction of overhanging DNA ends

The experiment was performed using T4-DNA polymerase which catalyses the synthesis of DNA in the 5'→3' direction and has a 3'→5' exonuclease activity. A total volume of 30 μ l containing 100 ng digested DNA, 100 μ M dNTP's, enzyme buffer, 2 μ g T4-DNA polymerase was placed for 15 min at 14°C followed by 15 min at 37°C . The mixture was heat inactivated (15 min at 75°C) and ligated followed by transformation.

2.2.2.7 Hybridization of oligonucleotides

A set of primers was hybridized by adding 2 μ l primer A (40 pmol/ μ l), 2 μ l primer B (40 pmol/ μ l), 4 μ l One-Phor-All buffer (10X), to 32 μ l H₂O. The mixture was transferred to a metal container, submersed for 5 min in boiling water, and incubated until the water reached RT. Then the annealed oligonucleotides were ligated into the vector (see 2.2.2.8).

2.2.2.8 Ligation of DNA fragments

Ligation was carried out in a total volume of 20 μ l containing 3 μ l dephosphorylated vector (20 ng/ μ l), 1 μ l DNA fragments, 1 μ l ligase, 5 μ l ligation buffer and H₂O. The ratio of dephosphorylated vector versus DNA fragments was 1/3. The amount of background colonies was controlled by ligation of dephosphorylated vector under the same conditions but without DNA fragments. The mixtures were submersed in a 14°C water bath for at least 1 hour. 10 μ l ligation product was used for transformation of competent bacteria, the rest was placed back in the water bath for 12-24 hours.

2.2.2.9 Generation of competent bacteria, DH5 α

Bacteria were plated onto LB-plates without antibiotics and incubated overnight at 37°C. The following morning a single colony was inoculated into 25 ml SOB medium and was incubated at 37°C in a shaker (220 rpm) for 6-8 hours. From this culture, 2 ml, 4 ml and 10 ml was inoculated into 1- or 2 liter flasks containing 250 ml SOB medium and shaken (150 rpm) at 18°C overnight. Then the OD was monitored until an OD of 0.55 was reached. The culture with the appropriate density was transferred to an ice-water bath for 10 min. The bacteria were harvested by centrifugation at 2.500xg for 10 min at 4°C, followed by aspirating the medium and resuspension of the bacteria in 80 ml ice cold TB buffer. Again the bacteria were harvested as described above and resuspended in 20 ml ice cold TB buffer. Under gentle swirling, 1.5 ml of DMSO was added to the bacterial suspension and stored for another 10 min in the ice bath. Then the suspension was aliquoted in microfuge tubes (100 μ l/tube) and immediately snap-frozen by immersing the tubes in a bath of liquid nitrogen and stored at -80°C.

2.2.2.10 Transformation of competent bacteria, DH5 α

10 μ l of ligation product was mixed with 100 μ l competent bacteria and placed on ice for 15 min. Meanwhile 100 μ l LB medium was warmed to 37 °C. The ligation/bacteria mixture was transferred to a heating block at 37 °C for 5 minutes. The pre-heated LB medium was added to the mixture and incubated for 15 min at 37 °C. After the incubation, the mixture was plated onto LB-plates containing Ampicillin or Kanamycin. The plates were placed in an incubator (37 °C) for 12-15 hours and 4-8 single colonies were picked to start bacterial cultures.

2.2.2.11 Isolation of DNA from bacteria cultures

Single colonies were grown overnight in 5 ml (miniprep) or 150 ml (midiprep) LB medium with appropriate antibiotics and DNA was isolated using the Nucleobond Plasmid kit, Nucleobond AX kit or the STET method.

Nucleobond Plasmid (for minipreps). Briefly, 5 ml bacterial cultures were pelleted (5 min, 3.200xg) and resuspended in buffer A1. Then lysis buffer A2 was added to the cell suspension and gently mixed by inverting the tubes. Buffer A3 was added to the lysate and incubated for 5 min at RT. The cell debris was precipitated by centrifugation (10 min, 11.000xg), the clear lysate was transferred to a NucleoSpin column (silica membrane) and centrifuged for 30 sec at 10.000xg. The flow-through was discarded and the column was washed with buffer A4. Plasmid DNA was eluted from the column with buffer AE and stored at 4°C.

Nucleobond AX (for midipreps). The 150 ml bacterial culture was harvested by centrifugation at 7.000xg for 10 min at 4°C and resuspended in buffer S1. Subsequently, the cells were lysed in buffer S2 and buffer S3 was added followed by precipitation of chromosomal DNA at 3.200xg for 10 min at 4°C. Directly after centrifugation, the clear lysate was poured through a filter. The flow-through was collected and loaded on a nucleobond AX cartridge. The cartridge was washed with buffer N3 and the DNA was subsequently eluted with buffer N5. The plasmid DNA was precipitated with 0.7-0.8 volumes of isopropanol, centrifuged at 16.000xg for 30 min at 4°C and washed with 75% ethanol, followed by a final centrifugation step (15.000xg for 10 min at 4°C). Finally the DNA was redissolved to a final concentration of 1 $\mu\text{g}/\mu\text{l}$ in sterile water.

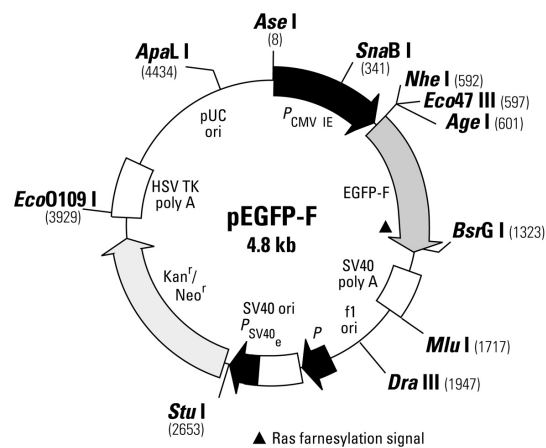
STET method. 1.5 ml of the bacterial culture was collected (30 sec at 16.000xg) and the medium was gently aspirated. Bacterial precipitates were resuspended in 350 μl STET and 25 μl lysozyme (10mg/ml) was added. The mixture was placed for exactly 40 seconds in boiling water and the lysate was centrifuged for 15 min at 16.000xg. The supernatant was transferred to a new 1.5 ml tube, 40 μl NaAc (3M) and 420 μl isopropanol was supplemented to precipitate the DNA. Subsequently the mixture was vortexed, incubated for 5 min at RT and centrifuged (16.000xg) for 10 min at RT or 4°C. The DNA/RNA precipitate was rinsed with cooled (4°C) 75% ethanol and resuspend in 50 μl TE (pH 8.0), store at 4°C (short time) or at -20°C (long term). Restriction enzyme digestion (see 2.2.2.1) of the DNA samples obtained with the STET method were performed in the presence of RNase (2mg/ml).

2.2.2.12 Amplification of DNA using PCR

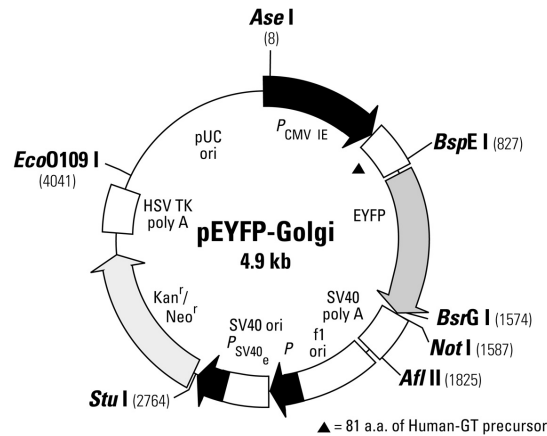
Amplification of DNA fragments from plasmid DNA using Pfu. In a 200 μ l reaction tube, 60 μ l sterile water contained 200-300 ng template DNA, 1 μ M of each primer and 0.2 mM dNTP's. This mixture was denaturated for 3 minutes at 92°C, paused and a second mixture, containing 1 μ l Pfu, 10 μ l buffer (10X) and 29 μ l H₂O, was added. Then the PCR was started, the setting for one PCR cycle was: denaturation: 30 sec at 94°C; annealing: 30 sec at X °C (T_M); and elongation: 1 min/kilobase at 72°C. The annealing temperature (T_M) was depending on the melting temperature of the primer with the lowest T_M and was calculated using the following formula: T_M = 4x(G+C) + 2x(A+T). The amount of cycles during amplification was varied from 15-25. When all cycles were completed there was a final elongation of 7 min at 72°C followed by cooling to 4°C.

2.2.2.13 Overview vectors

Overview cellular marker vectors

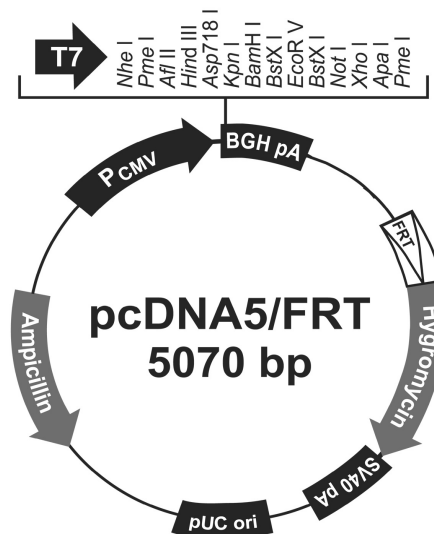
pEGFP-F vector

Vector encodes for a farnesylated enhanced green fluorescent protein. EGFP is tagged at the C-terminus with the farnesylated signal of c-Ha-Ras. The fusion protein is targeted to the plasma membrane.

pEYFP-Golgi

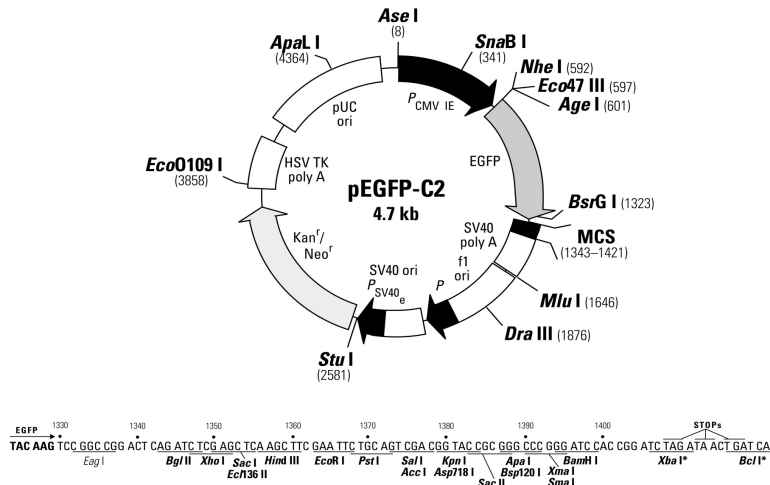
81 amino acids of the precursor of the human beta 1,4-galactosyltransferase are fused to the EYFP protein. The fusion protein allows specific labeling of the trans-medial region of the Golgi apparatus.

Overview cloning and expression vectors

pcDNA5/FRT

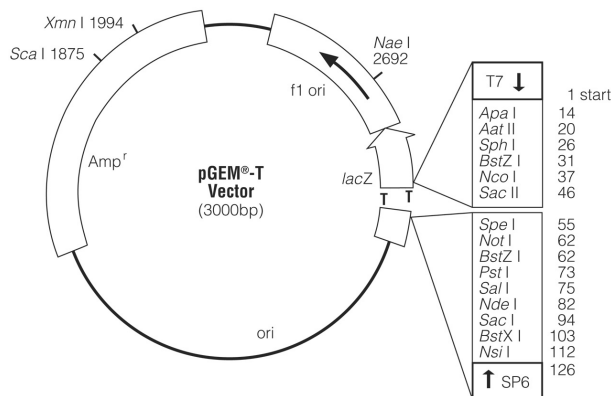
pcDNA5/FRT is a cloning vector used to incorporate channel DNA. The generated construct and pOG44 (coding for the Flp recombinase) are used together with Flp-In cell lines to generate cell lines stably expressing the channel. The integration of the gene of interest occurs between the FRT site in the plasmid, which will recombine with the FRT site in the FlpIn cells chromosome. This integration is catalyzed by the Flp recombinase. Furthermore, the vector contains the Hygromycin B resistance marker under the control of the SV40 early promoter. The ampicillin resistance gene is used to amplify the plasmid in bacteria.

pEGFP-C2



pEGFP-C2 is an expression vector used in cotransfection for electrophysiological measurements, it is also used to tag channels and study their distribution in the cell.

pGEM-T



pGEM-T vector is very convenient for cloning PCR products. When competent bacteria are transformed with vector containing an insert, this results in the formation white of colonies due to the interruption of the *lacZ* gene. If the vector does not contain an insert, the colonies will be blue.

2.2.2.14 Cloning strategies

Abbreviations of restriction enzymes

- | | | | | | |
|--------|---|--------|------|---|------|
| ACCI | = | ACCI | NotI | = | N |
| Alw44I | = | Alw44I | NsiI | = | NsiI |

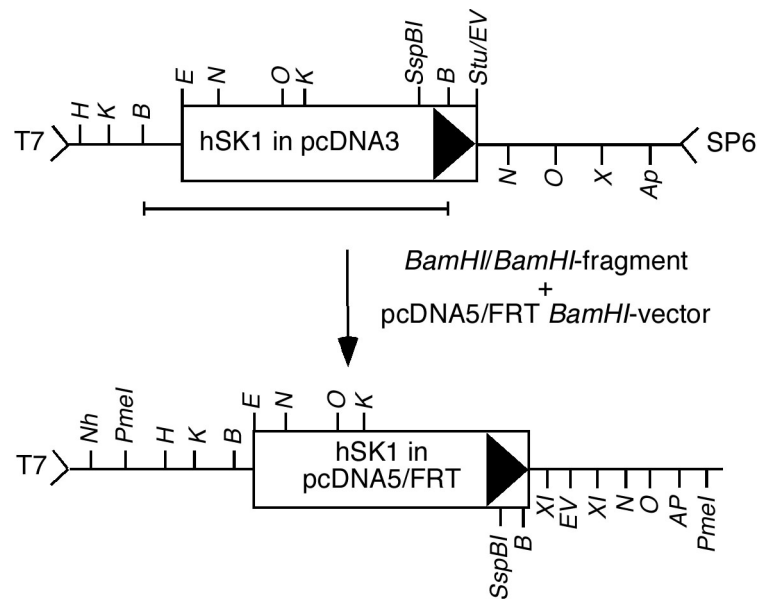
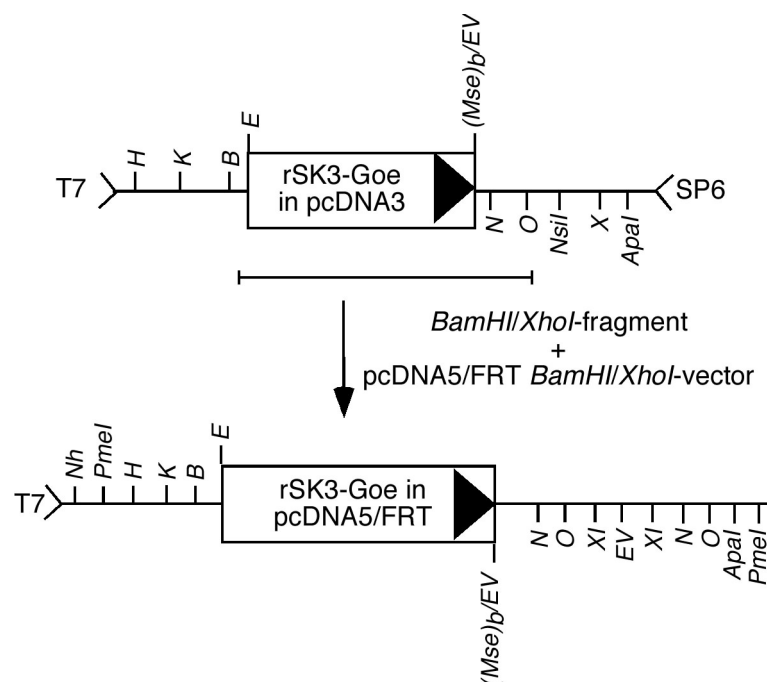
BamHI	= B	PstI	= P
BglII	= GII	PvuII	= VII
BstEII	= EII	SacI, SstI	= S
BstXI	= XI	SacII, SstII	= SII
ClaI	= C	SalI	= L
EcoRI	= E	SspBI	= SspBI
EcoRV	= EV	SmaI	= M
HindIII	= H	XbaI	= X
KpnI, Asp718	= K	XhoI	= O
NdeI	= Nd	XmaI	= Xml
NheI	= Nh		

Oligonucleotides

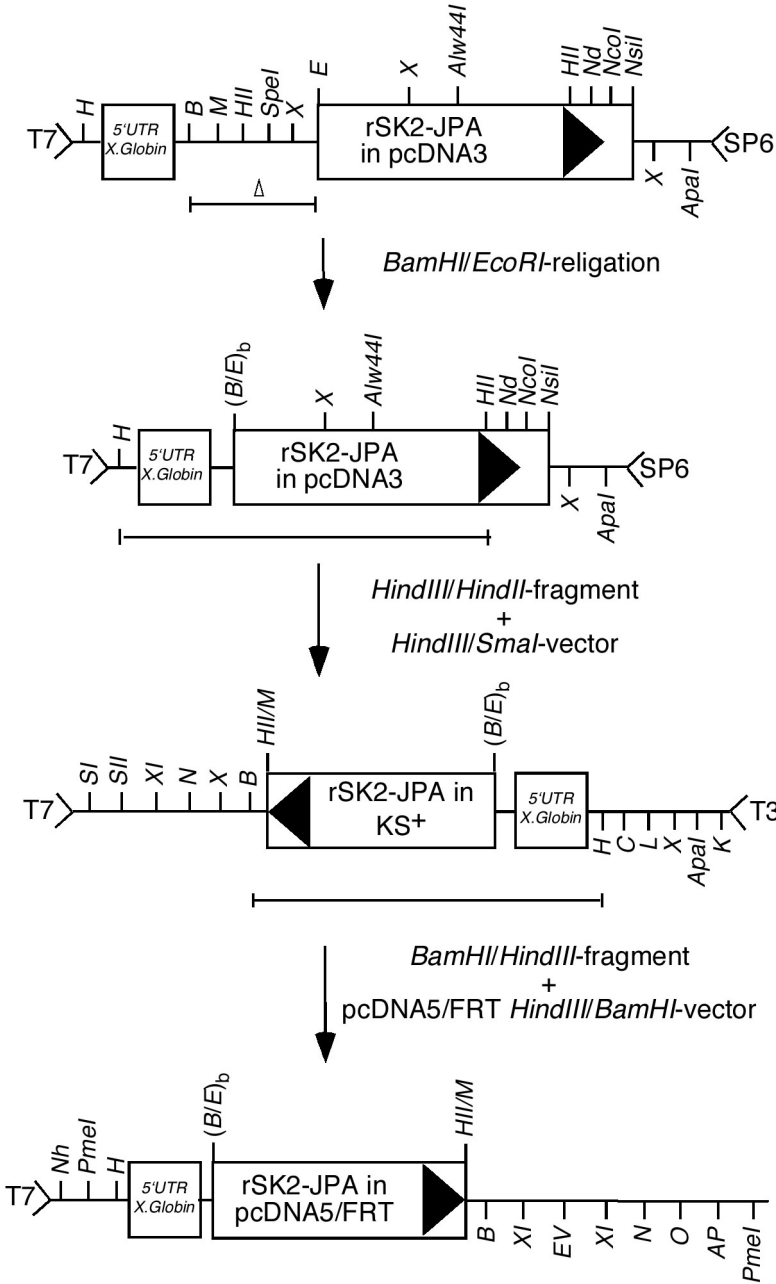
T7:	5' TAATACGACTCACTATAGGG 3'
T3:	5' ATTAACCCTCACTAAAGGGA 3'
SP6:	5' GATTTAGGTGACACTATAG 3'
p0973:	5' TGTTTCGAGCCTGTCAGGTAC 3'
p1605:	5' GACCGTACCGACCTGCCGC 3'
p2000:	5' GGGTTCCATGTCAGATCTGTAAAGC 3'
p2001:	5' CGGAAGATCTGACATGCACCACCCGCACCCGGCGCACCACC AGC 3'
p2002:	5' CTCAATGTGCTCGAGCTGACGCCGTC 3'
p2003:	5' GGCCTCGAGGTGCGGGTGGTGGTGAG 3'
p2019:	5' CCGCGGATCCCACCATGGAAACCCATTGCAGTTC 3'
p2020:	5' GATCCCACCATGTT 3'
p2021:	5' CCGGAACATGGTGG 3'
p2022:	5' GTACCTGCAGGAGCTCATGGCTATTTTCG 3'
p2026:	5' TGTTGTACACGCCACGACAGCTCGGTCTCGGTGACCATGAC CAC 3'

Cloning SK channels into pcDNA5/FRT

pcDNA5/FRT vector was used for the cloning the SK channel gene into the genome of the CHO-FlpIn or HEK-FlpIn cells.

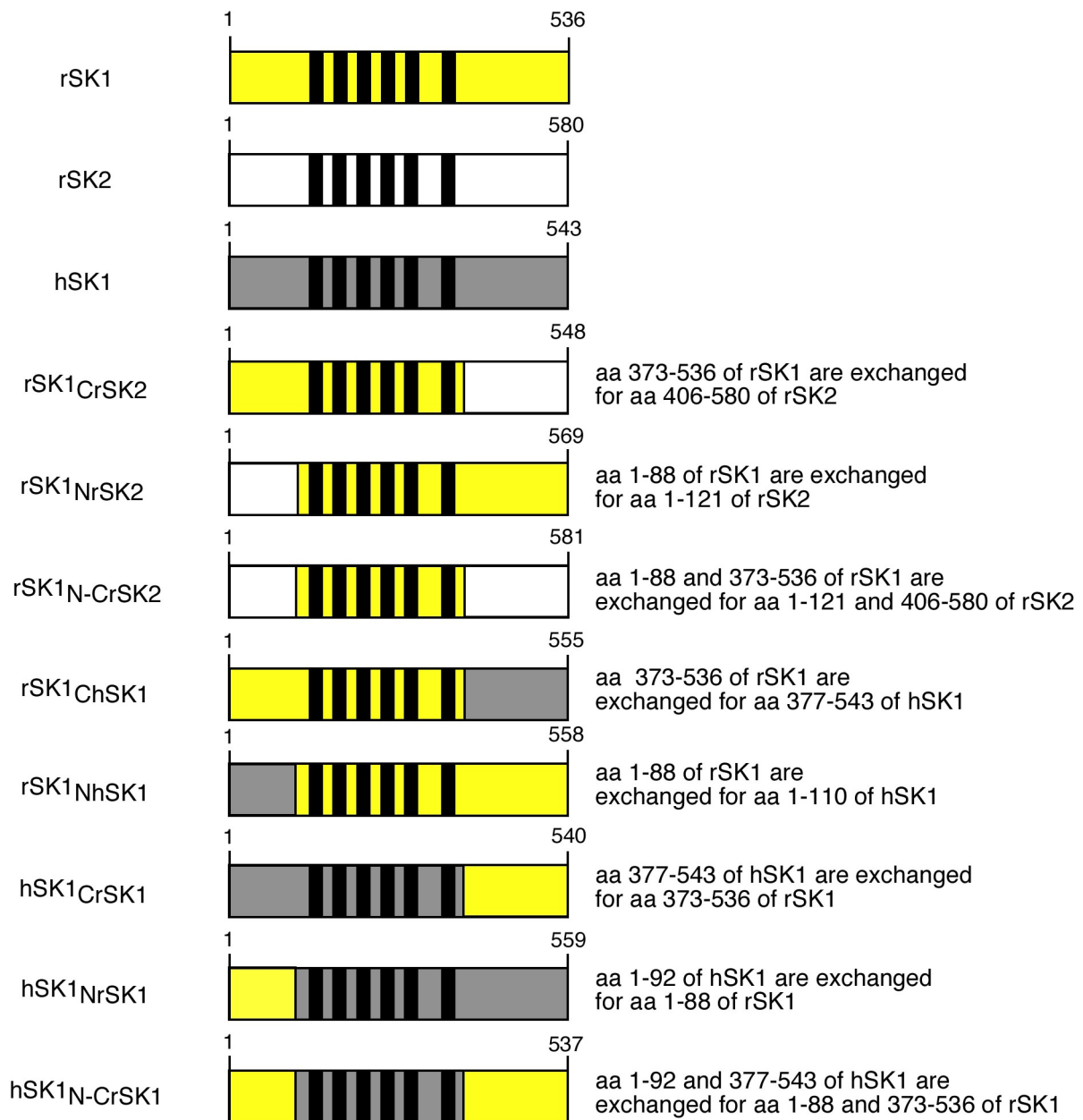
Cloning of hSK1 in pcDNA5/FRT*Cloning of rSK3-Goe in pcDNA5/FRT*

Cloning of rSK2-JPA into pcDNA5/FRT

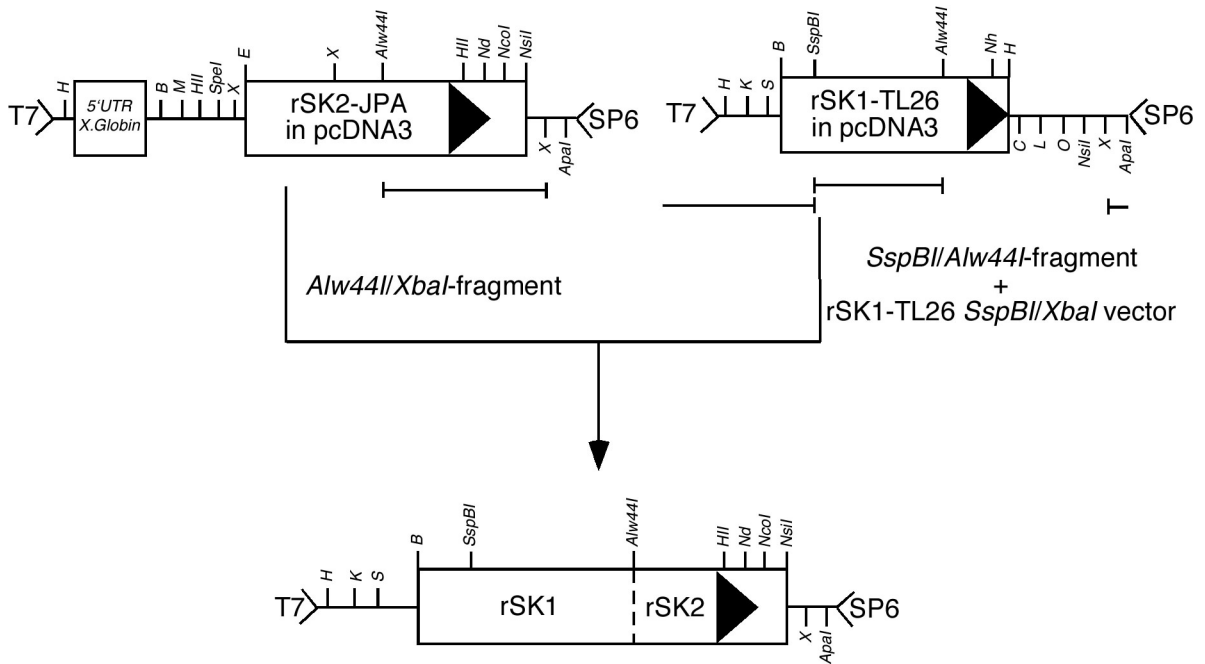


Cloning rSK1, hSK1 and rSK2 chimeras

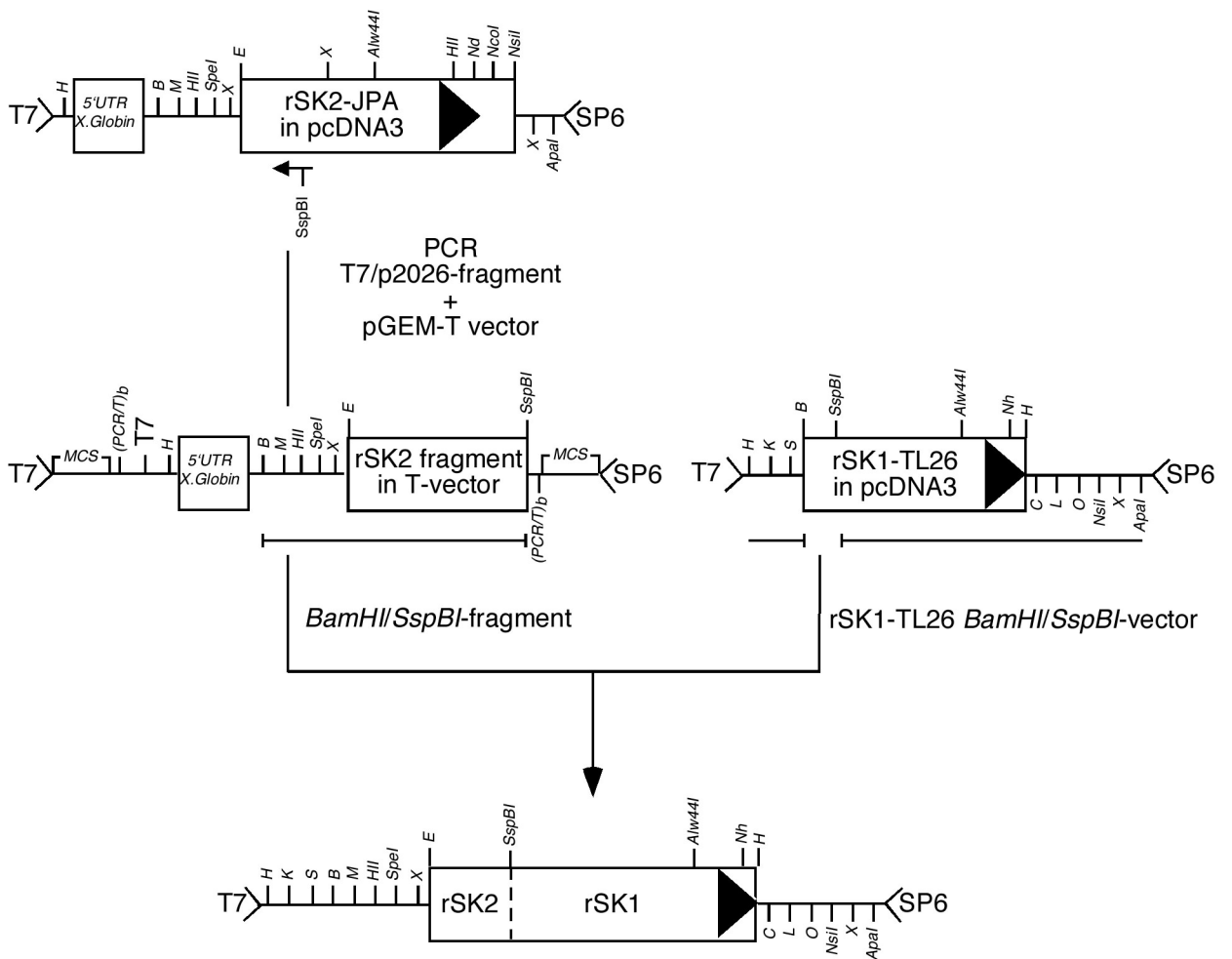
Overview of the generated chimeras. The 6 black boxes in the middle represent the membrane spanning segments of the channels. Corresponding amino acid sequences are presented in the appendix (appendix 1.2., 1.3. and 1.5.).



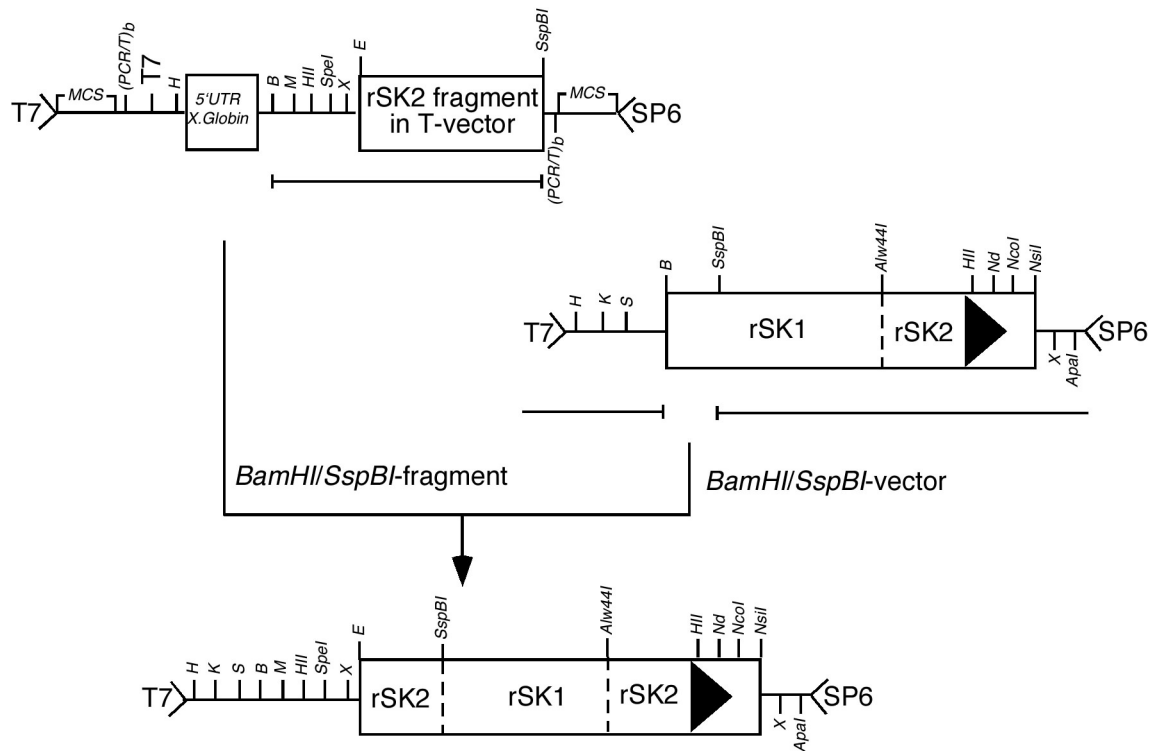
rSK1_{CrSK2} in pcDNA3



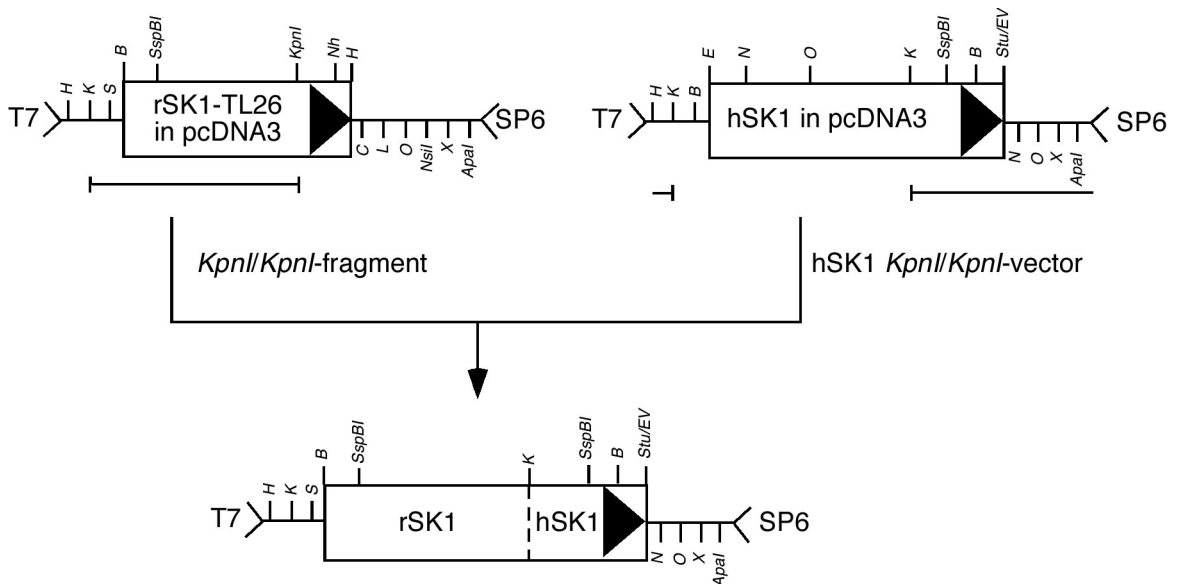
rSK1_{NrSK2} in pcDNA3



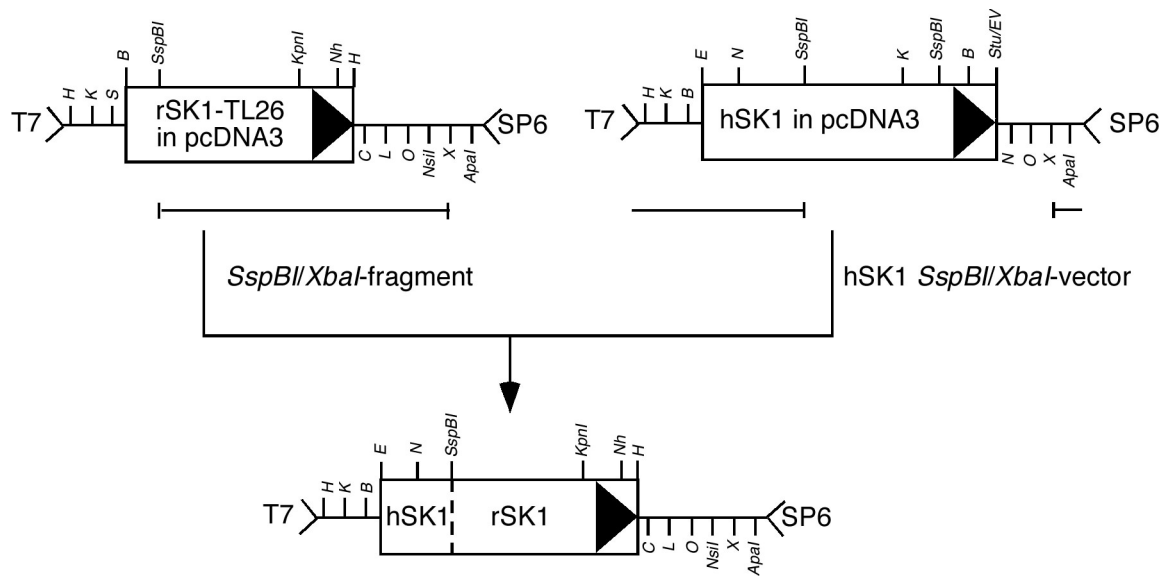
rSK1_{N-C_rSK2} in pcDNA3



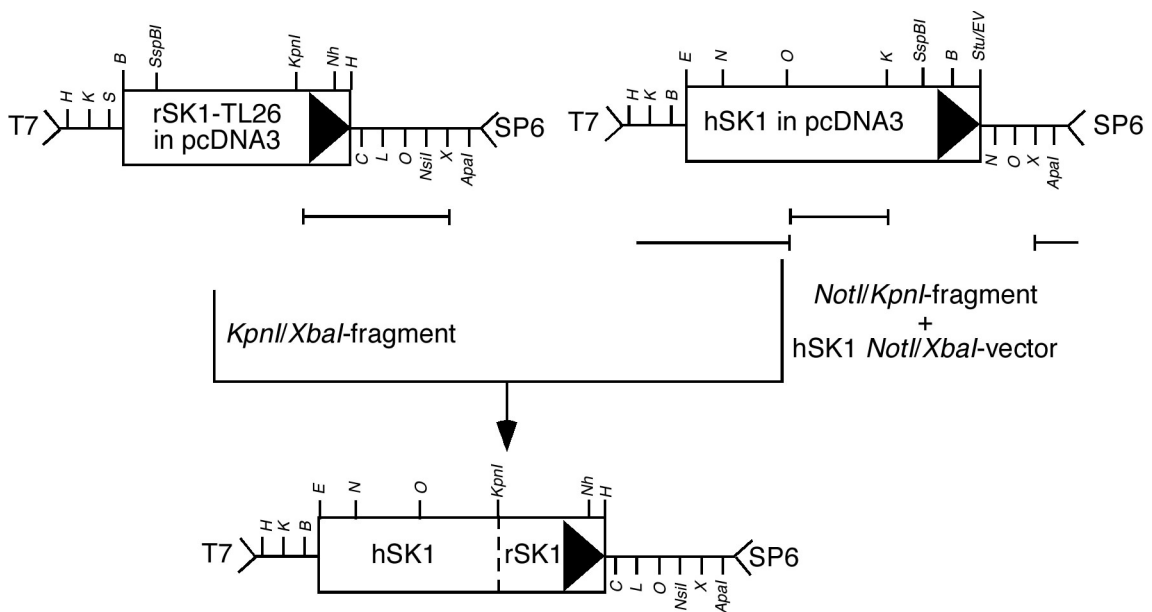
rSK1_{ChSKI} in pcDNA3



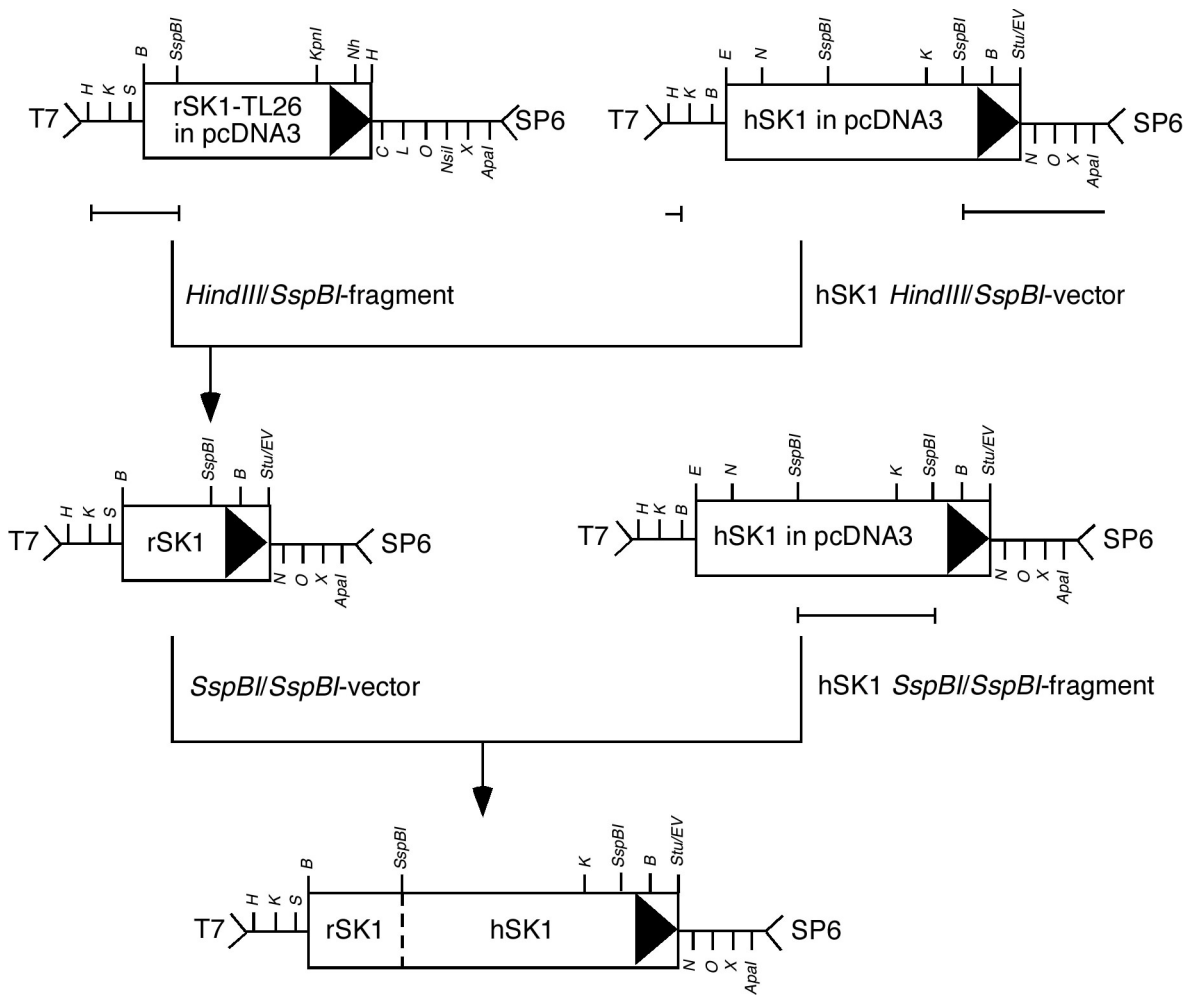
rSK1_{NhSK1} in pcDNA3



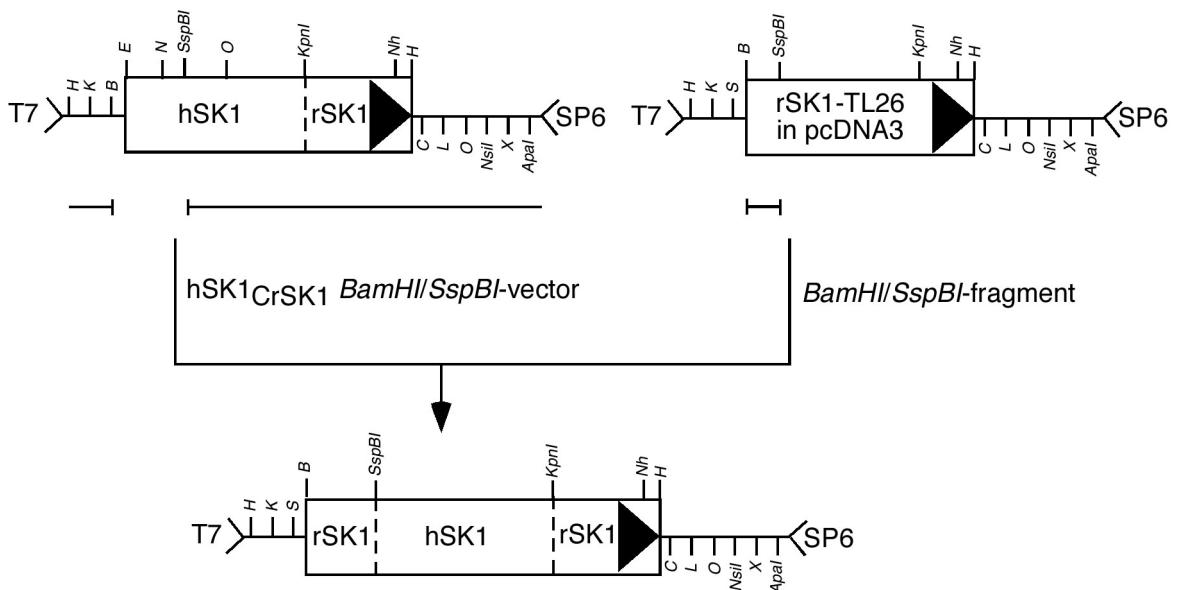
hSK1_{CrSK1} in pcDNA3



hSK1_{NrSK1} in pcDNA3

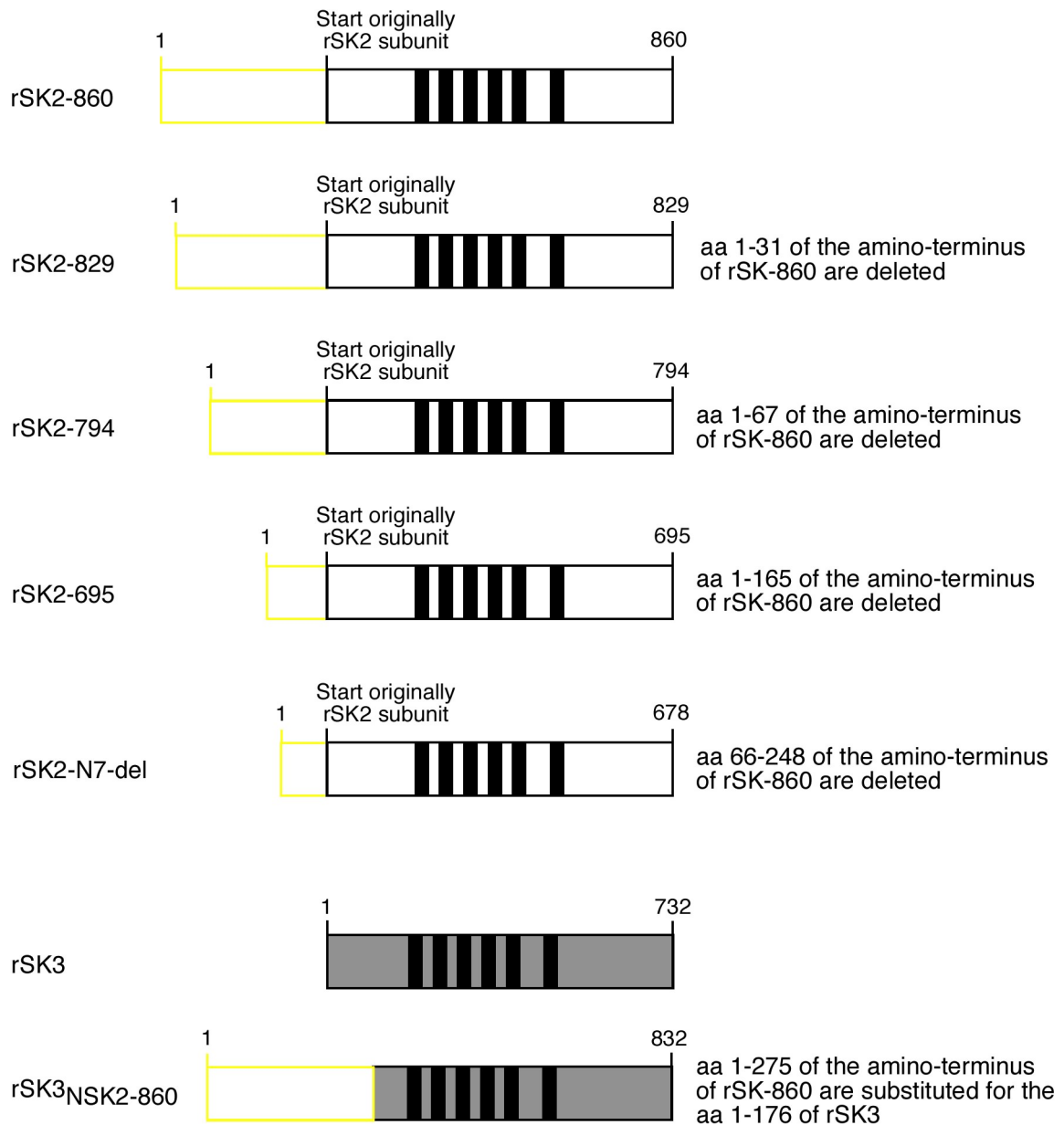


hSK1_{N-C_rSK1} in pcDNA3

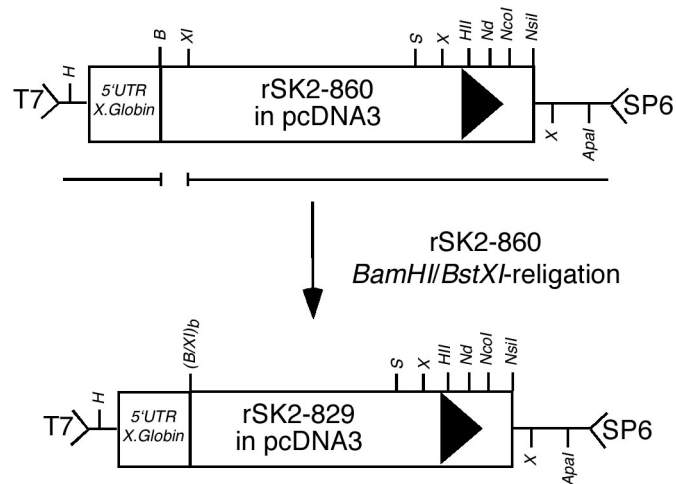


Truncations, deletion and substitutions of rSK2-860

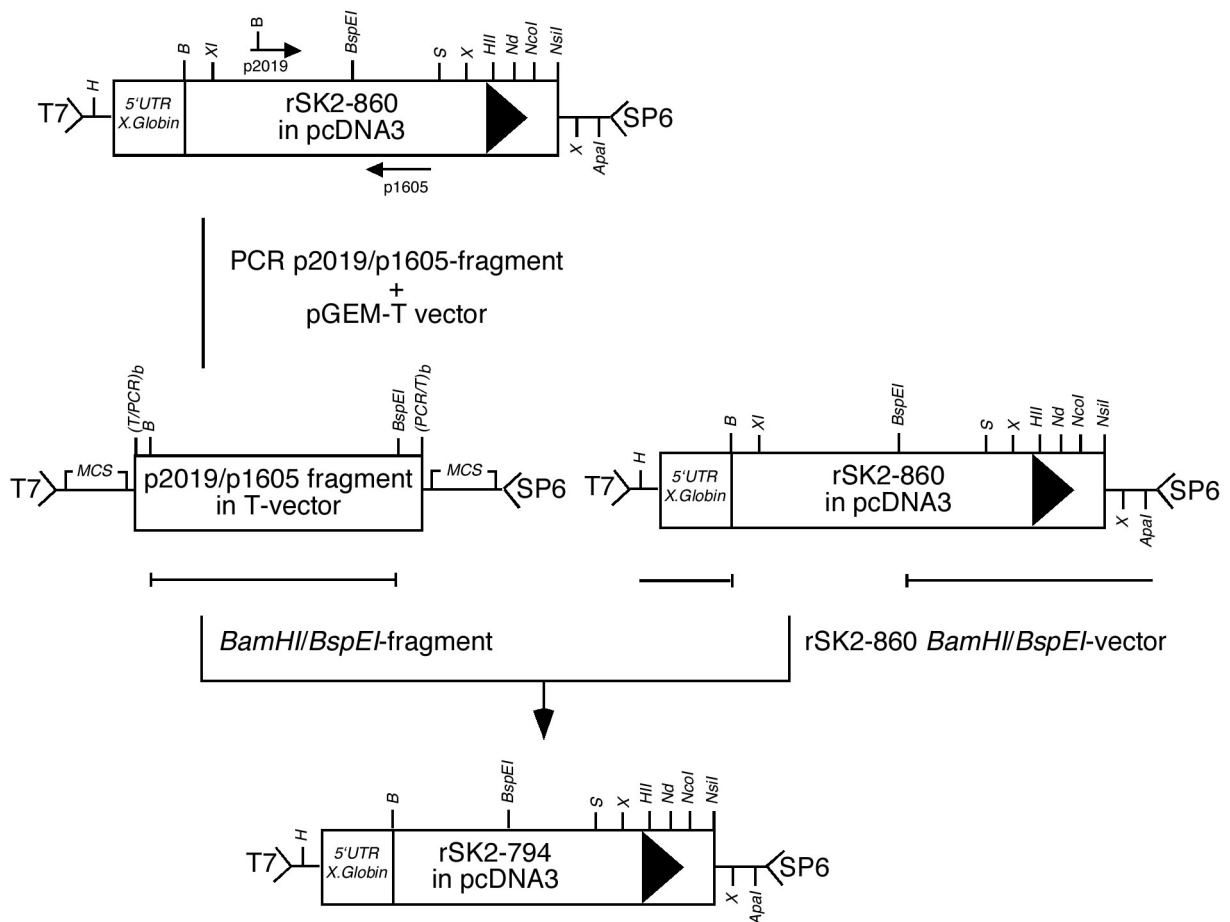
Overview of the generated amino-terminal rSK2-860 constructs. The 6 black boxes in the middle represent the membrane spanning segments of the channels. Corresponding amino acid sequences are presented in the appendix.



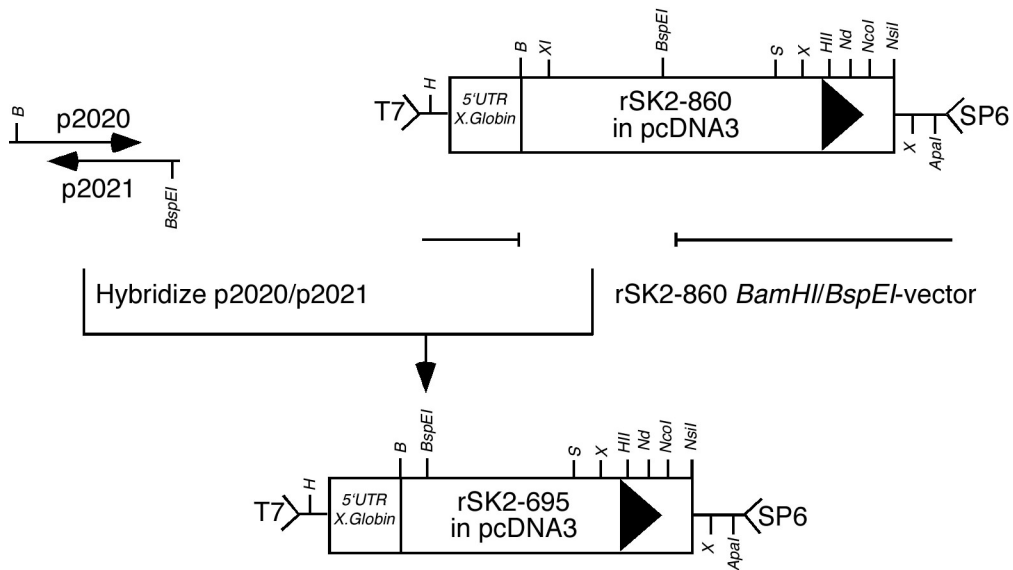
rSK2-829 in pcDNA3



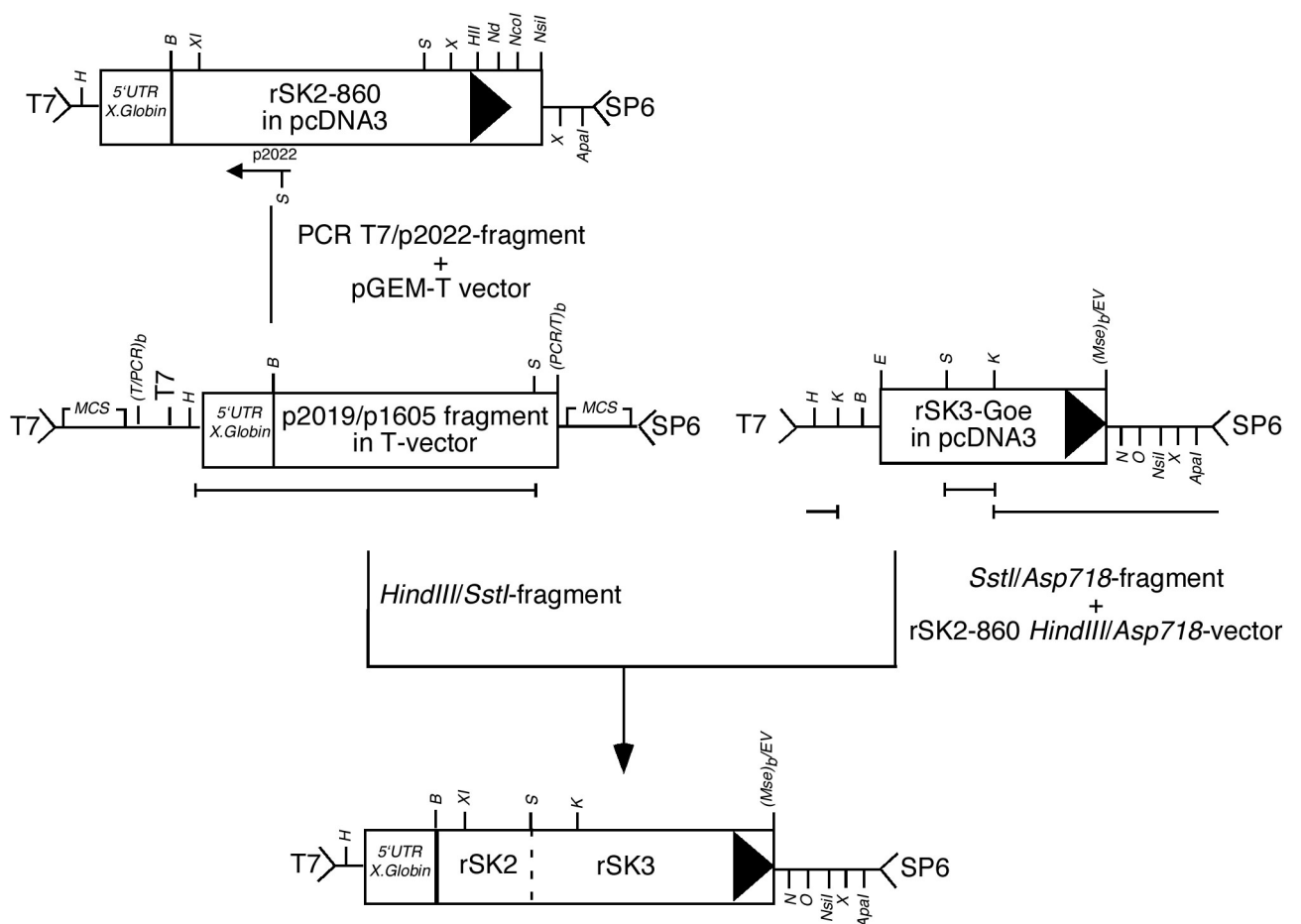
rSK2-794 in pcDNA3



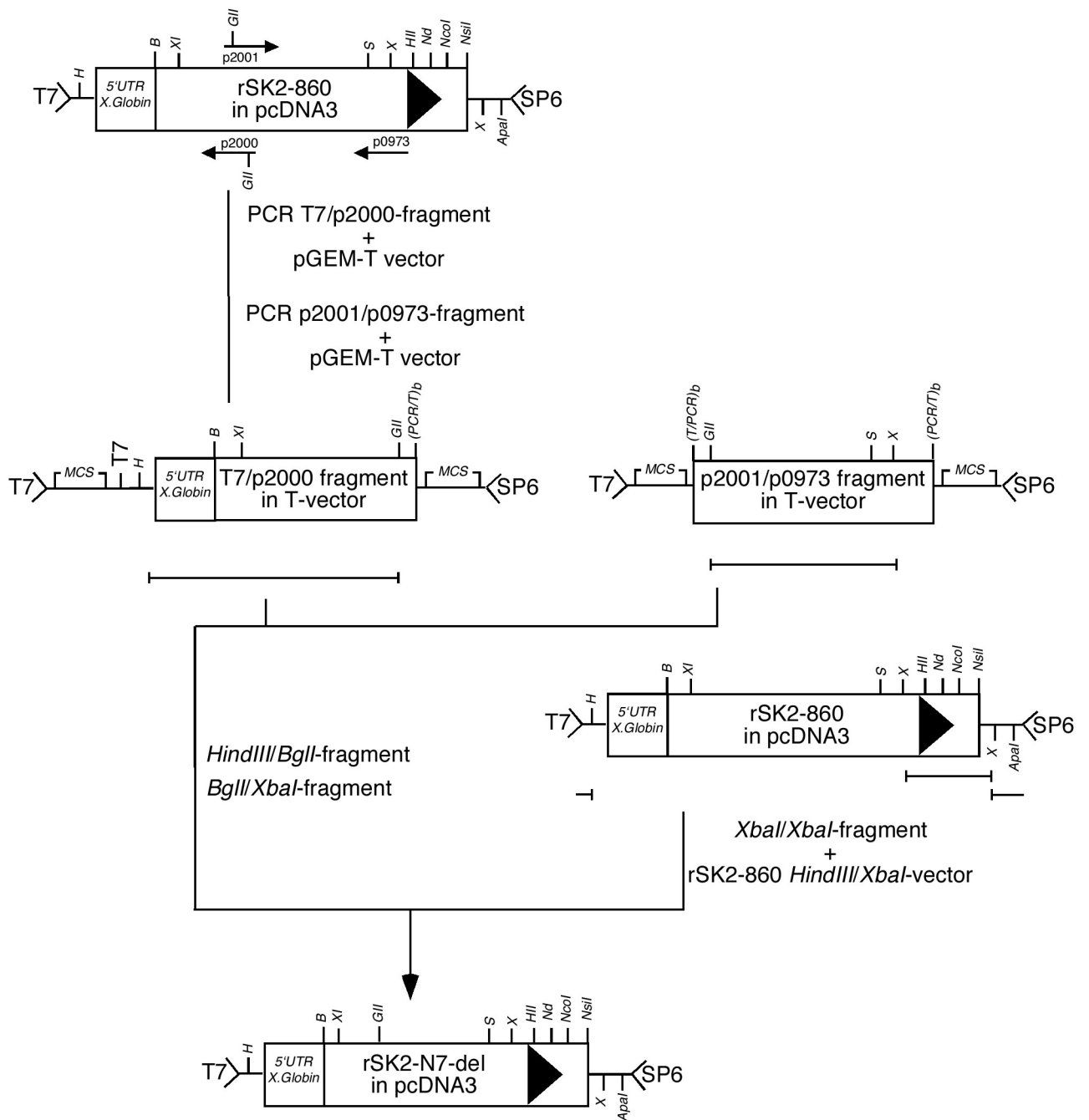
rSK2-695 in pcDNA3



rSK3_{NrSK2-860} in pcDNA3

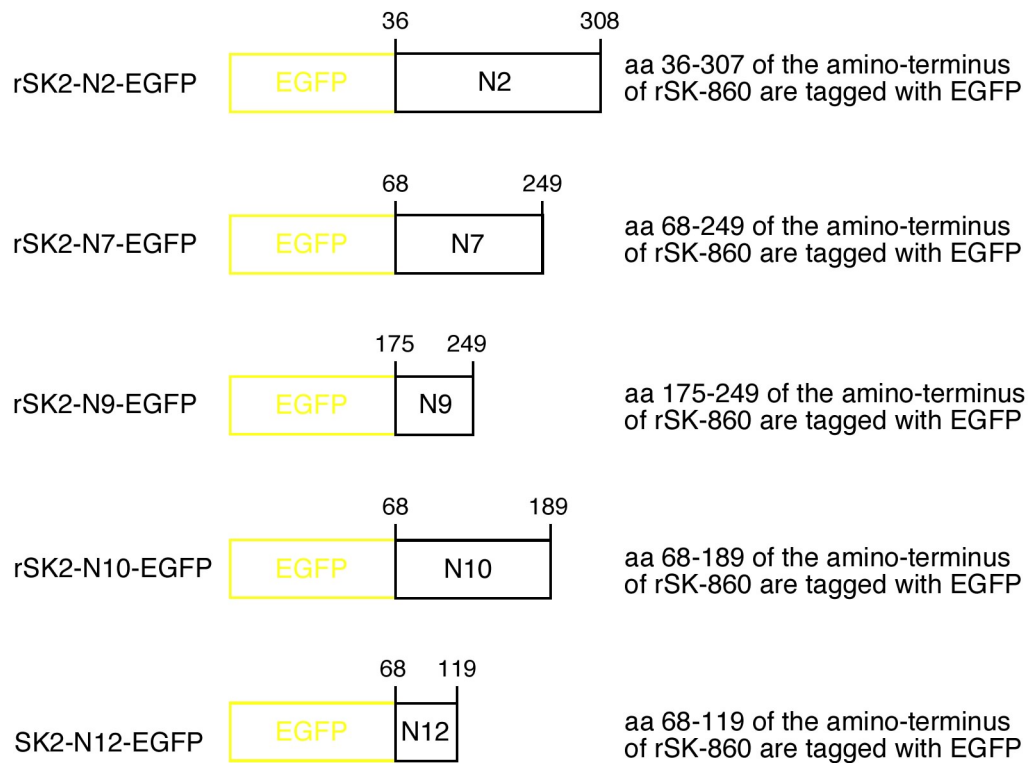


rSK2-N7-del in pcDNA3

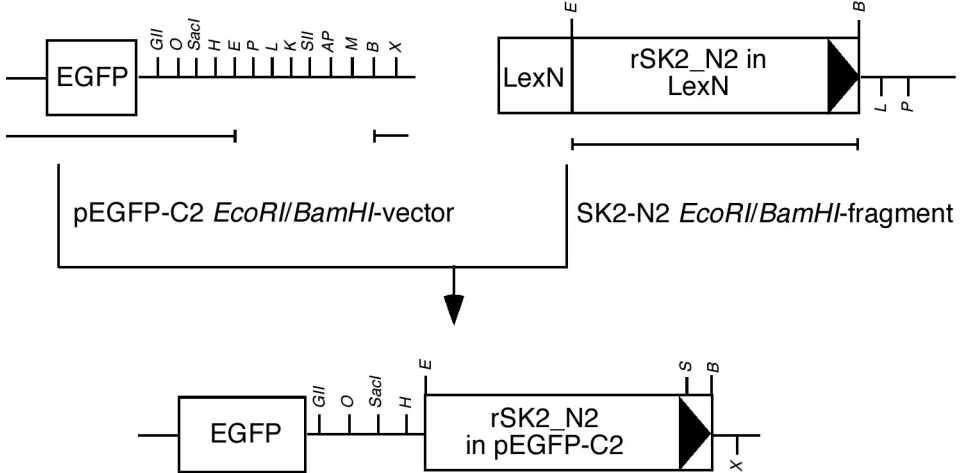


EGFP constructs of amino-terminal regions of rSK2-860

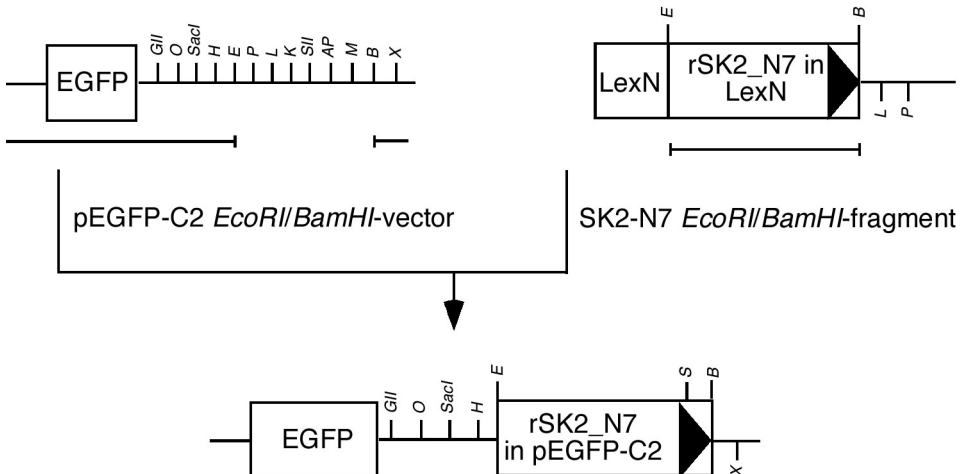
Overview of the EGFP tagged amino-terminal rSK2-860 constructs. Corresponding amino acid sequences are presented in the appendix .



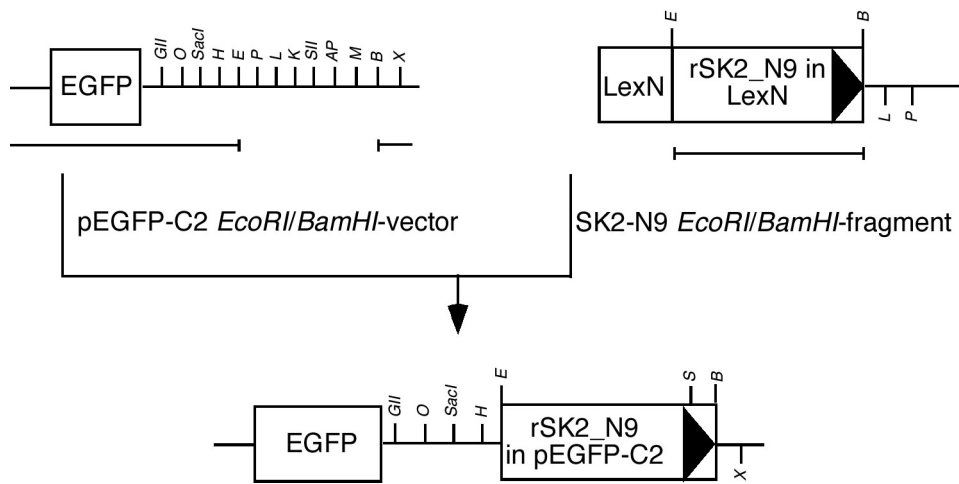
rSK2-N2 in pEGFP-C2



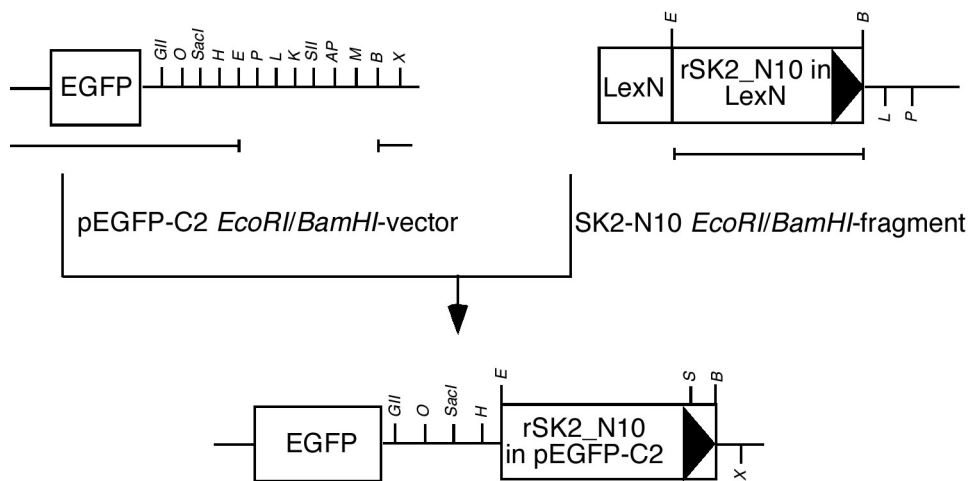
rSK2-N7 in pEGFP-C2

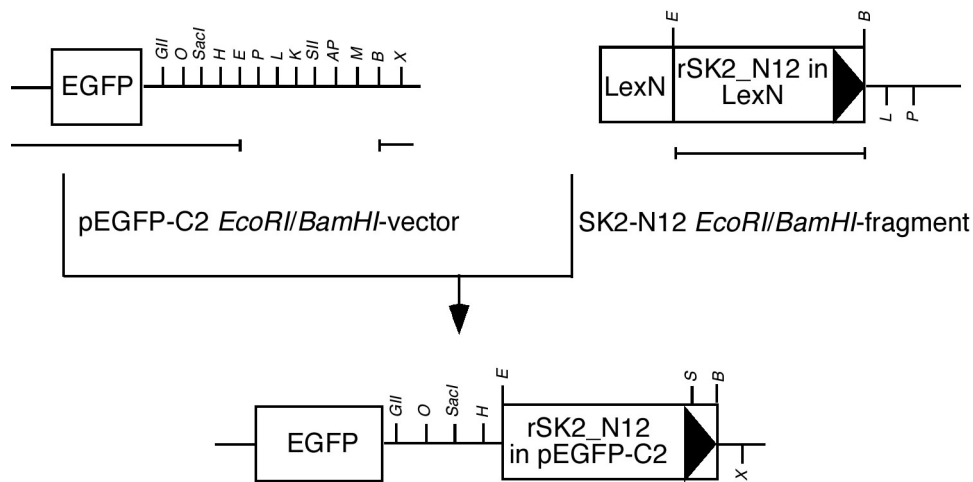


rSK2-N9 in pEGFP-C2



rSK2-N10 in pEGFP-C2



rSK2-N12 in pEGFP-C2

2.2.2.15 DNA sequencing

Purified plasmid DNA was sequenced using the BigDye terminator cycle sequencing kit combined with automated sequencing (ABI 377 and ABI 310 sequencers, ABI Perkin Elmer).

The sequencing reaction was performed in a total volume of 10 μ l containing 200 ng DNA, 2 μ l BigDye, 3.2 μ M primer and H₂O. The reaction was started with 1 min denaturation at 96°C followed by 25 cycles of denaturing (30 sec at 96°C), annealing (15 sec at 50°C) and an extension step (4 min at 60°C) in an AB GeneAmp PCR system 2400. The reaction was stopped by cooling to 4°C. The PCR product was precipitated by mixing 2 μ l NaAc (3M pH 4.6) and 50 μ l EtOH_{abs} for 10 min on ice. The mixture was centrifuged for 15 min at 4°C at max speed. Supernatant was discarded and 75% EtOH was added. Second centrifugation was performed for 5 min at 4°C maximum speed. Ethanol was removed and the pellet was air dried and resuspended in 4 μ l (for ABI 377) or 10 μ l Hi-Di formamide (for ABI 312) loading buffer. Samples were heated for 2 min at 93°C before loading on the sequencing gel.

2.2.3 Immunocytochemistry

2.2.3.1 Coating coverslips

Coverslips (22x22 mm) were washed for 45 min with absolute ethanol, rinsed three times with 75% ethanol and followed by baking for 6 hours at 200°C. Before use, the coverslips were coated for 10-60 min with poly-D-lysine (1 mg/10 ml) and rinsed three times with sterile water.

2.2.3.2 Immunofluorescence

Transiently transfected cells were plated onto poly-D-lysine coated coverslips 24 hours after transfection and incubated at 37°C (5% CO₂, 95% air) overnight. Cells expressing stably hSK1, rSK2 and rSK3 were plated on treated coverslips 24 hours before immunofluorescence was performed. HEK cells were grown in medium without serum in order to obtain nicely shaped cells the following day. CHO and COS cells were grown in the presence of serum. After overnight incubation, coverslips were processed by rinsing the cells three times with 1xPBS followed by fixation for 10 min with 4% PFA. Subsequently the cells were washed 2 times with PBS, permeabilized in 0.2% Triton X-100 in PBS for 2 min and washed 4 times for 5 minutes. Only for the experiments where the anti-Ubiquitin antibody was used, the cells were fixed for 10 min with cold methanol (-20°C) at RT followed by a 4 washing steps of 5 min each. Then the cells were transferred to a humidified box and incubated in blocking buffer at 37°C for 30 min. Afterwards, the blocking buffer was replaced by the primary antibody: 1/500 anti-NSK1, 1/1000 anti-NSK2, 1/500 anti-CSK2, 1/1000 N7-SK2 or 1/500 anti-NSK3, diluted in blocking solution. For colocalisation experiments the anti-SK channel antibodies were used in combination with anti-bodies against cellular markers; 1/1000 Lamin A/C, 1/1000 anti-Ubiquitin or 1/200 anti-Vimentin. The primary antibodies were applied to the cells for 1 hour at 37°C. The coverslips were washed 3 times for 5 min and the secondary antibody, fluorescein-linked donkey anti-rabbit antibody (1/500 dilution), Cy3-conjugated Goat anti-rabbit, Cy3-conjugated Goat anti-mouse or Cy5-conjugated Goat anti-rabbit, diluted in blocking buffer was applied. Cells were incubated for 30 min at 37 °C. Cy-conjugated antibodies were applied in 1/600 dilution onto the cells. Finally the cells were washed three times 5 min with PBS in the dark. Following the last washing step the cells were mounted with “Prolong” or “Slowfade” anti-fading solution. After the solution had dried the coverslips were sealed with nail polish. The immunostaining was visualized with a fluorescence microscope and pictures were taken with a CCD camera or a confocal microscope (filter settings for the confocal microscope are illustrated in the appendix).

2.2.4 Electrophysiology

2.2.4.1 Introduction

The patch-clamp technique was developed by the Nobel Prize winners Neher and Sakmann in the seventies (Neher and Sakmann, 1976, Hamill et al., 1981) and is used to measure

currents flowing through ion channels. In the voltage clamp mode a voltage is imposed on the patch on the cell under investigation and the changes in the current response are recorded. This configuration is commonly used to investigate ion channels. The method has been improved throughout the years, resulting in the establishment of different recording configurations (Fig 2.2 and point 2.2.4.3).

2.2.4.2 Electrophysiology recording equipment

The setup

The recording setup consists of a fluorescence microscope (Zeiss, axiovert 200) which is mounted on an air-table (TMC) in order to reduce the vibrations. Microscope and air-table are surrounded by a Faraday cage (custom made) to reduce the electrical noise from surroundings. A special carrier plate is mounted onto the microscope, in which the measuring chamber containing the cells is placed. The patch electrode is fixed in a holder which is connected to the headstage. An electrical micromanipulator (Luigs and Neumann) was used to control the movements of the patch electrode. Recordings were performed with an EPC9 patch-clamp amplifier (HEKA) using the acquisition software Pulse (HEKA) on a Macintosh computer.

Patch pipettes

Borosilicate glass (Kimax) was pulled using a vertical patch electrode puller, resulting in patch pipettes with a tip diameter of 2-3 μm . The pipettes were filled with intracellular solution (see material and methods 2.1.10) and showed a resistance of 2-3 MOhm. A chlorided silver wire inside the patch pipette formed an Ag/AgCl electrode allowing ionic currents flowing in the patch pipette solution to be seen as electrical currents by the headstage.

Electrical circuit

To measure the ionic currents, a second Ag/AgCl pellet in the recording bath is connected to the headstage ground point and completes the circuit from the bath solution to the headstage and back to the bath (Fig 2.1). To measure current flowing through ion channels expressed in the cell membrane, the cell can be approached in different ways, resulting in the formation of different patch configurations.

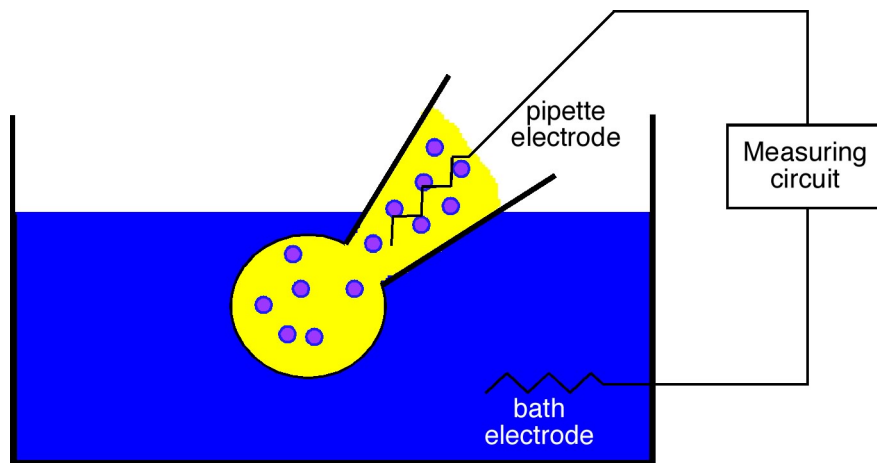


FIG 2.1 Electrical circuit. The current will flow in a closed circuit between the pipette electrode and the bath electrode. [adapted from The Axon Guide]

2.2.4.3 Patch-clamp measurement configurations

There are four basic patch-clamp recording configurations: cell-attached, inside-out, outside-out and whole cell patch. The first three configurations are mainly used to measure single channel currents in membrane patches, while the fourth is used to record currents through the whole cell membrane.

In order to obtain one of these configurations, a patch pipette (2-3 μm), filled with a salty intracellular solution, is lowered into the bath solution (extracellular solution, see 2.1.10). Before the patch pipette comes into contact with the extracellular solution a small positive pressure (pipette pressure between 7-12 cm H₂O) is applied to the patch pipette by giving a short blow into a tube which is in contact with the patch pipette. The positive pressure prevents the clogging of the patch pipette when it is lowered into the extracellular solution. Then the pipette tip is brought gently against the cell membrane, the positive pressure is released and immediately followed by a negative pressure (pipette pressure between -25 and -35 cm H₂O), resulting in the formation of a tight seal between the patch pipette and the cell membrane, also called gigaohm seal (normally ranging between 1-4 GOhm). This configuration is called the cell-attached patch configuration. When the cell-attached configuration is obtained, the pipette can be pulled away and the patch of membrane can be excised from the cell, forming the inside-out patch configuration. In this configuration the internal surface of the cell membrane is exposed to the bath solution. Another possibility after obtaining the cell-attached configuration is to disrupt the membrane patch, which was preventing the intracellular solution in the pipette to diffuse into the cell, by applying short pulses of suction (by mouth). This configuration is called the whole-cell patch recording. The last configuration, the outside-out patch configuration, is formed from the whole-cell configuration by simply pulling the pipette very slowly away from the cell.

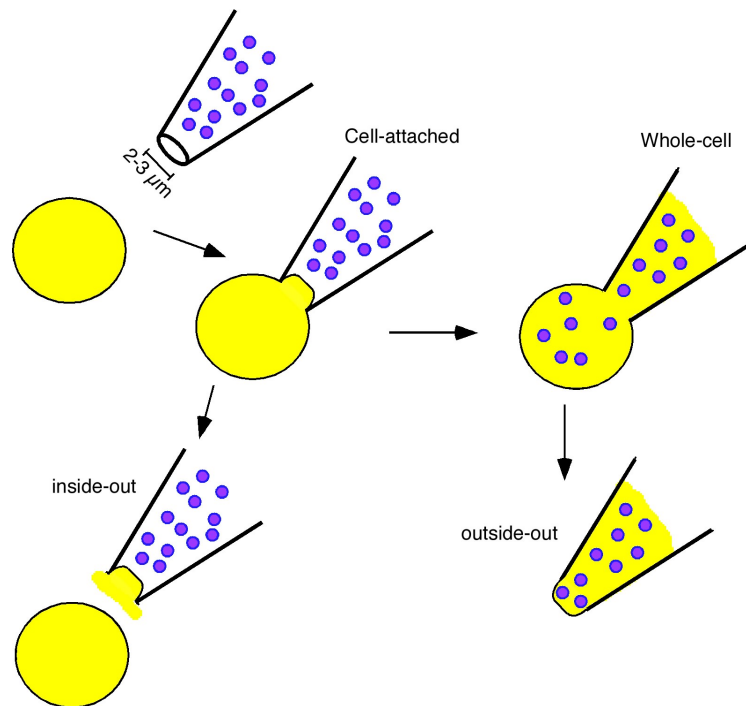


FIG 2.2 Simplified patch-clamp configuration. The cell-attached configuration is obtained when the pipette tip makes a tight seal on the cell membrane. Pulling back a patch of the cell membrane leads to the inside-out configuration. Alternatively, disrupting the membrane patch results in the whole-cell configuration. By withdrawing slowly the pipette from the whole-cell configuration, a small vesicle can be formed on the pipette tip resulting in the outside-out configuration. Blue circles represent the free calcium ions (normally $1 \mu\text{M}$ free calcium was in the pipette).

2.2.4.4 Recording of cells expressing channels

Preparation of cells for recording

Cells stably expressing hSK1, rSK2, rSK3 or transiently expressing the constructs of interest were plated on 10 mm coverslips. Then the coverslips were placed back in the incubator for 12-16 hours, in order to let the cells attach to the coverslips. The following day the coverslips were transferred one at a time to a customized recording chamber.

Measuring of the channels

SK channels and related constructs (SK chimeras) were measured in the whole-cell patch-clamp configuration (see patch-clamp measurement configuration). In the whole-cell configuration, the intracellular “pipette” solution diffuses into the cell after disrupting the membrane patch under the pipette tip. The intracellular solution contained, in the majority of the

experiments, 1 μM free calcium which is a saturating concentration to activate the calcium-dependent, voltage-independent SK channels (EC_{50} is 300 nM, Xia et al., 1998, Hirschberg et al., 1998). The amount of free calcium was calculated using the program Eqcal (Biosoft). In order to see a current we applied voltage changes (see further for ramp and step protocols) which changed the driving force for the ions.

SK currents were elicited using two different stimulation protocols, ramps and steps. The first and mostly used protocol was the ramp protocol (Fig 2.3A): currents were evoked by clamping the membrane potential from the membrane holding potential (V_m) to -100 mV followed by a 400ms-long ramp to $+40$ mV and returning to V_m for 10ms. This protocol was applied every 10 s. In the step protocol (Fig 2.3B), currents were elicited by the application of 30ms-long voltage steps from -100 mV to $+40$ mV with increments of 20 mV.

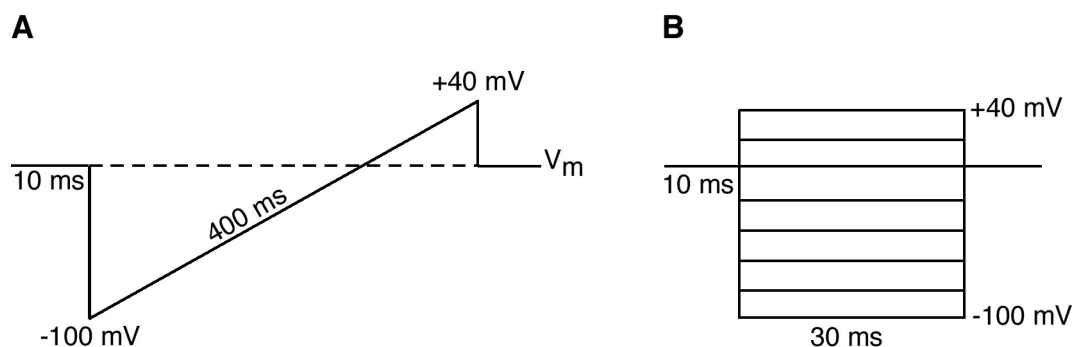


FIG 2.3 Schematic overview of the protocols. A, representation of the ramp protocol. The ramp was elicited after holding the cell for 10 ms at the membrane potential, followed by changing the voltage from -100 mV to $+40$ mV over a time span of 400 ms and then stepped back to the membrane potential for 10 ms, this was repeated every 10 sec. B, Overview of a step protocol, starting from the holding potential, 30 ms pulses are applied from -100 mV to $+40$ mV with increments of 20 mV.

The majority of experiments are performed in symmetrical conditions (similar potassium concentrations inside and outside the cell). The intracellular solution contained 130 mM K^+ while the extracellular solution contained 144 mM K^+ , this results, according to the Nernst equation in a reversal potential of ~ 0 mV, and represented in the figures by the ramp crossing x-axis (current, expressed in nanoAmpere, versus voltage, expressed in millivolt) at 0 mV. When testing the effect of tamapin, we also used asymmetrical conditions (different potassium concentrations inside and outside) to determine the effect of extracellular potassium on the binding of tamapin to the channel. Under this condition, the intracellular solution contained 130 mM K^+ but the extracellular solution was changed to 20 mM K^+ , resulting in a reversal potential of approximately -47 mV, seen in the figures by the ramp trace crossing the x-axis at approximately -47 mV. Furthermore, all experiments were finished by changing the extracellular solution to a solution with minimal K^+ concentration (4 mM K^+), resulting in a

reversal potential of approximately - 80 mV. This gave use an indication of the stability of the seal of the cell after the recordings had been made and the residual K⁺-dependent leak current. All these reversal potentials for the different K⁺ concentrations were estimated using the Nernst equation:

$$E_{\text{rev}} = \frac{RT}{F} \ln \frac{C_o}{C_i}$$

with E_{rev} ; reversal potential, R; the gas constant, T; absolute temperature, F; the Faraday constant, C_o ; potassium concentration outside and C_i ; potassium concentration inside.

Toxins and drugs were diluted in the extracellular solution and applied to the cell 3-5 minutes after obtaining a stable current baseline. After maximal block had occurred, the extracellular solution was replaced by solution without drugs, to allow for wash-out and to monitor the recovery of the current.

Data were sampled at 20 kHz and filtered at 5 kHz.

2.2.4.5 Data analysis

Data were acquired using the Pulse/Pulsefit software (HEKA electronic, Germany) and analyzed with Igor.

All the obtained data had to be corrected for the voltage error before we determined the IC₅₀ values. Correction for the voltage error was needed due to the very large currents we recorded, therefore we assumed a simple circuit called the voltage divider (Fig 2.4).

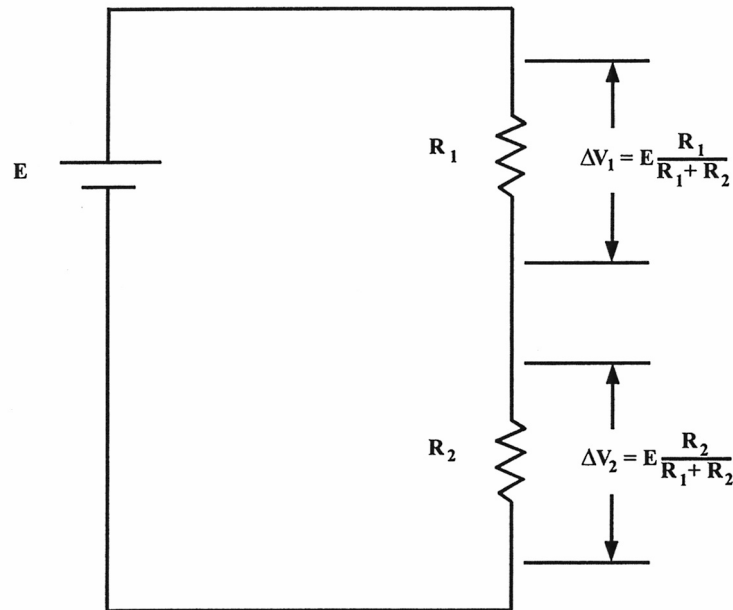


FIG 2.4 Overview a the circuit of a voltage divider in which two resistors are connected in series. R_1 and R_2 can be regarded as the pipette and cell resistance respectively. R_1 causes a voltage drop resulting in the application of a voltage to the cell which differs from the originally applied potential [adapted from The Axon Guide].

This circuit describes the proportion of the total applied voltage to the pipette and the cell membrane. Using this approach we could determine the voltage which was really applied to the cell membrane, presented in the figure by ΔV_2 . ΔV_2 can be obtained from the formula:

$$\Delta V_2 = E \frac{R_2}{R_{\text{tot}}}$$

with E; the applied voltage, $R_{\text{tot}} = E / \text{Amplitude}$ (comes from the Ohms law $V=IR$) and $R_2 = R_{\text{tot}} - R_1$ with R_1 the pipette resistance.

To determine the IC_{50} values (half maximal block of the channels) of apamin and d-tubocurarine on the stable cell lines, the following formula was used:

$$IC_{50} = \frac{\frac{I}{I_{\text{max}}} \times [\text{toxin}]}{\left[1 - \frac{I}{I_{\text{max}}} \right]}$$

with I_{max} ; the maximal current before block, I; current after maximal block had occurred and [T]; toxin concentration.

To determine the IC_{50} value for tamapin on the stable cell lines, the dose-respons curve was fitted with the DoseRespons function:

$$\frac{I}{I_{\max}} = \frac{1}{1 + \left[\frac{[\text{tamapin}]}{IC_{50}} \right]^n}$$

with I_{\max} ; the maximal current before block, I; current after maximal block had occurred; [tamapin]; tamapin concentration and n; the Hill coefficient

3 Results

3.1 Characterization of stable cell lines expressing SK channels

3.1.1 Immunocytochemistry

3.1.1.1 rSK2 α -subunit expression in HEK-293 and CHO-FlpIn cells

Cell lines stably expressing ion channels are useful: 1) to screen for different drugs; 2) to determine the interaction of the expressed subunit with other α -subunits and examine how this influences the pharmacological properties of the channel; 3) or to generate dominant negative α -subunits, which will then eliminate or reduce the current (current density, amount of current per surface area) elicited by the channels expressed in the stable cell lines. The advantage of stable cell lines is that every cell expresses the relevant ion channel, in our case one of the small conductance calcium-activated potassium (SK) channels. HEK-SK2 and HEK-SK3 stable cell lines were generated by transfecting HEK-293 cells with rSK2 or rSK3 (see material and methods). Each HEK-SK2 and HEK-SK3 cell line was generated from a single cell, guarantying genetically identical cells. To verify the stable expression of the rSK2 protein in HEK-293 cells, specific rabbit antibodies against the amino- and carboxy- terminus of rSK2 were used. Fig 3.1A shows the localization of the α -subunit, a membrane and cytoplasmic stain was observed when cells were incubated with the amino-terminal antibody (anti-NSK2), and similar results were obtained when the same cell line was incubated with the carboxy-terminal antibody (anti-CSK2) (Fig 3.1D). No signal was observed when the anti-NSK2 and anti-CSK2 antibodies were used on untransfected HEK-293 cells (Fig 3.1B, C, E and F). In all these experiments, a Cy3-conjugated goat anti-rabbit secondary antibody was used.

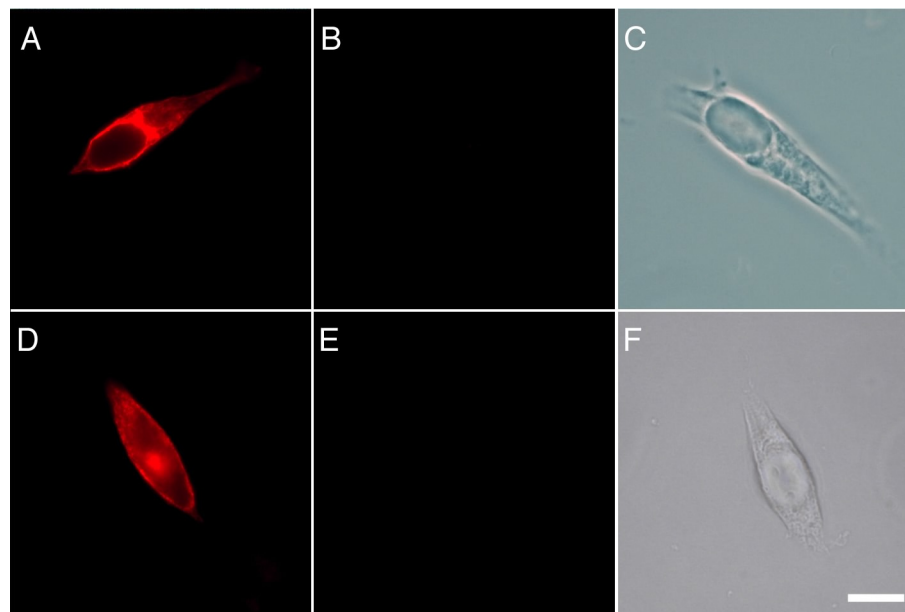


FIG 3.1. Immunofluorescence of HEK-293 cells stably expressing rSK2. A, Staining of rSK2 with the amino-terminal antibody, anti-NSK2 (1/1000 dilution). B, Empty HEK-293 cells exposed to the same antibody, no signal was detected. C, Bright field picture of cell reported in B. D, Immunofluorescence staining with the anti-CSK2 antibody (1/1000 dilution). E, Empty HEK-293 cell treated with the carboxy- terminal antibody, no signal was detected. F, Bright field picture of cell in E. A-F, the secondary antibody was Cy3-conjugated (1/600). Scale bar: 10 μm .

In order to determine if the host has no influence on the expression and properties of the SK2 α -subunits, a second stable cell line was generated in CHO cells by using the FlpIn system. FlpIn-CHO cells contain a single integrated Flp Recombination Target (FRT) site in the cell genome. Cells were transfected with a FlpIn expression vector containing the gene of interest (rSK2, rSK3 or hSK1) and the Flp recombinase expression plasmid. Stable cell lines expressing the channels were grown in a selection medium containing 100 $\mu\text{g/ml}$ hygromycin B. Expression of rSK2 in the CHO-FlpIn cells was tested by using anti-NSK2 (Fig 3.2A). No signal was detected when CHO-FlpIn cells stably expressing rSK2 were stained with an antibody directed against the amino terminus of rSK3 (anti-NSK3) (Fig 3.2B and C).

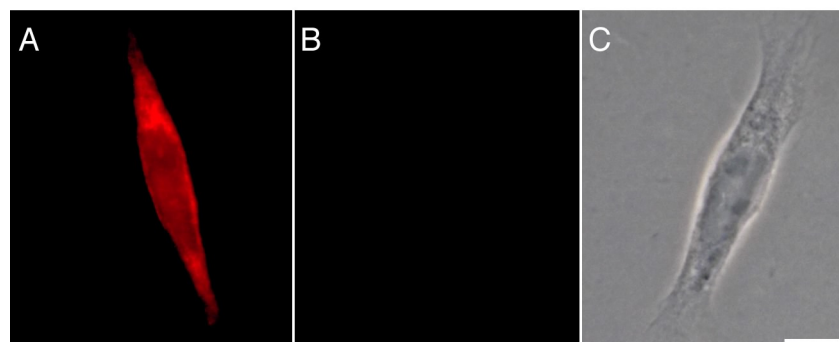


FIG. 3.2 CHO-FlpIn cells stably expressing rSK2. A, Immunostaining of rSK2 using the anti-NSK2 antibody (1/1000). B, CHO-FlpIn-SK2 cell incubated with antibody against the N-terminus of rSK3 (1/1000). C, Bright field picture of the cell shown in panel B. Scale bar: 10 μm

3.1.1.2 rSK3 α -subunit expression in HEK-293 and CHO-FlpIn cells

Throughout the generation of the SK3 stable HEK-293 cell lines, more than 10 independent SK3 expressing stable cell lines were generated. All of them were subjected to immunocytochemistry, and only one cell line was used for the experiments described on the following pages. This cell line had the highest expression level when the immunostaining was compared to the other generated rSK3 stable cell lines.

Stable expression of the rSK3 protein in HEK-293 was examined using an anti-SK3 carboxy terminal antibody (anti-CSK3), directed against a short specific C-terminal SK3 peptide. The secondary antibody used for this experiment was conjugated with fluorescein isothiocyanate. Fig 3.3A reveals a clear membrane stain when cells were incubated with the anti-CSK3 antibody. However, when the same conditions were used for empty HEK-293 cells, no immunostain was observed (Fig 3.3B).

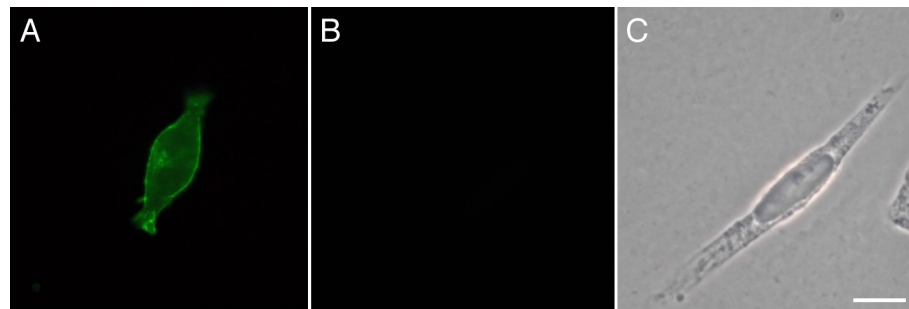


FIG 3.3. Immunostaining of HEK-SK3 stable cell line. A, Specific SK3 staining by the anti-CSK3 antibody. B, Control experiment of HEK-293 cells with the anti-CSK3 antibody, no signal was observed. C, Bright field picture of same cell as in B. Scale bar: 10 μ m

Stable expression of rSK3 in CHO-FlpIn cells was tested by using the same anti-CSK3 antibody (Fig 3.4 A), resulting in the detection of a signal in the stable expressing cells, while empty CHO-FlpIn cells did not show any signal (Fig 3.4B).

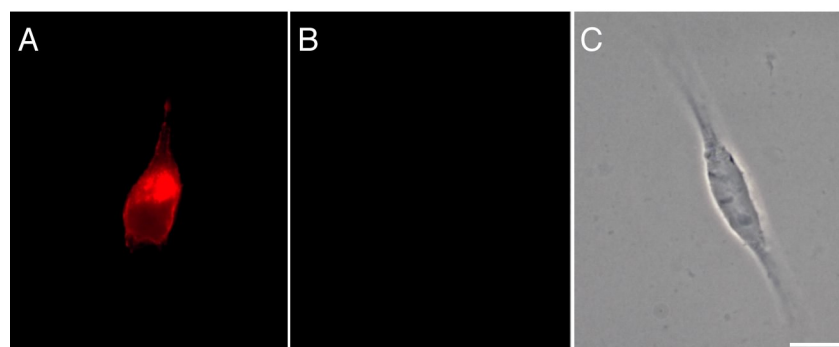


FIG 3.4. Immunostaining of CHO-Flp-SK3. A, Specific staining of rSK3 α -subunits in CHO-FlpIn cells using the anti-CSK3 antibody (1/500). B, Empty CHO-FlpIn cells treated with the anti-CSK3 antibody, no signal detected. C, Bright field picture of the same cell as in panel B. Scale bar: 10 μ m.

3.1.2 Pharmacology

3.1.2.1 Characterization of HEK-rSK2 stable cell line.

SK2 currents were activated by dialyzing the cell with $1\mu\text{M}$ free calcium and were recorded by applying ramp protocols from -100 mV to $+40\text{ mV}$ repeated every 10 sec (Fig 3.6A). Activation of rSK2 channels in HEK-293 cells is obtained by interaction of intracellular calcium with the constitutively bound calmodulin (CaM). Calcium was present in the patch pipette and diffused into the cell upon disrupting of the membrane patch, which was established after a formation of a gigaseal between the pipette tip and the cell membrane. The majority of the experiments were performed in high K^+ (144 mM) on the extracellular side of the cell. According to the Nernst equation, this would result in a reversal potential for K^+ of approximately -2 mV , as observed in the experiments. To control the stability of the cell patch, the experiment was finished by switching the extracellular solution to a more physiological solution, containing 4 mM potassium. This results in a change of the reversal potential to -80 mV and an I-V curve going through -80 mV could be observed (Fig 3.6A).

In the presence of a calcium concentration close to the physiological resting one (100 nM free calcium), SK2 channels were not activated. However, application of EBIO (1 mM), a compound known to enhance the calcium sensitivity of SK channels (Pedarzani et al., 2001), to the bath solution induced a robust activation of rSK2 current even at low calcium concentrations (Fig 3.5B). To examine if HEK-293 cells contained endogenous SK channels, EBIO (1 mM) was applied to the empty cells. No detectable current could be observed (Fig 3.5A), suggesting that the HEK-293 cells are not expressing any endogenous SK channels. A set of experiments using different concentrations of free calcium in the pipette showed that rSK2 channels were maximally activated when 500 nM free calcium diffused into the cell. EBIO was not able to increase any further the SK2 current in the presence of 500 nM calcium (Fig 3.5C). For this reason, in most experiments an intracellular solution containing $1\mu\text{M}$ free calcium was used. $1\mu\text{M}$ free calcium is a saturating concentration, presumably activating all the SK channels in the cell (Fig 3.5D).

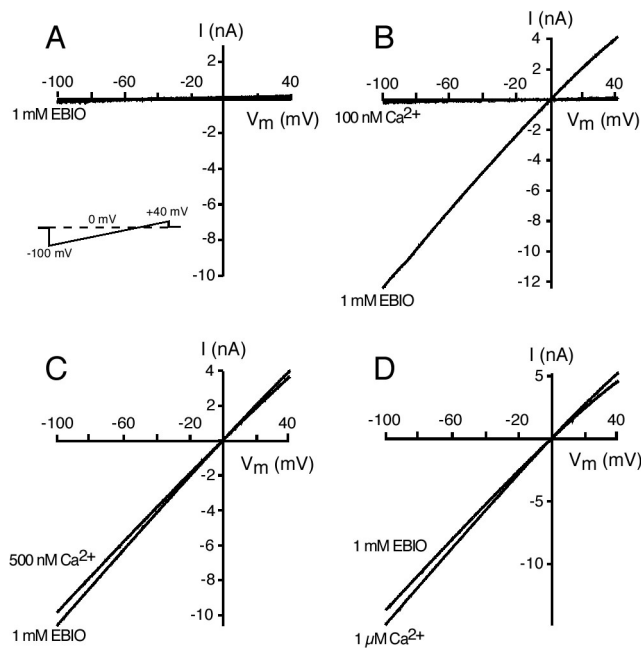


FIG 3.5. Calcium dependent activation of rSK2 channels. SK currents were recorded in symmetrical high K^+ conditions. A, Empty HEK-293 cells are not responding to the SK channel enhancer, EBIO. Inset: ramp protocol, 400 ms ramps from -100 mV to $+40$ mV are repeated every 10 sec. B, HEK-293 cells stably expressing rSK2 are not activated by 100 nM Ca^{2+} , but in the presence of 1 mM EBIO a SK2 current can be observed. C, 500 nM free Ca^{2+} maximally activates SK2 channels. In the presence of this calcium concentration, EBIO did not further increase the current. D, EBIO did not increase the amplitude of SK2 currents at the saturating Ca^{2+} concentration of 1 μM .

SK currents can be blocked by several SK channel blockers. One of the most commonly used and well characterized SK channel blockers is apamin. Apamin has been shown to block SK2 channels with high affinity, with an IC_{50} varying in different studies between 27 and 140 pM (see table 1 in Introduction). Application of 100 pM apamin reduced the SK2 current to $32.2 \pm 2.48\%$ of its original amplitude ($n=3$). The calculated IC_{50} was 47.3 ± 4.9 pM (Fig 3.6B).

d-Tubocurarine (dTC), a small organic compound, also reduced rSK2 currents. 10 and 20 μM dTC reduced the SK2 current by 64.5 and 84.2% respectively (Fig 3.6C). The calculated IC_{50} was 5.1 ± 0.3 μM ($n=6$). IC_{50} values for dTC reported by other groups varied between 2.4 and 17 μM (see table 2 in Introduction).

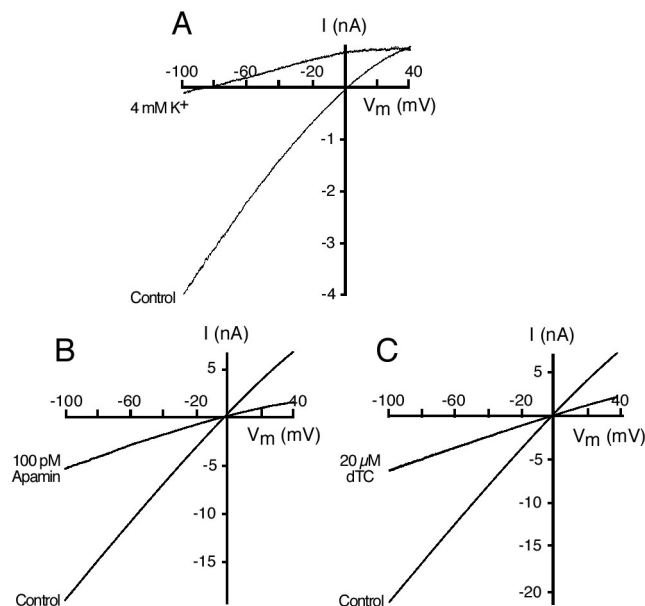


FIG 3.6. Pharmacological characterization of SK2 currents. A, Typical current elicited by a ramp protocol from -100 mV to 40 mV. Application of 4 mM extracellular K^+ , results in a left wards shift of the reversal potential to -80 mV. B, Reduction of the SK2 current (control) upon application of apamin (100 pM). C, Inhibition of rSK2 current by d-tubocurarine (20 μ M).

3.1.2.2 Characterization of HEK-rSK3 stable cell line

To characterize SK3 channels with respect to their basic pharmacology, the channels were expressed in HEK-293 cells. SK3 currents were activated by a pipette solution having 1 μ M free calcium. Fig 3.7A shows the whole-cell current elicited by a voltage ramp in symmetrical high K^+ solutions. The inward current was reduced by application of low K^+ outside resulting in a small background inward K^+ current.

Application of apamin to the extracellular solution resulted in a reduction of the rSK3 current (Fig 3.7B). 100 pM and 500 pM apamin reduced the currents by 76% ($n=3$) and 83.2% ($n=6$), respectively. The calculated IC_{50} of apamin for rSK3 channels was 95.6 ± 28.4 pM. To further characterize the cell line, the sensitivity for d-tubocurarine was measured using 10 and 20 μ M dTC (Fig 3.7C). Application of 10 μ M dTC reduced the rSK3 current by 30.1% , 20 μ M dTC by 45.9% . The calculated IC_{50} of dTC for rSK3 channels was 28.3 ± 6.2 μ M ($n=6$).

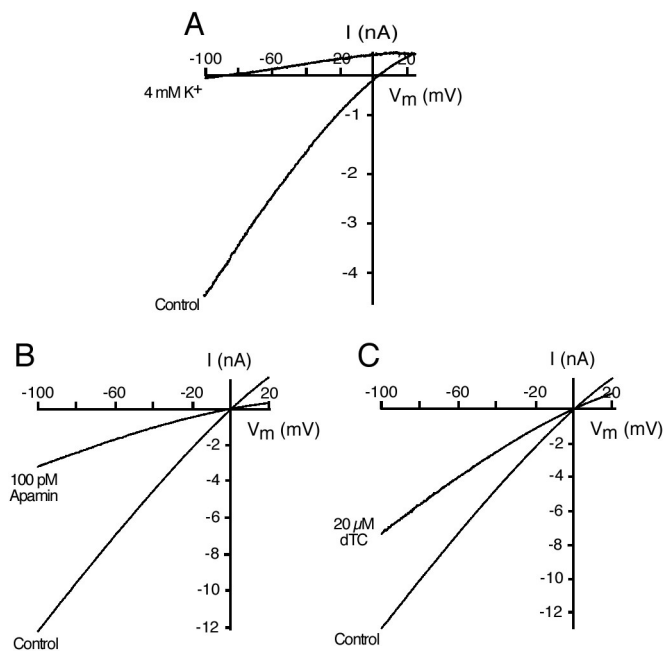


FIG 3.7. Expression of rSK3 in HEK-293 cells. A, rSK3-current recorded upon application of voltage ramps from -100 mV to $+40$ mV. B, Inhibition of rSK3-current by 100 pM apamin. C, 20 μ M dTC reduced the current by 45.9% .

3.1.2.3 Characterization of CHO-Flp-hSK1 stable cell lines

In recent years different groups have shown that expression of hSK1 in mammalian cell lines gave rise to apamin-sensitive channel (Shah and Haylett, 2000, Strobaek et al., 2000). Although hSK1 can be blocked by apamin, it is the least sensitive SK subunit, with IC_{50} values between 0.7 - 12 nM (see table 1 in Introduction). Thus, SK1, 2 and 3 channels can be distinguished on the basis of their different level of apamin sensitivity.

hSK1 channels stably expressed in CHO-FlpIn cells were activated by dialyzing the cells with 1 μ M free calcium. As previously shown for rSK2 and rSK3, the hSK1 current was elicited by voltage ramps from -100 mV to $+40$ mV. When the extracellular high K^+ solution was exchanged for high Na^+ solution, the hSK1 inward current was decreased, demonstrating a high selectivity for K^+ over Na^+ of hSK1 (Fig 3.8A). Application of low K^+ solution leaves a small inward potassium current.

10 nM apamin blocked $65.1 \pm 4.1\%$ of the initial hSK1 current (Fig 3.8B). The IC_{50} value was 6 ± 1.3 nM ($n=5$).

d-Tubocurarine (50 μ M) blocked the hSK1 current by 66% (Fig 3.8C). The estimated IC_{50} value was 23.8 ± 2.8 μ M ($n=5$).

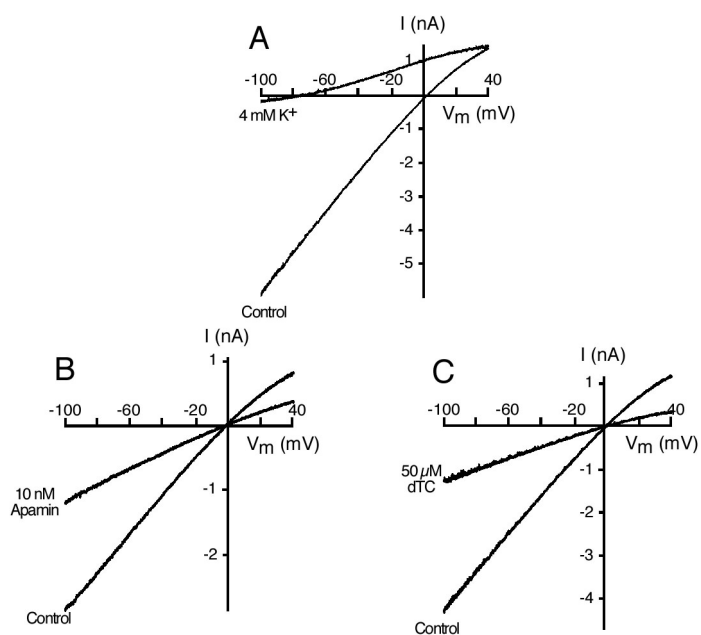


FIG 3.8 Characterization of CHO-FlpIn cells expressing hSK1. A, hSK1 current elicited by application of voltage ramps from -100 mV to $+40$ mV. 4 mM K^+ decreased the inward current dramatically and shifted the reversal potential to -80 mV. B, Inhibitor of hSK1 current in the presence of 10 nM apamin. C, 50 μ M dTC blocked 66% of the hSK1-current.

3.2 Tamapin: a venom peptide from the Indian red scorpion (*Mesobuthus tamulus*) which targets SK channels.

3.2.1 Introduction

The Indian red scorpion (*Mesobuthus tamulus*) causes annually a large number of deaths, especially among young children on the Indian subcontinent. Its venom has been a rich source for highly specific potassium channel blockers such as iberiotoxin and tamulustoxin (Galvez et al., 1990, Strong et al., 2001). The venom was screened for other selective ion channel blockers and one of the isolated peptides proved to be highly efficient in inhibiting the binding of monoiodo-¹²⁵I-apamin to rat brain synaptic plasma membranes (Pedarzani et al., 2000). This last technique is well established and commonly used to determine the presence of SK channel blockers in venoms.

Two active peptides, tamapin and tamapin-2 were isolated. Both are 31 amino acids long and tamapin-2 differs by a single amino acid residue from tamapin. Tamapin and tamapin-2, contain at position 31 a tyrosine and a histidine, respectively. Tamapin shares 77% amino acid sequence similarity with scyllatoxin and contains six cysteine residues at the same positions (Fig 3.9). Scyllatoxin was isolated from the scorpion *Leiurus quinquestriatus* and is a SK channel blocker which has an IC_{50} of 240 pM for rSK2 channels (Castle and Strong, 1986, Auguste et al., 1990, Cao et al., 2001; see table 2 in Introduction).

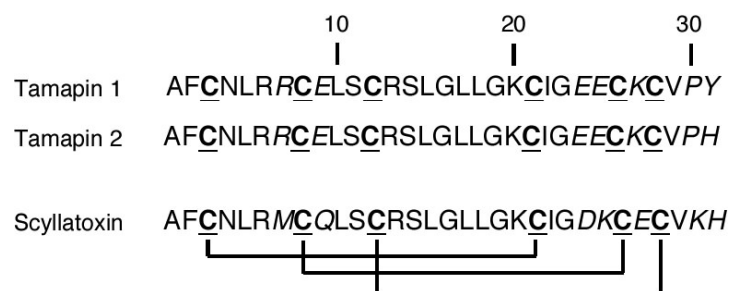


FIG 3.9. Alignment of tamapin, tamapin-2 and scyllatoxin. All 3 toxins are 31 amino acids long and contain at the same positions the cysteines (bold and underlined). Different amino acids between tamapin and scyllatoxin are given in italic.

Knowing that tamapin was able to displace ¹²⁵I-apamin and that it shared a high similarity with scyllatoxin, it was of great interest to determine the specificity and efficiency of tamapin in blocking the different cloned SK channels.

3.2.2 Effect of acetonitrile on SK α -subunit

The concentrated stock of purified tamapin ($2 \mu\text{M}$) was stored in a 30% acetonitrile solution. Therefore, as control the maximal concentration of acetonitrile (0.3%) to which the cells were exposed during tamapin application was applied ($n=9$, 3 for each SK channel subtype). No significant effect of acetonitrile on the SK currents was observed (Fig 3.10).

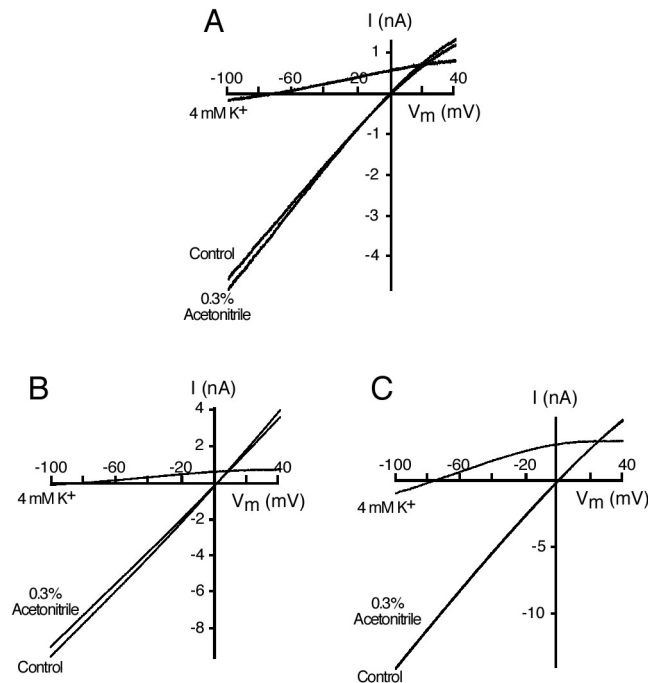


FIG 3.10. Effect of 0.3% acetonitrile on cells stably expressing SK channels. SK currents were elicited by applying a ramp from -100 to $+40$ mV, channels were activated by dialyzing the cells with $1 \mu\text{M}$ free calcium. No effect of 0.3% acetonitrile was observed on CHO-FlpIn cells expressing hSK1 (A), HEK-293 stably expressing rSK2 (B) and rSK3 (C).

3.2.3 Effect of tamapin on rSK2 channels stably expressed in HEK-293

rSK2 channels were activated by dialyzing the cell with intracellular solution containing $1 \mu\text{M}$ free calcium, as previously described. All the experiments were performed in symmetrical conditions (144 mM K^+ outside). SK2 currents were elicited by applying voltage ramps or voltage steps.

Fig 3.11A shows that in the presence of 500 pM tamapin the rSK2 current was dramatically reduced. The block was rather fast and partially reversible (Fig 3.11C). rSK2 currents elicited by voltage steps were likewise blocked by 500 pM tamapin (Fig 3.11B). In order to obtain the IC_{50} value for tamapin on SK2 channels, a range (1 pM to 10 nM) of different concentrations of tamapin were tested on HEK-rSK2 cells ($n=45$). After fitting the concentration-response curve with the Hill equation (see Methods), an IC_{50} value of 24 pM and a Hill coefficient of 1.0 were obtained (Fig 3.11D).

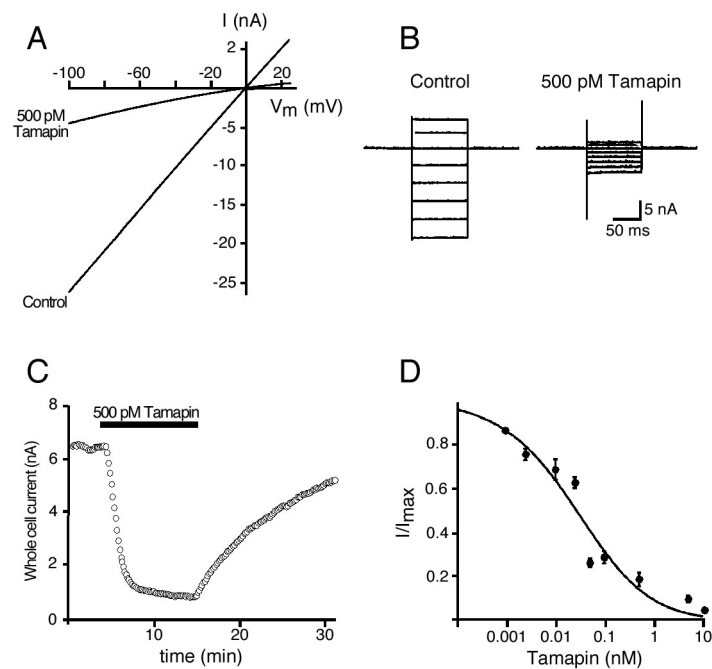


FIG 3.11. Effect of tamapin on rSK2 currents. A, The whole-cell SK2 current triggered by a voltage ramp, before and after addition of 500 pM tamapin. B, Example of the block by tamapin on the currents produced by voltage steps C, Current versus time plot for a single dose experiment in which 500 pM tamapin was applied to a rSK2 expressing cell during the time indicated by the bar. Fast block of rSK2 current followed by a partial wash-out. D, Concentration-response curve for tamapin on HEK-293 cells stably expressing rSK2.

3.2.4 Influence of external K^+ and voltage on tamapin block

To elucidate the influence of external potassium on toxin binding, the extracellular potassium concentration was lowered from 144 mM K^+ to 20 mM K^+ , by exchanging KCl with NaCl. As a result the equilibrium potential for K^+ shifted to a more negative value and was estimated to be around -49 mV. When the cell was held at -49 mV no net ion flux will occur instead at voltages above -49 mV an outward current was observed, and at more negative voltages an inward current occurred. Fig 3.12 presents rSK2 current through the activated rSK2 channels in an extracellular solution containing 20 mM K^+ after applying a ramp protocol. The channels were activated by 1 μ M free calcium. A profound inward rectification of the current at positive potentials was observed under these ionic conditions, as reported by Soh and Park (2001). Characteristic for the inward rectifying I-V relationship is the reduction or decrease of the current at potential more positive than the equilibrium potential. No further experiments were performed to explain this phenomenon.

Fig 3.12A shows that in the presence of 10 pM tamapin ($n=4$) the rSK2 current was reduced by 24% at -70 mV, 26% at 0 mV and 28% at 10 mV. After application of 100 pM (Fig 3.12B) only 29% current was left at -70 mV, 29% at 0 mV and 30% at 10 mV. The calculated

IC_{50} at the voltages -70mV , 0mV and 10mV were respectively $38.5 \pm 4.5 \text{ pM}$, $36.8 \pm 4.0 \text{ pM}$ and $35.4 \pm 4.3 \text{ pM}$ ($n=21$, 7 for each voltage). IC_{50} values at potentials higher than 10 mV were not calculated due to the pronounced inward rectification. Fig 3.12C shows a plot of the IC_{50} values obtained at different voltages in the symmetrical (full circles) and asymmetrical K^+ conditions (open circles). No significant difference was observed between the IC_{50} values in symmetrical and asymmetrical K^+ . This result suggests not only that the block was not voltage dependent, but also that it was not significantly influenced by external potassium.

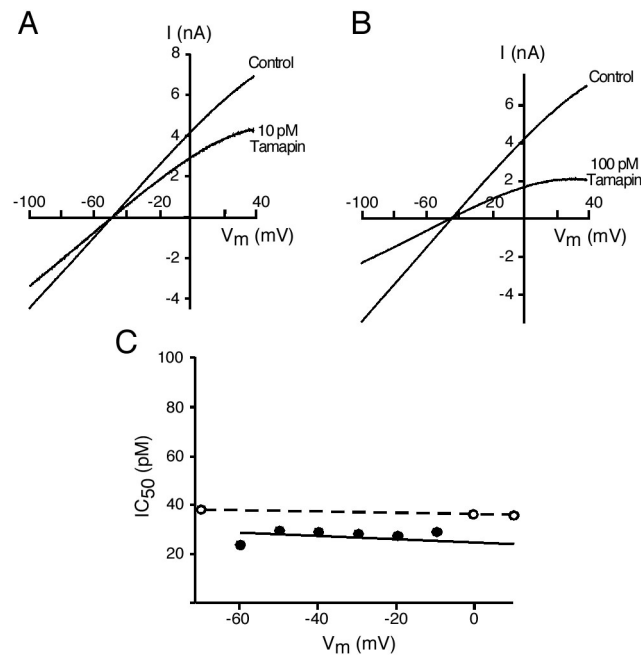


FIG 3.12. Voltage and potassium dependent block of rSK2 currents by tamapin. A, B, Effect of 10 pM and 100 pM tamapin on HEK-293 cells expressing rSK2. Measurements were performed under asymmetrical K^+ conditions and currents were elicited by application of voltage ramps. C, IC_{50} versus voltage plot. IC_{50} values in symmetrical K^+ conditions are shown as full circles, IC_{50} values in asymmetrical conditions are displayed as open circles. A regression line was fitted through the points.

3.2.5 Effect of tamapin on rSK3 and hSK1 expressing cell lines

To examine if the other SK α -subunits were sensitive to tamapin, the cells expressing rSK3 and hSK1 channels were measured in the presence of this toxin. In both cases the experiments were performed in symmetrical K^+ conditions. As previously done for rSK2, currents were elicited by dialyzing the cells with $1 \mu\text{M}$ free calcium and ramp voltage protocols were applied. When 50 nM tamapin was applied to hSK1 expressing cells, the current was partially inhibited (Fig 3.13A). The IC_{50} for tamapin on hSK1 was $41.6 \pm 7.8 \text{ nM}$ ($n=6$). The SK3-mediated current was partly inhibited by 1 nM tamapin (Fig 3.13B), and the estimated IC_{50}

was 1.7 ± 0.5 nM ($n=7$). The inhibition of rSK3 and hSK1 channels by tamapin was reversible (insets in Fig 3.13B and C).

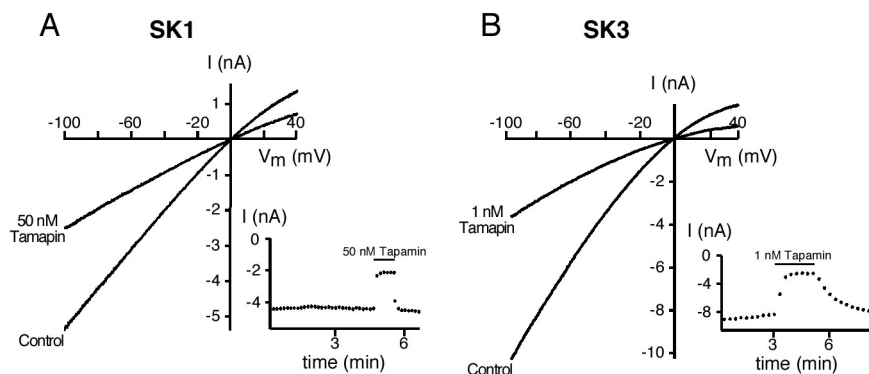


FIG 3.13. Inhibition of hSK1-mediated and rSK3 mediated currents by tamapin. A, CHO-FlpIn cells stably expressing hSK1 were activated by $1 \mu\text{M}$ free calcium. Currents were elicited by voltage ramps from -100 mV to $+40$ mV for 400 ms, and repeated every 10 sec. The SK1-mediated current was partially inhibited by 50 nM tamapin. The calculated IC_{50} value was 41.6 ± 7.8 nM. B, The same protocol as in A was applied to HEK-rSK3 cells. The rSK3 current was partly blocked by 1 nM tamapin. The estimated IC_{50} for the block of SK3 channels by tamapin was 1.7 ± 0.5 nM. Inset in A, shows that 50 nM tamapin blocked hSK1 almost instantaneously upon toxin application. The toxin block was completely and fast reversible. Inset in B, 1 nM tamapin reduced the rSK3 current upon application and the block was also completely reversible.

3.2.6 Effect of tamapin on IK channels stably expressed in HEK-293 cells

HEK-293 cells expressing IK channels were a kind gift of W.J. Joiner and L.K. Kaczmarek. IK channels are intermediate conductance calcium-activated potassium channels. The amino acid sequence is related to, but distinct from, the small conductance calcium-activated potassium channel subfamily (Joiner et al., 1997, Logsdon et al., 1997, Ishii et al., 1997a). Like SK channels, these IK channels are activated by submicromolar concentrations of intracellular calcium (300 nM). It has been shown that IK channels are insensitive to apamin (100 nM) but are blocked by charybdotoxin (Joiner et al., 1997, Logsdon et al., 1997, Ishii et al., 1997a, Jensen et al., 1998).

Fig 3.14 presents the effect of apamin (A), charybdotoxin (CTX) (B) and tamapin (C) on IK channels. Measurements were performed in symmetrical K^+ conditions (144 mM K^+), and IK-mediated currents were elicited by voltage ramps after the cells were dialyzed with $1 \mu\text{M}$ free calcium. In the presence of 100 nM apamin (A), no effect on the current was observed ($n=3$). When 50 nM CTX (B) was applied ($n=5$), the IK current was reduced and resulted in a calculated IC_{50} of 28.9 ± 2.4 nM. Finally tamapin was tested on IK channels stably expressed in HEK-293 cells. The IK current was not affected by 50 nM tamapin ($n=3$, Fig 3.14 C).

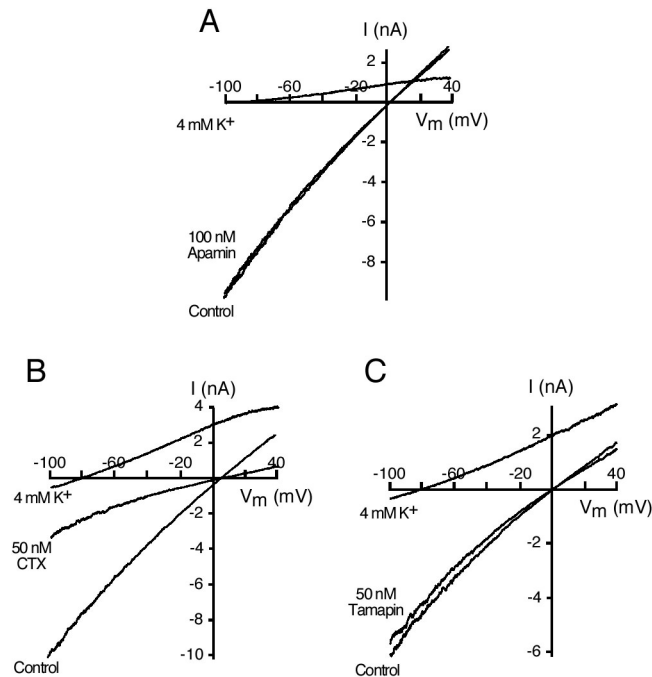


FIG 3.14. Characterization of HEK-293 cells stably expressing hIK. IK currents were elicited by a ramp protocol from -100 to $+40$ mV, with $1 \mu\text{M}$ free Ca^{2+} in the pipette. A, Application of 100 nM apamin did not affect the current. B, 50 nM CTX decreased the IK current. C, IK current was not affected by 50 nM tamapin. Upon application of 4 mM K^+ , the reversal shifted to -80 mV, as predicted.

3.2.7 Conclusion

We have characterized a new toxin, tamapin, which is more potent in blocking rSK2 than apamin (Fig 3.11 and see table 1 Introduction). In spite of the a high similarity between tamapin and scyllatoxin (77% similarity), tamapin has shown to be more efficient in blocking the SK channels (Fig 3.11, fig 3.13, see table 1 Introduction). Tamapin showed different efficiency in blocking the different SK subtypes (Fig 3.11 and 3.12). Furthermore, the block by tamapin was neither voltage dependent nor potassium dependent (Fig. 3.12). Therefore, tamapin should be a good pharmacological tool to determine the native molecular basis of SK currents in various tissues. It could also be a helpful tool to design similar peptides, which could result in more efficient SK channel blockers, possible even more selective for SK channel subtypes.

3.3 Domain analysis of the calcium-activated potassium channel SK1 from rat brain: Functional expression and toxin sensitivity.

3.3.1 Introduction

In the last years, work by our group and others has focused on the rSK2, rSK3 and hSK1 channels expressed in different types of expression systems and displaying different pharmacological profiles (see paragraph 1.3 in Introduction).

However, only little information was available on the SK1 channels from rat brain (rSK1). Although this channel was originally cloned with the other SK subunits (Kohler et al., 1996, Joiner et al., 1997), only one report mentioned that it could not be functionally expressed (Bowden et al., 2001). The human homologue (hSK1) was instead able to form functional channels with a sensitivity to apamin that varied depending on the expression system (Strobaek et al., 2000, Shah and Haylett, 2000, See table 1 in Introduction). When compared to hSK1, the rSK1 subunits presents a 84% sequence identity (Fig 3.15).

In order to determine the molecular mechanism that prevents the formation of functional rSK1 channels, a set of chimeras containing different regions of rSK1 were made. All clones were transiently transfected into HEK-293 cells, while for the pharmacology on hSK1 the CHO-Flp-hSK1 stable cell lines was used. Expression of the native channels or the chimeras was determined by immunocytochemistry and/or by electrophysiology.

3.3.2 Expression of rSK1 in HEK-293 cells

Our group generated an antibody against the amino-terminal portion of the rat SK1 subunit (anti-NSK1) to identify and localize the rSK1 channel subtype. HEK-293 cells were transiently transfected with the rSK1 subunit in three independent transfections. Anti-NSK1 (1/500 dilution) detected a diffuse pattern of rSK1 protein in the cell, with a higher concentration in intracellular structures, most likely corresponding to the endoplasmatic reticulum and the Golgi apparatus (Fig 3.16B). The anti-NSK1 antibody did never generate any signal when applied to non-transfected HEK-293 cells (Fig. 3.16C).

```

hSK1  MNSHSYNNGSVGRPLGSGPGALGRDPPDDPEAGHPPQPPHSPGLQVVAKSEPARPSPGSPR 60
rSK1  MSSRSHNGSVGRPLGSGPGELGMEPVVDPEAGRPRQPTQGPGLQMM-AKGQPAGLSPSSGPR 59

S1
hSK1  GQPQDQDDDDEDDEEDEEAGRQRASGKPSVWGHRLGHRRALFEKRKRLSDYALIFGMFGIVV 120
rSK1  GHISQAQEEEEEEEDDEDD---RPGSGKPPTVSHRLGHRRALFEKRKRLSDYALIFGMFGIVV 116

S2
hSK1  MVTETELSWGVYTKESLYSFALKCCLISLSTAILLGLVVLYHAREIQLFLVMDNGADDWRIA 180
rSK1  MVTETELSWGVYTKESLCSFALKCCLISLSTVILLGLVILLYHAREIQLFLVDNGADDWRIA 176

S3
hSK1  MTCERVFLISLELAVCAIHPVPGHYRFTWTARLAFTYAPSVAEADVDVLLSIPMFLRLYL 240
rSK1  MTWERVSLISLELAVCAIHPVPGHYRFTWTARLAFSLVPSAAEADVDVLLSIPMFLRLYL 236

S4
hSK1  LGRVMLLHSKIIFTDASSRSIGALNKITFNTRFVMKTLMTICPGTVLLVFSISSWIIAAWT 300
rSK1  LARVMLLHSRIIFTDASSRSIGALNRVTFNTRFVKTKLMTICPGTVLLVFSISSWIVAAWT 296

P-region
hSK1  VRVCERYHDKQEVTSNFLGAMWLISITFLSIGYGMVPHTYCGKGVCLLTGIMGAGCTAL 360
rSK1  VRVCERYHDKQEVTSNFLGAMWLISITFLSIGYGMVPHTYCGKGVCLLTGIMGAGCTAL 356

S6
hSK1  VVAVVARKLELTKAEKHVHNFMMDTQLTKRVKNAANVLRETWLIYKHTRLVKKPDQARV 420
rSK1  VVAVVARKLELTKAEKHVHNFMMDTQLTKRVKNAANVLRETWLIYKHTRLVKKPDQSRV 416

hSK1  RKHQRKFLQAIHQAQKLRSVKIEQGKLNDQANTLIDLAKIQIIVMYDLVSELHAQHEELEA 480
rSK1  RKHQRKFLQAIHQAQKLRVKIEQGKVNDQANTLADLAKAQSTAYVVSELQAQQEELEA 476

hSK1  RLAITLESRLDALGASLQALPGLIAQAIRPPPPLPPRPGPGPQDQAARSSPCRWIPVAS 540
rSK1  RLAALESRLDVLGASLQALPSLIAQAICPLPPP---WGPSHLTTAAQSQSHWLPITAAS 533

hSK1  DCG 543
rSK1  DCG 536

```

FIG 3.15 Alignment of the primary sequences of rSK1 and hSK1. rSK1 shows 84% sequence identity with hSK1. S1-S6 are the putative transmembrane domains (yellow boxes); P-region is the pore region (green box). In black boxes are the amino acids that differ in the two sequences.

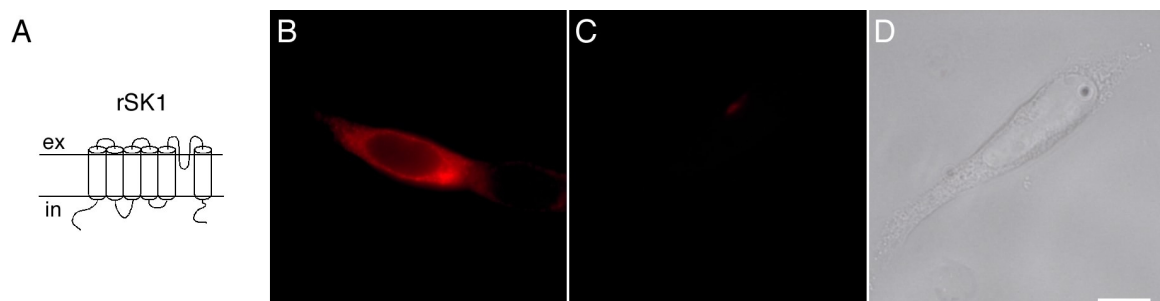


FIG 3.16. Expression of rSK1 α -subunit in HEK-293 cells. A, Nomenclature and schematic drawing of rSK1. B, Specific rSK1 stain by anti-NSK1 antibody. C, No signal was observed with anti-NSK1 on HEK-293 cells. D, Bright field picture of the same cells as mentioned in panel C. Scale bar: 10 μ m

To determine the specificity of anti-NSK1 and anti-NSK2 antibodies, the antibodies were applied to cells transfected with rSK2 and rSK1 α -subunits, respectively. Anti-NSK2 antibody (1/1000 dilution) did not detect any signal in cells expressing rSK1 protein (Fig 3.17B), neither did the anti-NSK1 antibody (1/500 dilution) detect any signal in cells transfected with rSK2 (Fig 3.17C). This result demonstrates that the anti-NSK1 and the anti-NSK2 antibodies do not display any unspecific cross-reactivity.

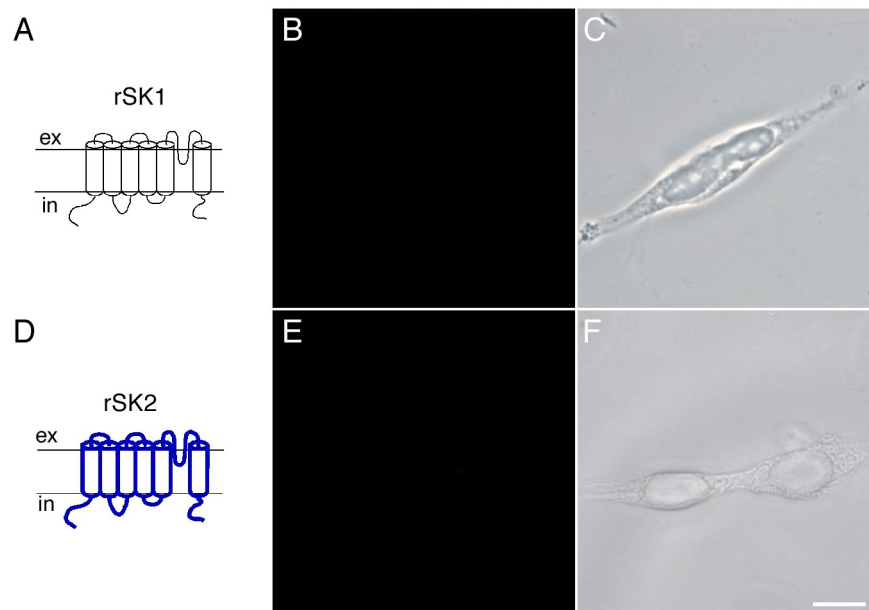


FIG 3.17. Specificity of anti-NSK1 and anti-NSK2 antibodies. A, D, Schematic overview of rSK1 and rSK2 α -subunits. Thin black lines correspond to rSK1, blue thick lines correspond to rSK2. B, No signal detected with anti-NSK2 on HEK-293 cells transfected with rSK1. C, bright field picture corresponding to the cell in B. E, No staining was observed with anti-NSK1 on HEK-293 cells transfected with rSK2. F, bright field picture of the cell in panel E. Scale bar: 10 μ m.

3.3.3 Expression of rSK1 and rSK1 core chimeras.

In order to assess the functional properties of rSK1 channels, electrophysiological measurements in the whole cell configuration were performed. The channels were activated by 1 μ M free Ca^{2+} in the pipette. In spite of the presence of rSK1 protein as detected by immunofluorescence (Fig 3.16B), no current above background could be measured in rSK1 transfected cells. (Fig 3.19A and 3.22).

The biggest differences between rSK1 and rSK2 lie in their amino- and carboxy-terminal regions. To identify the molecular determinants responsible for the lack of functional expression of rSK1, a chimera containing the rSK1 transmembrane domains (S1-S6) and the amino- and carboxy-terminal of rSK2 was generated (Fig 3.18E). The rSK1_{N-CtSK2} protein was detected using the anti-NSK2 antibody (Fig 3.18F). Furthermore, electrophysiological recordings demonstrated

that the rSK1_{N-CrSK2} chimera formed a functional channel. When transfected cells were dialysed with 1 μ M free Ca²⁺, the channels were activated and a K⁺ current was observed (Fig 3.19D). To narrow down the region responsible for the lack of expression of the rSK1 α -subunit, chimeras containing rSK1 and either the amino- or the carboxy-terminus of rSK2 were generated (Fig 3.18A, D). The chimeras rSK1_{NrSK2} and rSK1_{CrSK2} were transfected in HEK-293 cells. Expression of the proteins rSK1_{NrSK2} and rSK1_{CrSK2} was tested by using anti-NSK2 and anti-NSK1 antibodies, respectively. A diffuse expression pattern of both proteins was observed (Fig 3.18B, C). Although both chimeras showed expression, only one chimera was functional. Activation of rSK1_{NrSK2} and rSK1_{CrSK2} by 1 μ M Ca²⁺ resulted in a K⁺ current only for the chimera rSK1_{CrSK2} (Fig 3.19C), showing that, like rSK1_{N-CrSK2}, rSK1_{CrSK2} assembled into functional K⁺ channels. However, the substitution of the amino-terminus of rSK1 by the amino-terminus of rSK2 was not sufficient for formation of functional channels (Fig 3.19B). Furthermore, exchange of the carboxy-terminus of rSK1 by the corresponding region of hSK1 in the chimeric rSK1_{ChSK1} (Fig 3.19H) resulted in the formation of functional K⁺ channels (Fig 3.19F) which were detected with the anti-NSK1 antibody (Fig 3.18G). In contrast, replacement of the amino-terminus of rSK1 by hSK1 amino-terminal region, rSK1_{NhSK1} did not yield a rescue of rSK1 functional expression (Fig 3.19E).

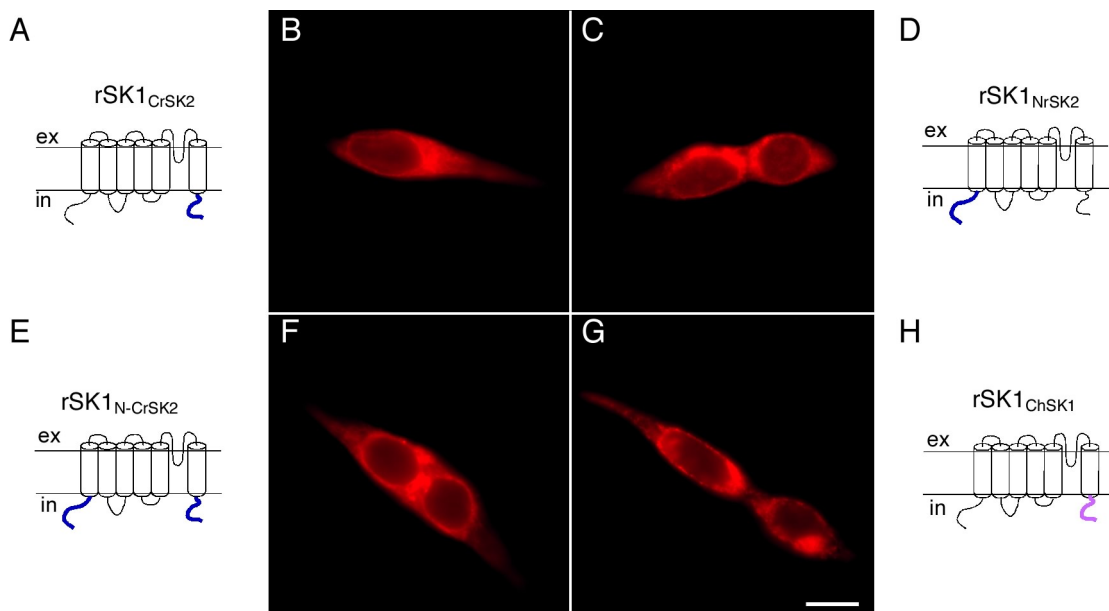


FIG 3.18. Expression of rSK1 chimeras. A, D, E and H, Schematic overview of the chimeras, thin lines correspond to rSK1 regions, dark blue lines correspond to rSK2 regions and violet lines correspond to hSK1 parts. B, Immunofluorescence of the rSK1_{CrSK1} construct as pictured in A, protein was visualized using the anti-NSK1 antibody. C, rSK1_{NrSK2} was detected with the anti-NSK2 antibody. F, Specific staining of rSK1_{N-CrSK2} with the anti-NSK2 antibody. G, Expression of rSK1_{ChSK1} was detected with the anti-rSK1 antibody. Scale bar; 10 μ M

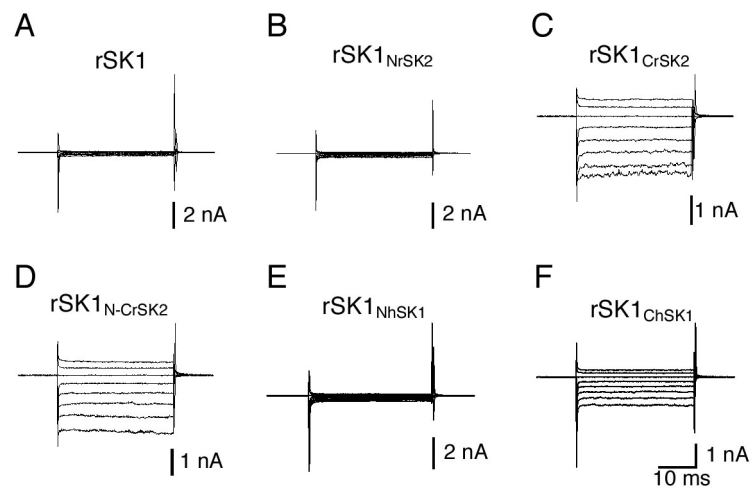


FIG 3.19. Recordings of rSK1 and chimeras. All measurements were performed in the whole cell configuration of the patch clamp technique. K^+ currents were elicited by voltage pulses from -100 to $+40$ mV in 20 mV steps, lasting 30 ms, in the presence of $1 \mu\text{M}$ free Ca^{2+} . In A, B and E no current above background was observed. In C, D and F, K^+ currents were observed upon application of voltage steps.

3.3.4 Expression of hSK1 core chimeras.

In the attempt to elucidate whether the carboxy-terminus of rSK1 is per se capable of hindering the formation of functional channels when attached to normally expressing SK subunits, a chimera containing the hSK1 core and the carboxy-terminus of rSK1 was generated. Surprisingly, transfection of this chimera, hSK1_{CrSK1}, into HEK-293 cells resulted in the formation of functional channels. K^+ currents were observed after transfected cells were dialyzed with $1 \mu\text{M}$ free Ca^{2+} (Fig 3.21B). Similarly, replacing the amino-terminus of hSK1 by that of rSK1 in hSK1_{NrSK1} led to the formation of functional channels (Fig 3.21C). Expression of the hSK1_{NrSK1} α -subunit was detected by the anti-NSK1 antibody (Fig 3.20B). By contrast, functional expression was hindered when both amino- and carboxy-termini of rSK1 were substituted for the corresponding regions of hSK1 (Fig 3.20D). Fig 3.20C shows a specific stain by anti-NSK1 for the hSK1_{N-CrSK1} chimera expressed in HEK-293 cells.

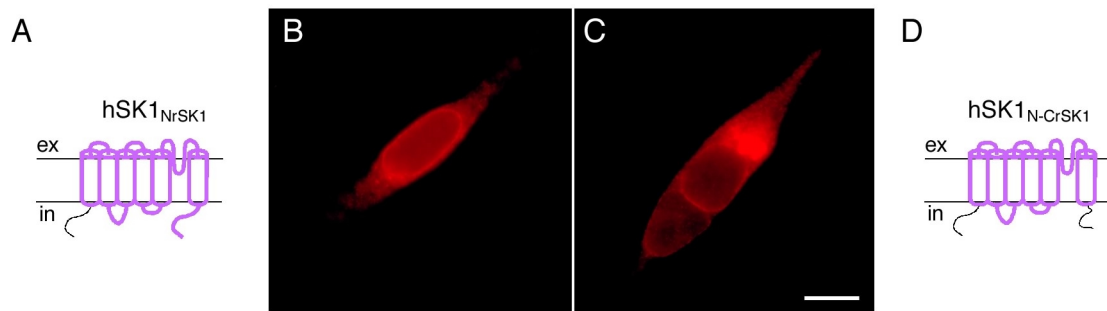


FIG 3.20 Immunocytochemistry of hSK1 chimeras. A, D, Schematic drawings of the hSK1 constructs. Thick violet lines correspond to the hSK1 region. Thin black line corresponds to the rSK1 parts. B, Specific anti-NSK1 stain of hSK1_{NrSK1} transiently transfected in HEK-293 cells. C, hSK1_{N-CrSK1} protein expression was detected with anti-NSK1 antibody.

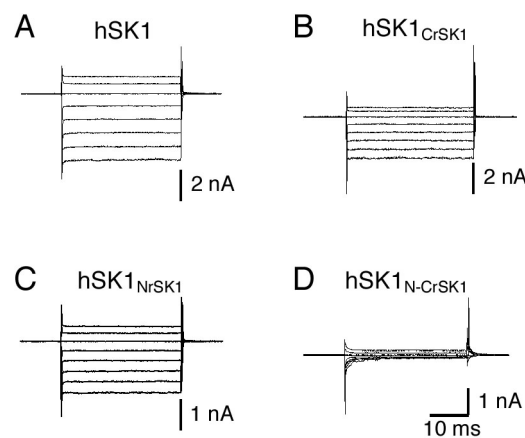


FIG 3.21 Expression of hSK1 and hSK1 core chimeras. Measurements were performed in the whole cell patch clamp technique. Channels were activated by 1 μ M free Ca^{2+} in the pipette and K^+ currents were evoked after applying voltage pulses from -100 mV to 40 mV with 20 mV steps for 30 ms. A, hSK1 currents through hSK1 channels stably expressed in CHO-FlpIn cells. B and C, hSK1 core chimeras reveal K^+ currents upon application of voltage steps. D, No K^+ currents above background were observed for chimera hSK1_{N-CrSK1}.

Fig 3.22 represents an overview of the absolute current (A) and of current density (B) (amount of current per surface area) for all the different constructs. The data showed that rSK1, rSK1_{NrSK2}, rSK1_{NhSK1} and hSK1_{N-CrSK1} expression in HEK-293 cells did not result in the formation of functional channels, although rSK1 and the chimeras rSK1_{NrSK2} and hSK1_{N-CrSK1} were expressed in the cells, as shown by immunocytochemistry. The currents were not different from the background K^+ currents measured in non-transfected HEK-293 cells. In two occasions, for constructs rSK1_{NrSK2} and hSK1_{N-CrSK1}, also 10 μ M free calcium was tested in an attempt to activate the channels (black diagrams Fig 3.22A and B). However, a 10-fold increase in intracellular calcium concentration did not alter the current amplitude or current density .

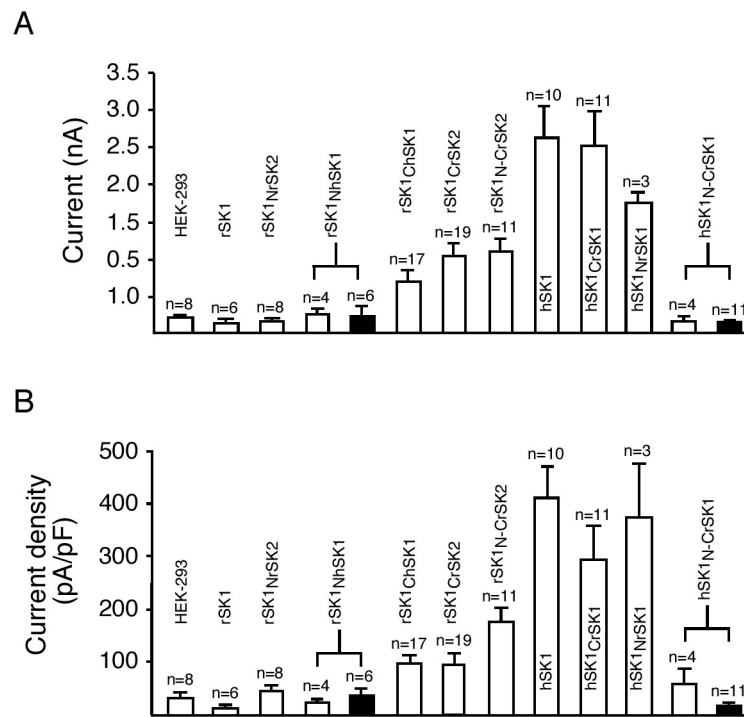


FIG 3.22 Summary of the current amplitudes and current densities of all constructs. A, Bar diagram of the maximum current of all constructs measured at -80 mV. B, current densities at -80 mV. Black bars represents cells measured with $10 \mu\text{M}$ free calcium. “n” corresponds to the number of cells measured; error bars are SEM.

3.3.5 Effect of apamin and d-tubocurarine on the chimeras

The pharmacological properties of rSK1 could not be investigated so far because this subunit does not form functional channels. Thanks to the chimeras, it was possible to determine the apamin and d-tubocurarine sensitivity of channels containing large portions of rSK. The chimeras used in the experiments contained the pore as well as the transmembrane domains of rSK1, while only the intracellular amino- and/or carboxy-terminals were exchanged for those of rSK2 or hSK1. As shown in earlier experiments, rSK1_{CrSK2}, rSK1_{ChSK1} and rSK1_{N-CrSK2} expression resulted in the formation of functional channels. To our surprise these chimeric channels did not show sensitivity for the SK channel blockers apamin (Fig 3.23A, B, C) and d-tubocurarine (Fig 3.24A, B, C). Even high apamin (100 nM) and d-tubocurarine ($50 \mu\text{M}$) concentrations did not alter the K_{Ca} currents through the rSK1_{CrSK2} and rSK1_{N-CrSK2} chimeras. By contrast, the chimeras hSK1_{CrSK1} and hSK1_{NrSK1}, which contain the pore and transmembrane domains of hSK1, were sensitive to the applied drugs. 10 nM apamin was sufficient to block more than half of the hSK1, hSK1_{CrSK1} and hSK1_{NrSK1} current (Fig 3.23D, E, F). Also application of $50 \mu\text{M}$ d-tubocurarine resulted in a reduction of the hSK1 and hSK1_{CrSK1} current (Fig 3.24D, E).

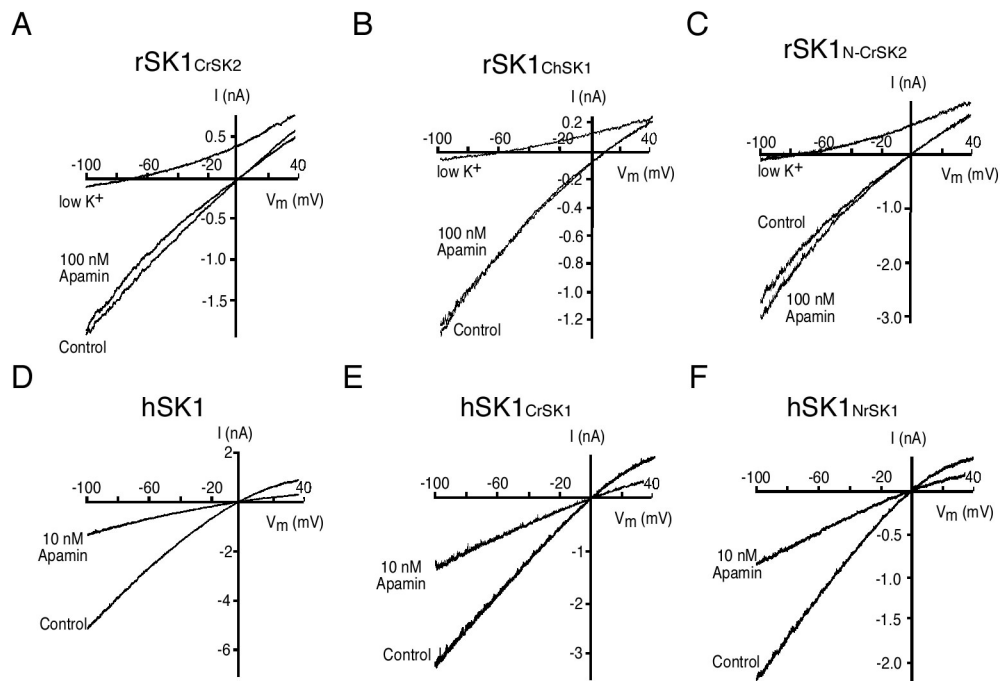


FIG 3.23 Effect of apamin on chimeric rSK1 and hSK1 channels. All experiments were performed in the whole cell configuration of the patch-clamp technique. K⁺ currents were evoked by voltage ramps with 1 μ M free calcium in the pipette. A, B and C, Application of 100 nM apamin to chimeras with transmembrane and pore regions of rSK1 did not affect the currents. Low potassium (4 mM K⁺) was applied after each experiment to determine the stability of the seal, the reversal potential was approximately around -80 mV under these conditions. D, E and F, 10 nM apamin was sufficient to reduce K⁺ currents mediated by chimeras containing the hSK1 transmembrane and pore regions.

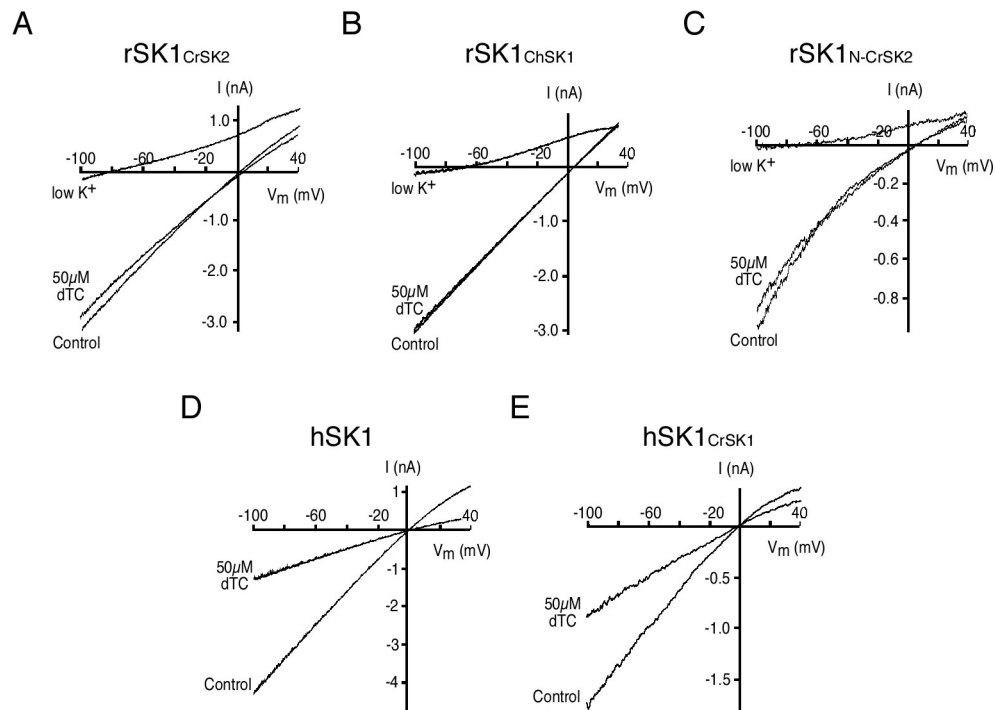


FIG 3.24 Effect of d-tubocurarine on chimeric rSK1 and hSK1 channels. HEK-293 cells expressing SK channels and chimeras were measured in the presence of $1 \mu\text{M}$ intracellular Ca^{2+} . Voltage ramps from -100 mV to $+40$ mV (duration: 400 ms) were applied. A-C, The rSK1_{CrSK2} (A), rSK1_{ChSK1} (B) and the rSK1_{N-CrSK2} chimeras (C) yielded currents that were not suppressed by $50 \mu\text{M}$ dTC. Application of low K^+ resulted in a shift of the K^+ equilibrium potential to -80 mV. D-E, hSK1 (D) as well as hSK1_{CrSK1} generated currents that were largely blocked by $50 \mu\text{M}$ dTC.

3.3.6 Conclusion

We generated a novel antibody against a unique sequence in the amino-terminal region of rSK1, which specifically recognized the rSK1 α -subunits expressed in HEK-293 cells (Fig 3.17). We also showed that the rSK1 protein is expressed in the cells (Fig 3.16), however electrophysiological measurements of HEK-293 transfected with rSK1 did not show the formation of functional K^+ channels. Furthermore, when the amino- and carboxy-terminus of rSK1 subunits were swapped for the same region of rSK2, functional K^+ channels were formed, characterized by the evoked K^+ currents after dialyzing the cells with $1 \mu\text{M}$ free calcium (fig 3.19D). When the amino-terminus of rSK1 was exchanged for the amino-terminus of hSK1 or rSK2, no functional K^+ channels were formed (Fig 3.19B, E), although immunofluorescence showed that the chimeras were expressed (Fig 3.18A, H). When only the carboxy-terminus of rSK1 was replaced by the corresponding region of hSK1 or rSK2, functional K^+ currents were observed (Fig 3.19 C, F). In addition, when the amino-terminal region of hSK1 was exchanged for the corresponding region of rSK1, functional chimeric channels were formed (Fig 3.21C). Surprisingly, substitution of the carboxy terminus of hSK1 by the carboxy-terminus of rSK1 also

resulted in the formation of functional K⁺ channels (Fig 3.21B), but when the amino- as well as the carboxy-termini of hSK1 were exchanged for the amino- and carboxy-termini of rSK1, no functional chimeric channels were formed (Fig 3.21D).

Although hSK1 and rSK1 α -subunits share the same pore region sequence (Fig 3.15), functional chimeras containing the rSK1 core domain (transmembrane regions and the pore) did not show any sensitivity for apamin (Fig 3.23A, B, C) and d-tubocurarine (Fig 3.24A, B, C). However, the functional chimeras expressing the core domain of hSK1 proved to be sensitive to apamin (Fig 3.23E, F) as well as to d-tubocurarine (Fig 3.24E).

In conclusion, rSK1 transfected in the HEK-293 cells forms α -subunits, but is not able to form functional homotetrameric K⁺ channels. Furthermore, chimeras containing the rSK core domain (transmembrane domains and pore region) were not sensitive to apamin and d-tubocurarine.

3.4 Characterization of a novel splice variant of the calcium-activated potassium channel rSK2, rSK2-860.

3.4.1 Introduction

Our group has recently identified a new splice variant of rSK2, called rSK2-860, because the expressed protein is 860 amino acids (aa) long (Manuscript in preparation; Dr. Stocker's personal communication). The rSK2-860 cDNA codes for a protein which is 275 amino acids longer at the amino terminus when compared to the rSK2 channel originally cloned (Kohler et al., 1996).

Transfection of rSK2-860 in different cell lines resulted in a surprising expression pattern of the protein. Immunofluorescence as well as electrophysiological recordings have shown that rSK2 expresses in the cell membrane of different cell lines. However, transfection of the new splice variant in HEK-293, CHO or COS cells resulted in the formation of intracellular clusters, particularly numerous around the cell nucleus. The 275 aa additional stretch in the amino-terminus of the rSK2 protein resulted in an apparent retention and clustering of the rSK2-860 α -subunits.

Several studies have focused on the identification of signal sequences, which are responsible for the retention of proteins in the ER or Golgi (see for example: Munro and Pelham, 1987, Munro, 1991, Lewis and Pelham, 1992, Nilsson and Warren, 1994, Sharma et al., 1999, Zerangue et al., 1999). Besides these specific signals, recent studies have shown that trafficking of channels or other proteins to special compartments are regulated by interactions with other proteins, such as ubiquitin, through specific sequences (Bachmai and Varshavsky, 1989, Hicke, 1997, Laney and Hochstrasser, 1999, Hicke, 2001, Bishop et al., 2002, Polo et al., 2002, Lelouard et al., 2002, Raiborg et al., 2002). Recently it has been shown that a specific motif, RXR, at the carboxy-terminus of an α -subunit or between transmembrane domains, is responsible for the retention of the channel in the ER (Zerangue et al., 1999, Margeta-Mitrovic et al., 2000). Thorough investigation of the primary sequence of rSK2-860 revealed the presence of RXR motifs at the amino-terminus of the α -subunit, but no other signal sequences were found.

The aim of the work described in the following part was to identify in which cell compartment the rSK2-860 α -subunit clusters occur and to determine the molecular mechanism responsible for the distinct behaviour of this subunit, in the hope that this might help elucidating its functional role.

3.4.2 Primary sequence of the new splice variant of rSK2

The difference between the new splice variant and the originally cloned rSK2 α -subunit is situated in the amino-terminus of the protein. The splice variant contains 275 amino acids more than rSK2. The rest of the sequence behind the longer amino acid stretch is completely identical. Fig 3.25 presents a schematic drawing of the alignment of both rSK2 subunits. The yellow and blue part of the drawing corresponds to the originally cloned rSK2 subunit. The white box represents the extended 275 amino acid-long part at the amino terminus of rSK2, resulting in the expression of a protein of 860 amino acids. The red box on top of the drawings marks the region used to generate the anti-NSK2 antibody. The green box shows the region used to generate a specific antibody against rSK2-860, called anti-N7-SK2. Throughout the thesis, I used mainly the anti-NSK2 antibody to detect rSK2-860, unless otherwise stated.



FIG 3.25. Schematic illustration of the rSK2 and rSK2-860. Upper part presents the originally cloned rSK2 α -subunit, with the transmembrane domains, S1-S6 (blue). Lower drawing shows the rSK2-860 subunit. The only difference between both subunits lies in the longer amino terminus of rSK2-860 (white box).

3.4.3 Expression of rSK2 and rSK2-860 in HEK-293 cells

HEK-293 cells were transfected with rSK2 or rSK2-860, and 48 hours later they were fixed with PFA and the expression of protein was detected by using the anti-NSK2 antibody, which detected rSK2 as well as rSK2-860 α -subunits. Pictures were made with a confocal microscope at different levels through the z-axis (depth) of the cell. Fig 3.26 shows the expression pattern of rSK2 channels in two transiently transfected HEK-293 cells. As seen from the picture, the channel has a diffuse pattern throughout the cell but does not result in the formation of protein clusters.

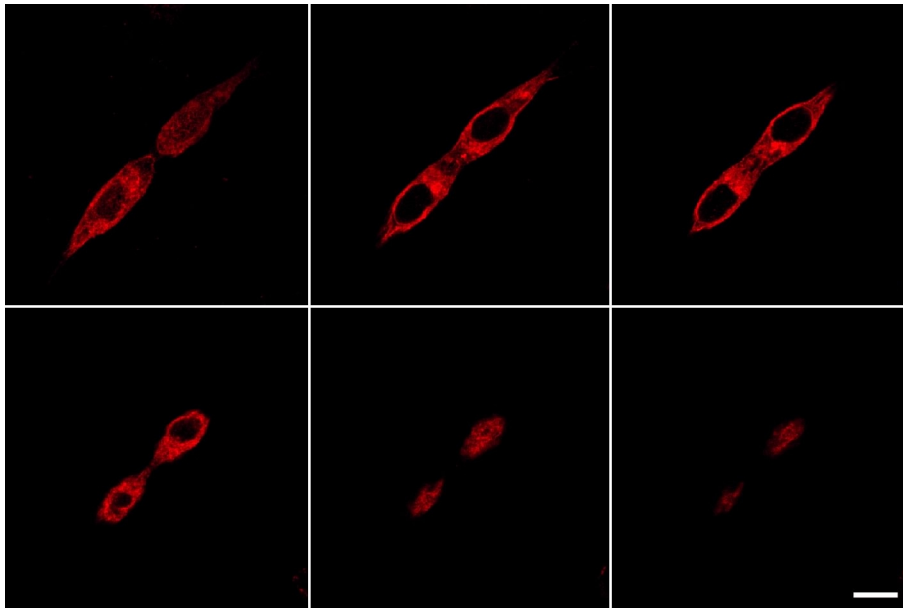


FIG 3.26. Expression of rSK2 α -subunits in HEK-293 cells. This panel shows 6 sections of the same cells expressing rSK2. HEK-293 cells were transfected with rSK2 and detected using the anti-NSK2 antibody (1/1000 anti-NSK2). A diffuse pattern of rSK2 subunits in cytoplasm and cell membrane was detected. Scale bar: 10 μ m

Cells expressing rSK2-860 showed a distinct pattern. The protein was not detected in the cell membrane and there was no diffuse expression in the cytoplasm. As visible in Fig 3.27, clusters of protein were observed intracellularly and especially around the nucleus of the cells.

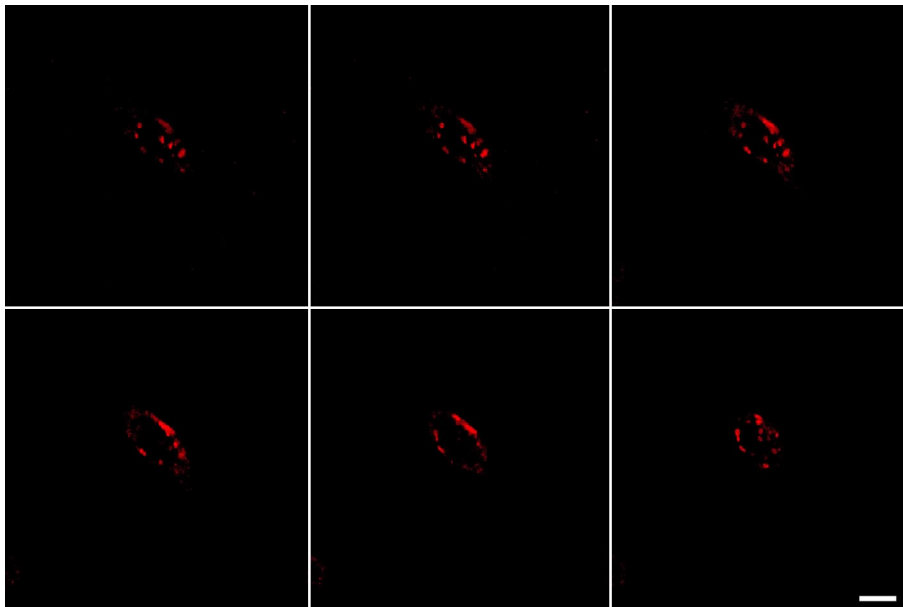


FIG 3.27. Expression of rSK2-860 subunits in HEK-293 cells. HEK-293 cells were transfected 48 hours before immunocytochemistry. The expression of rSK2-860 proteins were detected with anti-NSK2. The stain shows the formation of clusters around the nucleus. Scale bar: 10 μ m

3.4.4 Expression of rSK2 and rSK2-860 in COS and CHO cells.

To eliminate the possibility that this distinct expression pattern of rSK2-860 was related to the HEK cell expression system, COS and CHO cells were transiently transfected with rSK2-860, and with rSK2 as a control. Transfection of COS cells with different lipidic transfection reagents, FuGENE or LipofectAMINE, did not change the expression pattern of rSK2 or rSK2-860. COS cells transfected with rSK2 showed a diffuse expression pattern of the protein. No α -subunit clusters were observed in the cells (Fig 3.28).

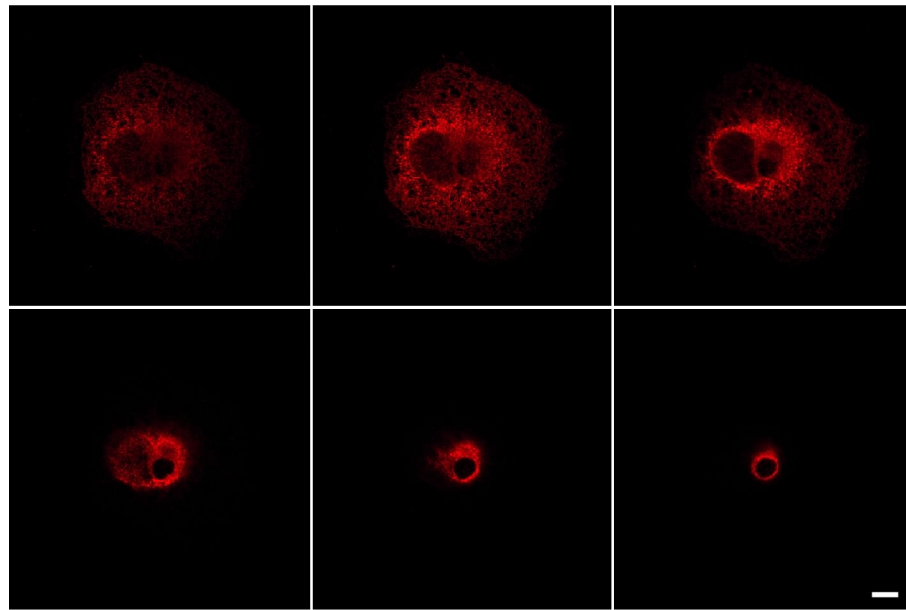


FIG 3.28. Expression of rSK2 in COS cells. rSK2 α -subunits were detected in transiently transfected COS cells by the anti-NSK2 antibody (1/1000). The immunostaining showed a diffuse pattern of expression in the cell. The six panels correspond to confocal optical sections of one transfected COS cell. Scale bar: 10 μ m

However, when rSK2-860 was expressed in COS cells, a change in the protein expression was observed (Fig 3.29). Instead of the characteristic diffuse pattern of expression, clusters of protein were observed, especially around the cell nucleus, similarly to what observed in HEK-293 cells.

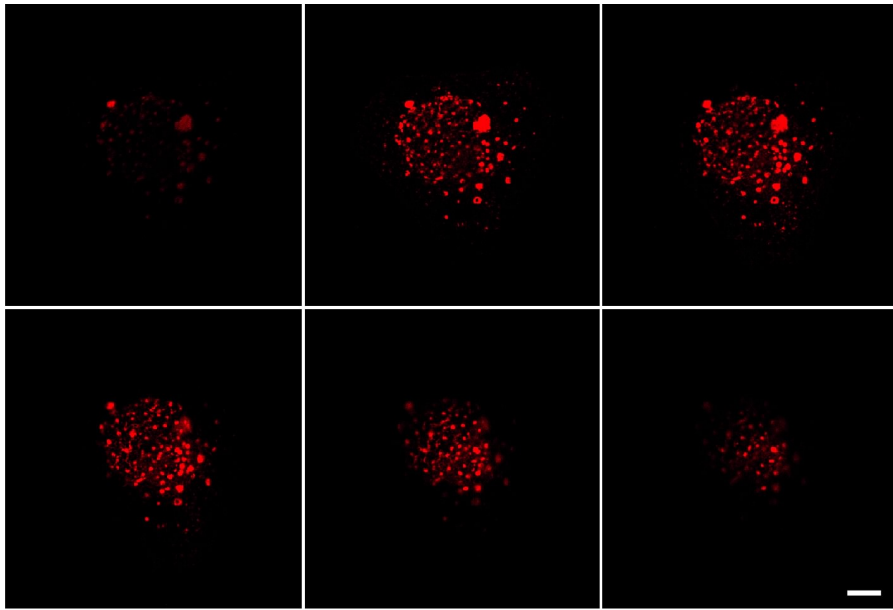


FIG 3.29. Immunostaining of rSK2-860 in COS cells. A specific rSK2-860 signal was obtained using the anti-NSK2 antibody. The six panels are consecutive confocal optical sections across a single COS cell transfected with rSK2-860. The protein formed clusters throughout the cell. Scale bar: 10 μm

Finally, rSK2 and rSK2-860 channels were expressed in CHO cells and analyzed by immunofluorescence, with the anti-NSK2 antibody. As previously shown in HEK-293 and COS cells, the expression of rSK2 in CHO cells resulted in a uniform distribution of rSK2 α -subunits throughout the cytoplasm and cell membrane (Fig 3.30).

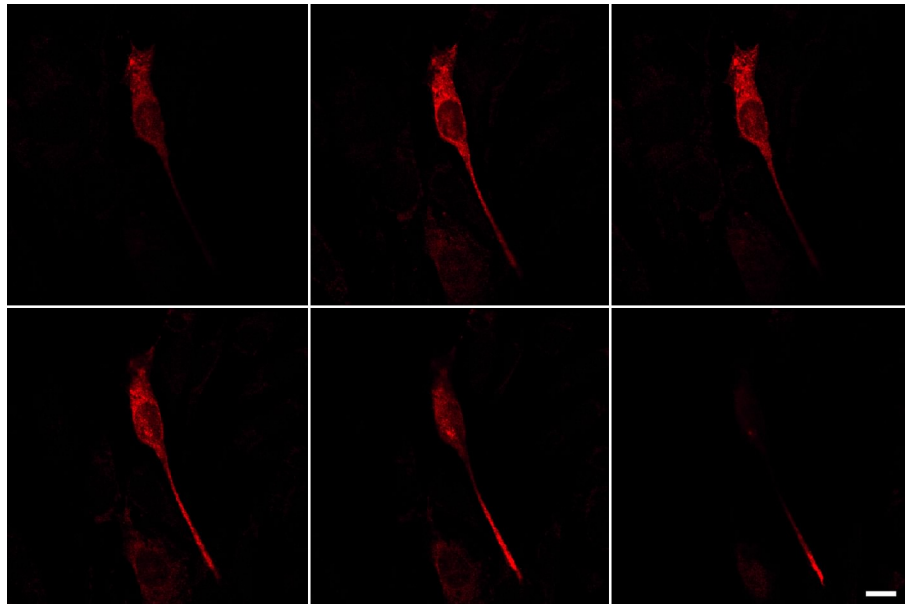


FIG 3.30. Immunofluorescence of CHO cells transiently expressing rSK2. This picture presents 6 different levels (stacks) of the same cell expressing rSK2. A signal was detected using the anti-NSK2 (1/1000). Scale bar: 10 μm

Expression of rSK2-860 in CHO cells confirmed the pattern observed in COS or HEK-293 cells. As in the other cell lines, rSK2-860 expression resulted in numerous protein clusters, apparently intracellular (Fig 3.31).

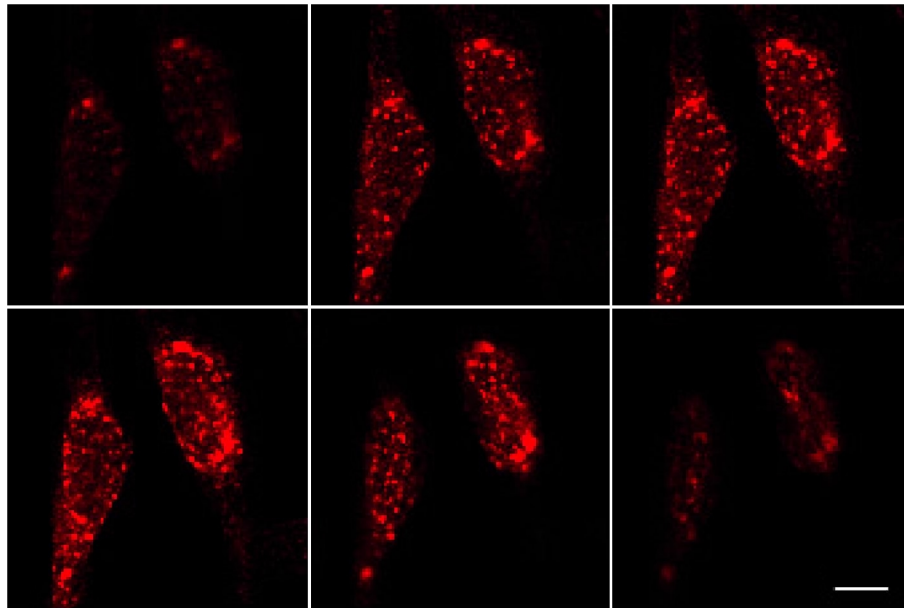


FIG 3.31. Expression of rSK2-860 in CHO cells. Immunocytochemistry was performed using 1/1000 dilution of the anti-NSK2 antibody. Protein clusters were observed throughout the cytoplasm of the two CHO cells. Scale bar: 10 μ m.

3.4.5 Role of the rSK2-860 amino-terminus in protein trafficking: chimera

To address the question whether the specific sequence of the amino-terminus of rSK2-860 is alone responsible for the expression pattern of rSK2-860, a rSK3 chimera containing the amino-terminus of rSK2-860 was generated. As shown in figure 3.3A, rSK3 is highly expressed in the cell membrane. In order to determine if the amino-terminus of rSK2-860 is capable of altering the membrane expression of rSK3, the 275 aa-long stretch was cloned in frame with the amino-terminus of rSK3. The resulting chimera rSK3_{NrSK2-860} was transfected in HEK-293 cells and detected with a specific anti-CSK3 antibody (1/500 dilution) (Fig 3.32) and with the antibody generated against the long amino-terminus of rSK2, anti-N7-SK2 (1/1000 dilution) (Fig 3.33). The substitution of the amino-terminus of rSK3 for the amino-terminus of rSK2-860 resulted in the formation of clusters, especially around the cell nucleus. This result suggests that the amino-terminus of rSK2-860 contains a specific signal which is able to retain proteins in clusters in the cytoplasmatic compartment.

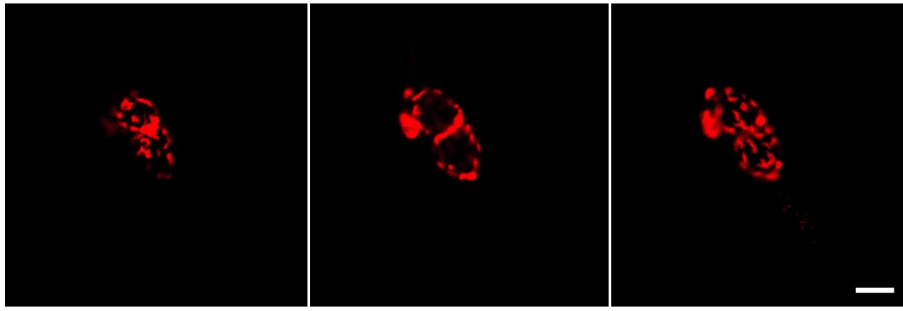


FIG 3.32. Detection of rSK3_{NrSK2-860} using the anti-CSK3 antibody. The chimera was detected using a specific antibody against the carboxy-terminus of rSK3. Shown are three confocal optical sections through a HEK-293 cell transiently transfected with rSK3_{NrSK2-860}. Scale bar: 10 μ m.

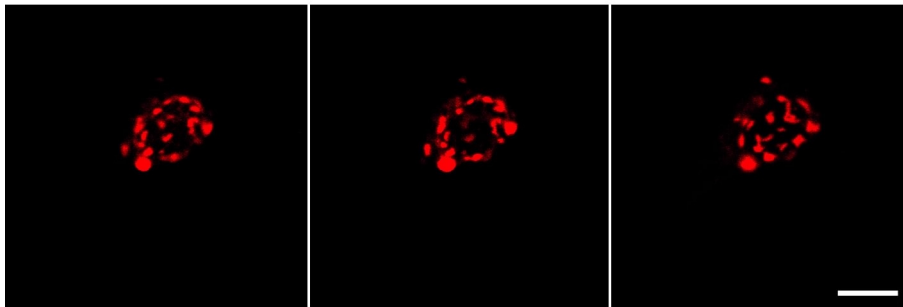


FIG 3.33. Expression of rSK3_{NrSK2-860} in HEK-293 cells. Cells were immunostained 48 hours after transfection with the chimera. Expression was detected with a specific antibody generated against the amino-terminus of rSK2-860, anti-N7-rSK2. The expression pattern of the chimera was similar to the one of rSK2-860 expressed in HEK-293 cells. The three panels represent consecutive confocal optical sections of a single transfected cell. Scale bar: 10 μ m

3.4.6 Role of rSK2-860 amino-terminus in protein trafficking: truncations and deletion.

In order to assess which domain of the amino-terminus of rSK2-860 is responsible for the intracellular retention and clustering of the channel, a set of truncated α -subunit constructs were generated. Fig 3.34 shows an overview of the truncated proteins.

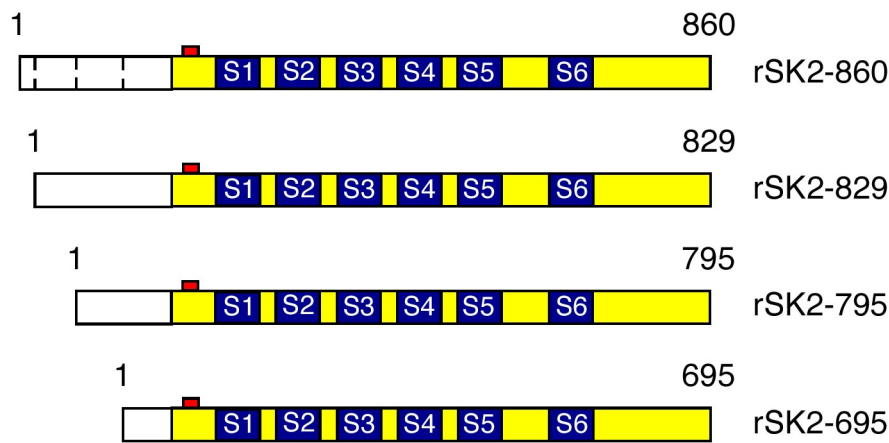


FIG 3.34. Representation of the truncated rSK2-860 subunits. The upper construct corresponds to the original rSK2-860. Dashed lines in the white box represent the positions where the truncated proteins start. rSK2-860 codes for a protein of 860 amino acids. rSK2-829 has the first 31 amino acids at the amino terminus truncated, resulting in a protein that is 829 amino acids long. rSK2-795 misses the first 65 amino acids and expression results in a protein of 795 aa. The last construct codes for a protein of 695 aa. 165 aa have been eliminated at the amino terminus of rSK2-860 in order to obtain rSK2-695.

The first construct, rSK2-829, missed the first 31 amino acids at the beginning of the protein. At position 21-23 in the amino acid sequence of rSK2-860 is a RTR motif. It has been reported that this sequence at the carboxy-terminus or in the lobes between transmembrane domains of certain channels is responsible for their retention in the ER (Zerangue et al., 1999, Margeta-Mitrovic et al., 2000). We wondered whether this motif at the amino terminus of rSK2-860 had the same function, and used the rSK2-829 subunit, which is missing this RTR motif, to test this hypothesis.

Expression of rSK2-829 in HEK-293 cells did not result in an altered expression pattern (Fig 3.35). The truncated channel resulted in the formation of clusters around the cell nucleus, similar to the pattern obtained for rSK2-860 expressed in various expression systems.

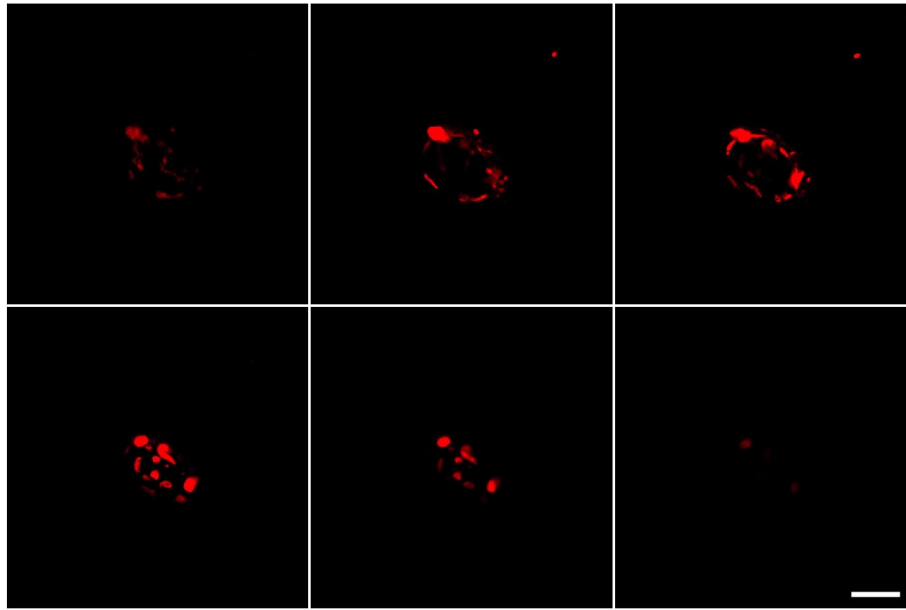


FIG 3.35. Expression of rSK2-829. Expression rSK2-860, missing the first 31 amino acids at its amino terminal did not alter the expression pattern. Intracellular clusters were still observed, especially around the cell nucleus. Six panels present different confocal sections of the same transfected HEK-293 cell. The protein was detected using anti-NSK2 antibody. Scale bar: 10 μ m.

In order to narrow down the domain responsible for the retention of the protein, a larger part of the amino-terminus of rSK2-860 was eliminated (rSK2-795). This resulted in a truncated protein missing the first 65 amino acids at its amino-terminus. However, transfection of this protein in HEK-293 cells did not change the expression pattern. As shown in Fig 3.36, the protein was still clustering intracellularly, particularly around the cell nucleus. This result suggests that the first 65 amino acids are not responsible for clustering of the protein.

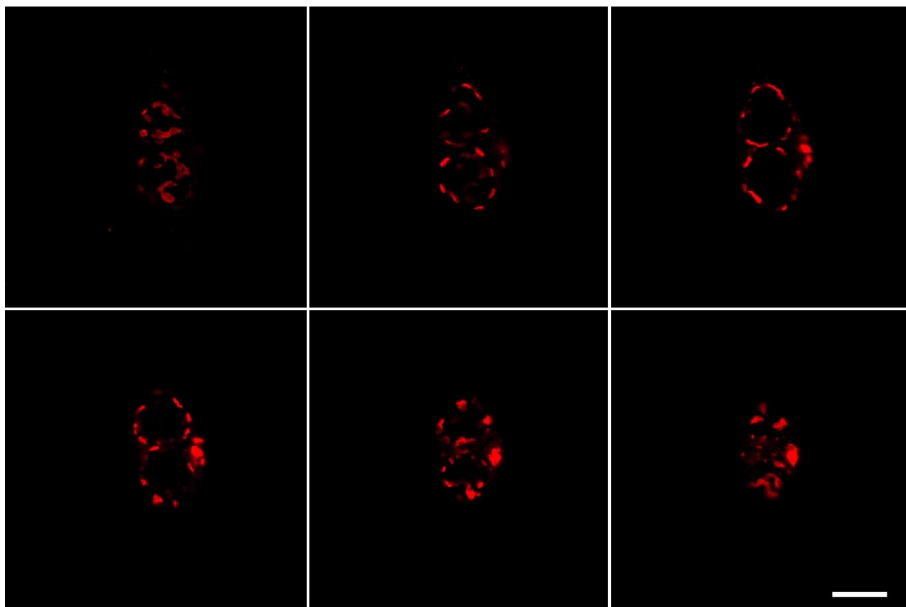


FIG 3.36. Immunofluorescence staining of rSK2-795 expressed in HEK-293 cells. Protein was detected using the specific anti-NSK2 antibody. Shown are the channel clusters surrounding nuclei of 2 cells. Six different confocal optical sections are shown, from the bottom of the cells to the top. Scale bar: 10 μ m

Next, an even longer stretch of the amino-terminus was eliminated. In total 165 amino acids were truncated from rSK2-860, leaving a final protein of 695 amino acids. This protein still contained 110 amino acids more at its amino-terminus than the originally cloned rSK2 protein. When this protein was expressed in HEK-293 cells, a difference in expression pattern was observed (Fig 3.37). Instead of the formation of intracellular clusters mainly around the nucleus, a faint membrane stain was observed. However a very small amount of protein clusters could still be detected in the cell cytoplasm. Furthermore, preliminary electrophysiological recordings revealed the presence of functional rSK2-695 channels in the membrane, characterized by the presence of K^+ currents upon activation of the channels with $1\mu M$ free calcium (data not shown). This result suggests that the intracellular clustering and retention of rSK2-860 is mediated by a region comprising this last truncated 100 amino acids.

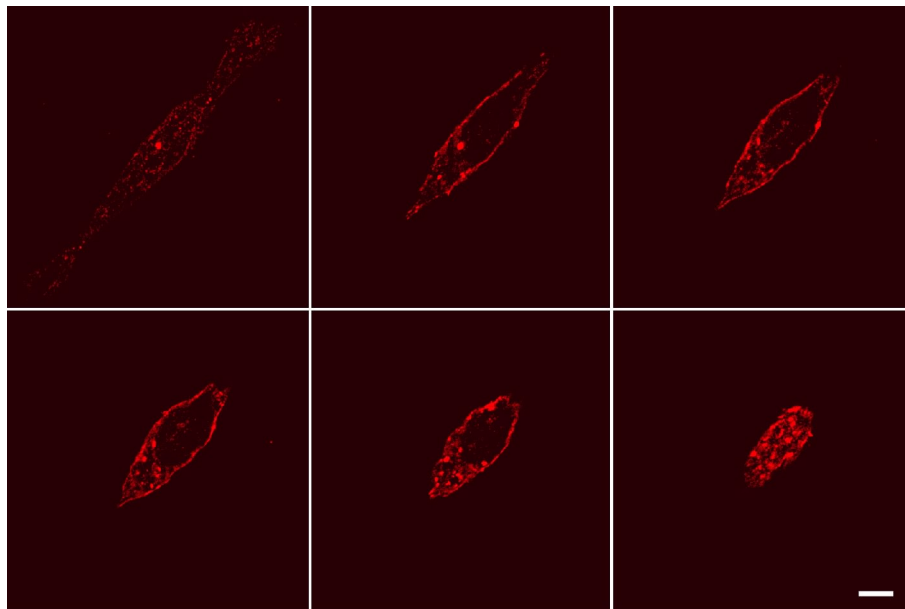


FIG 3.37. Transient expression of rSK2-695 in HEK cells. rSK2-695 was detected with the anti-NSK2 antibody (1/1000). A clear membrane stain was detected, while a small amount of protein clusters was still observed. Presented are six panels of confocal sections of the same cell. Scale bar: $10\mu m$.

Therefore, a deletion mutant, rSK2-N7-del, was generated in which more than 183 amino acids were eliminated, including this 100 amino acid stretch (Fig 3.38). Fig 3.39 presents the specific stain of the rSK2-N7-del protein using the anti-NSK2 antibody. As observed, a high expression of the protein was visible in the cell plasma membrane. These data are supported by preliminary electrophysiological experiments which reveal K^+ currents after the cells have been dialyzed with $1\mu M$ free calcium, suggesting that rSK2-N7-del forms functional channels in the membrane. These data confirm that this 100 amino acid long sequence is involved in the intracellular clustering of the α -subunit.

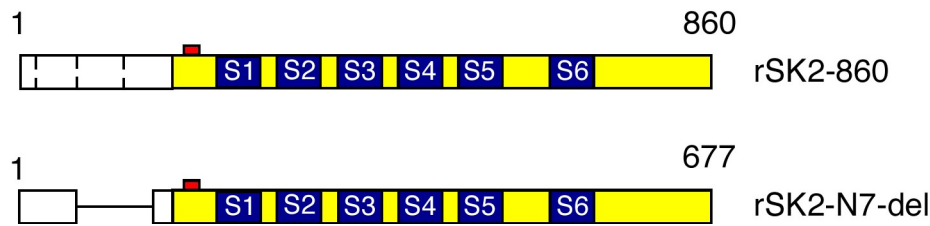


FIG 3.38. Schematic overview of rSK2-860 deletion construct. The upper construct represents the original long variant of rSK2-860, rSK2-860. White box corresponds to the longer amino-terminus. The lower construct, rSK2-N7-del, codes a protein in which 183 aa are deleted in the amino-terminus, represented by the black line in the white box.

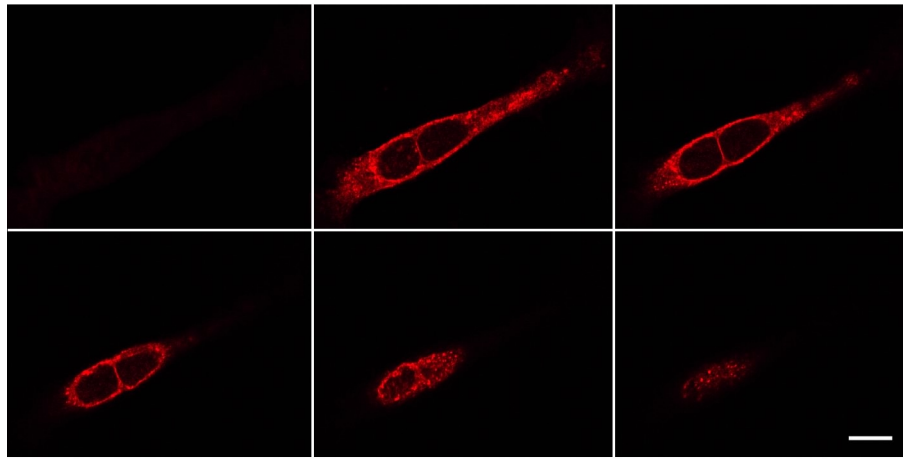


FIG 3.39 Detection of rSK2-N7-del with the anti-NSK2 antibody. Transiently transfected cells were incubated with the specific antibody against the amino terminus of rSK2 (anti-NSK2, 1/1000 dilution). Shown are six different confocal sections through the same cell. A clear signal is observed in the membrane. Scale bar: 10 μ m.

3.4.7 Role of the rSK2-860 amino-terminus in protein trafficking: targeting of fusion proteins containing different parts of the amino-terminus of rSK2-860.

A second strategy to determine which part of the amino-terminus of rSK2-860 is involved in the retention and formation of intracellular clusters is by using fusion proteins. The fusion proteins contained an amino-terminal enhanced green fluorescent protein-tag (EGFP) followed by a certain part of the amino-terminus of rSK2-860. Five different constructs were generated (Fig 3.40) and expressed in HEK-293 cells. Upon expression of each of these fusion proteins, a green signal was observed after excitation. As a control, HEK-293 cells were transfected with the plasmid coding for the EGFP protein alone. This resulted in the homogenous expression of EGFP throughout the cell cytoplasm (Fig 3.41F). Expression of some constructs in HEK-293 cells resulted in the formation of intracellular protein clusters (Fig 3.41A, B and D), while other constructs did not form these characteristic clusters (Fig 3.41C and E).

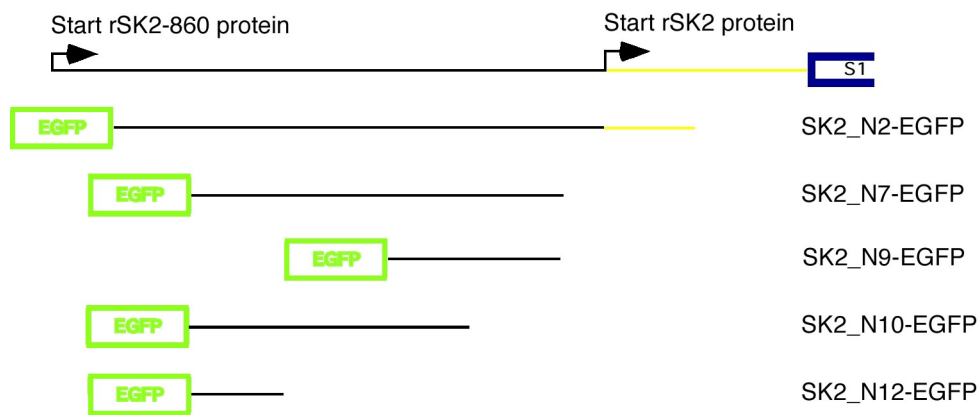


FIG 3.40 Schematic drawing of the EGFP-rSK2-860 fusion proteins. The upper drawing present the first part of rSK2-860 until the first transmembrane segment. The black line represents the amino-terminus of rSK2-860 followed by the yellow line which is the originally cloned rSK2 part. The lower drawings are the amino-terminal portions of the amino-terminus of rSK2-860 fused to EGFP.

Thus, expression of SK2_N2-EGFP in HEK-293 cells resulted in the formation of protein clusters concentrated at one side of the cell (Fig 3.41A). This pattern was visible in more than 70% of transfected cells. The rest of the transfected cells showed a more distributed pattern of protein clusters.

A similar pattern was observed for HEK-293 cells transfected with SK2_N7-EGFP, 70-80% of the cells displayed a diffuse pattern of EGFP tagged protein with strong accumulation of clusters at one side of the cell (Fig 3.41B). In the remaining 20% of the cells a very faint diffuse pattern of distribution of the fusion protein was observed.

SK2_N9-EGFP transfected in HEK-293 cells resulted in a diffuse expression pattern of the protein in the cells (Fig 3.41C). More than 95% of the cells presented this type of distribution. No clusters could be detected for this fusion protein.

Transfection of SK2_N10-EGFP yielded a diffuse pattern of EGFP tagged protein with the formation of a cluster at one side of the cell (Fig 3.41D). This pattern was similar to the one obtained after transfection of HEK cells with SK2_N7-EGFP.

Finally expression of rSK2_N12-EGFP did not result in the formation of clusters, a diffuse pattern of EGFP-tagged protein was observed throughout the cell cytoplasm (Fig 3.41E). The data obtained using the GFP- tagged amino-terminal rSK2-860 constructs is in good agreement with the data from the truncations and deletion study. It shows that constructs which contain the critical 100 amino acid long stretch identified by truncations are forming protein clusters in the cytoplasm.

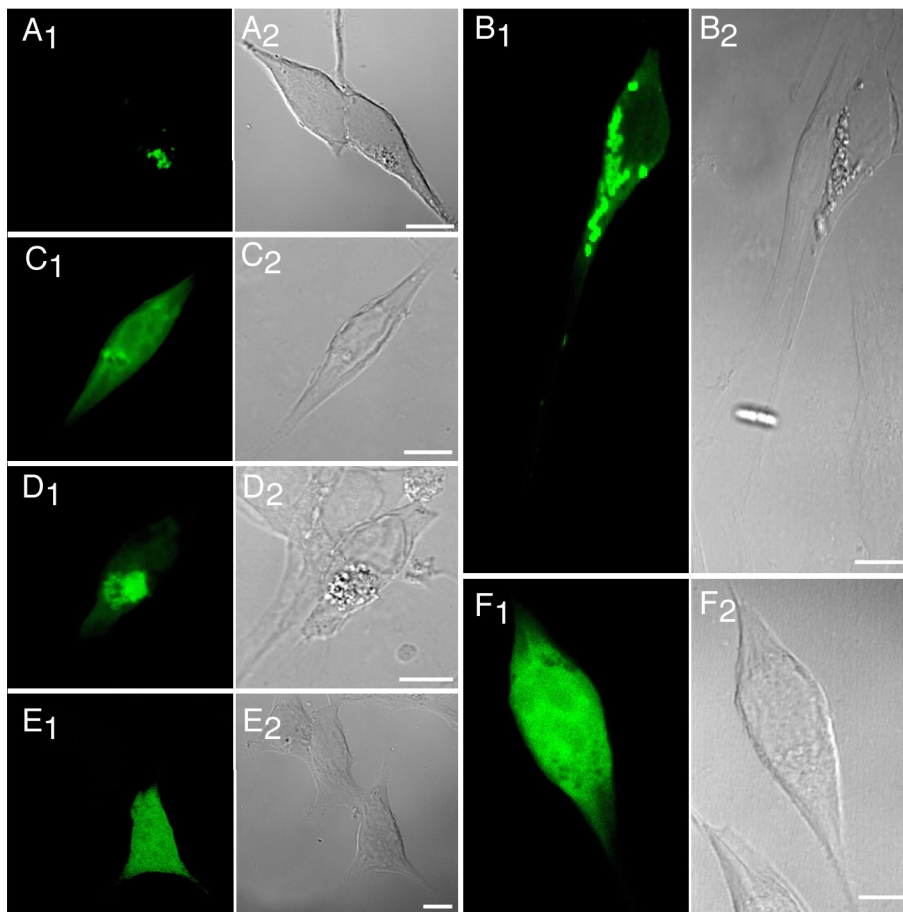


FIG 3.41. Expression of EGFP-tagged amino-terminal portions of the N-terminus of rSK2-860. A₁-E₁, Fluorescence of EGFP-tagged proteins. A₂-E₂ Bright field pictures of the corresponding cells. Expression of SK2_N2-pEGFP (A), SK2_N7-pEGFP (B), SK2_N9-pEGFP (C), SK2_N10-pEGFP (D) and SK2_N12-pEGFP (E). F, Control, HEK-293 cells transfected with the EGFP protein alone, F₁ Distribution of EGFP in HEK cells. F₂, Bright field picture of the cell presented in F₁. Scale bars: 10 μ m

3.4.8 Interaction of rSK2-860 with rSK2

An important question for the possible functional relevance of rSK2-860 is its capability of interaction with the rSK2 α -subunits. To address this question, rSK2-860 was co-expressed with rSK2-myc, constructed by tagging the rSK2 protein at its carboxy-terminus with a myc epitope. The tagged rSK2 protein could be detected with a specific anti-myc antibody, while for the rSK2-860 protein the specific anti-N7-SK2 antibody was used. The secondary antibodies were conjugated with Cy3 and Cy5 to detect rSK2-myc and rSK2-860, respectively.

When both, rSK2 and rSK2-860 were expressed in HEK-293 cells, a partial overlap in their cellular localization was observed. This suggested that the interaction between both α -subunits was not hindered by the longer amino-terminus of rSK2-860. Interestingly, rSK2 subunits were partially localized in clusters (Fig 3.41C). However, a certain portion of rSK2 α -subunits escaped from these protein clusters (Fig 3.41B). An explanation could be that the

expression of rSK2-myc protein was higher and, after the protein clusters formed by rSK2-rSK2-860 complexes reached saturation, the remaining rSK2-myc protein diffused into the cytoplasm and possibly the cell membrane. The distribution pattern of rSK2-860 was not changed upon interaction with the rSK2 subunit (Fig 3.42A).

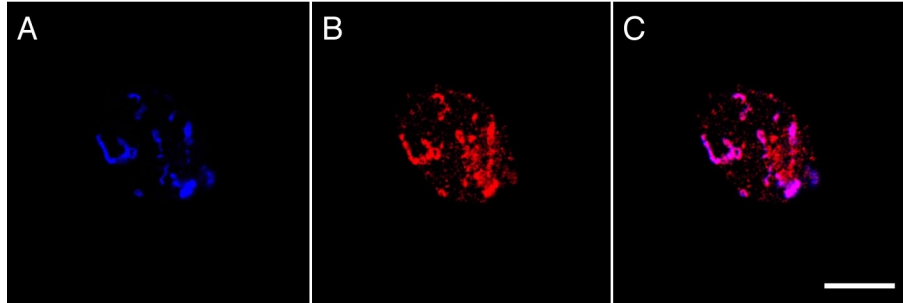


FIG 3.42. Co-expression of rSK2-long with rSK2-myc. A, Immunostaining of rSK2-860; the protein was detected using the anti-N7-rSK2 antibody (1/1000 dilution). B, Expression of rSK2-myc detected with an anti-myc antibody (1/400 dilution) in the same cell as in A. C, Overlay of rSK2-long and rSK2-myc immunostaining. Scale bar: 10 μ m

3.4.9 Subcellular localization of rSK2-860

To determine in which intracellular organelle or compartments the rSK2-860 clusters are formed, rSK2-860 was co-expressed with various EGFP or enhanced yellow fluorescent protein (EYFP) tagged subcellular markers (see Material and Methods). The marker protein and rSK2-860 were co-transfected in HEK-293 cells in a ratio of 1:1. 48 hours after transfection, the cells were immunostained using the specific antibody, anti-NSK2. Cy5 was used as a fluorophore conjugated to the secondary antibody to avoid cross emission of the different dyes.

First, rSK2-860 was co-expressed with the pEGFP-F vector. The vector is encoding a farnesylated EGFP. EGFP is fused at its C-terminus to the farnesylation signal of c-Ha-Ras, which directs the EGFP to the plasma membrane. Fig 3.43 shows the co-expression of rSK2-860 with pEGFP-F; no overlap between the two proteins could be observed, suggesting that the rSK2-860 protein was not expressed in the plasma membrane.

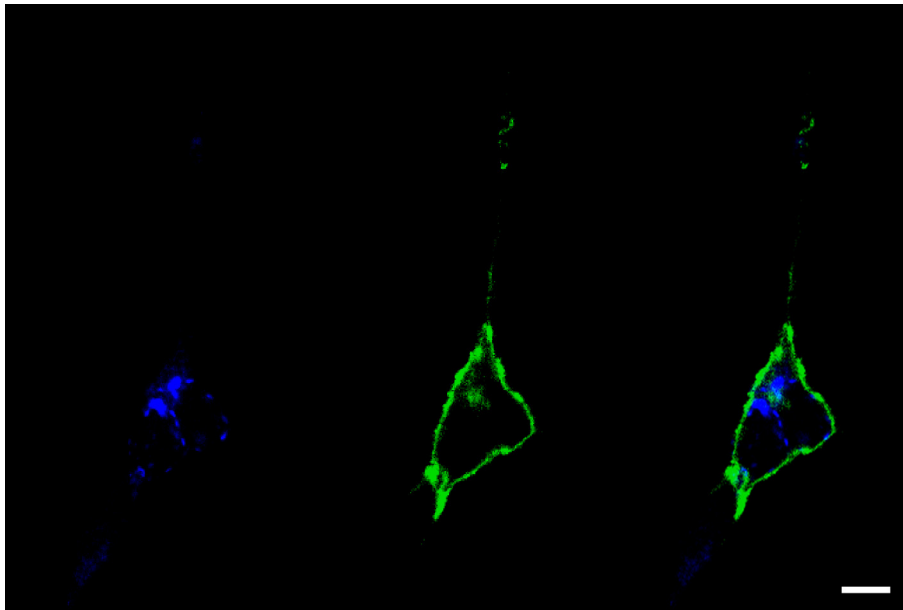


FIG 3.43. Co-expression of rSK2-long with pEGFP-F. A, Specific immunostain of rSK2-860 using the anti-NSK2 antibody (1/1000 dilution). The secondary antibody was conjugated with Cy5. B, Expression of pEGFP-F, showing a plasma membrane stain due to the tagged EGFP containing a specific plasma membrane signal. C, Merged picture of A and B. Presented is a confocal section. Scale bar: 10 μ m

In some of the HEK-293 cells overexpressing of rSK2-860 a rather big cluster of protein was observed. This observation suggested that the proteins could be partially trapped in the Golgi-apparatus. In order to test this hypothesis, rSK2-long was co-expressed with pEYFP-Golgi. In pEYFP-Golgi, the amino-terminus of EYFP is fused to the amino-terminal 81 amino-acids of the human β 1,4-galactosyltransferase, thereby resulting in an EYFP which is targeted to the Golgi. No overlap in the cellular distribution of pEYFP-Golgi and the rSK2-860 protein was detected (Fig 3.44).

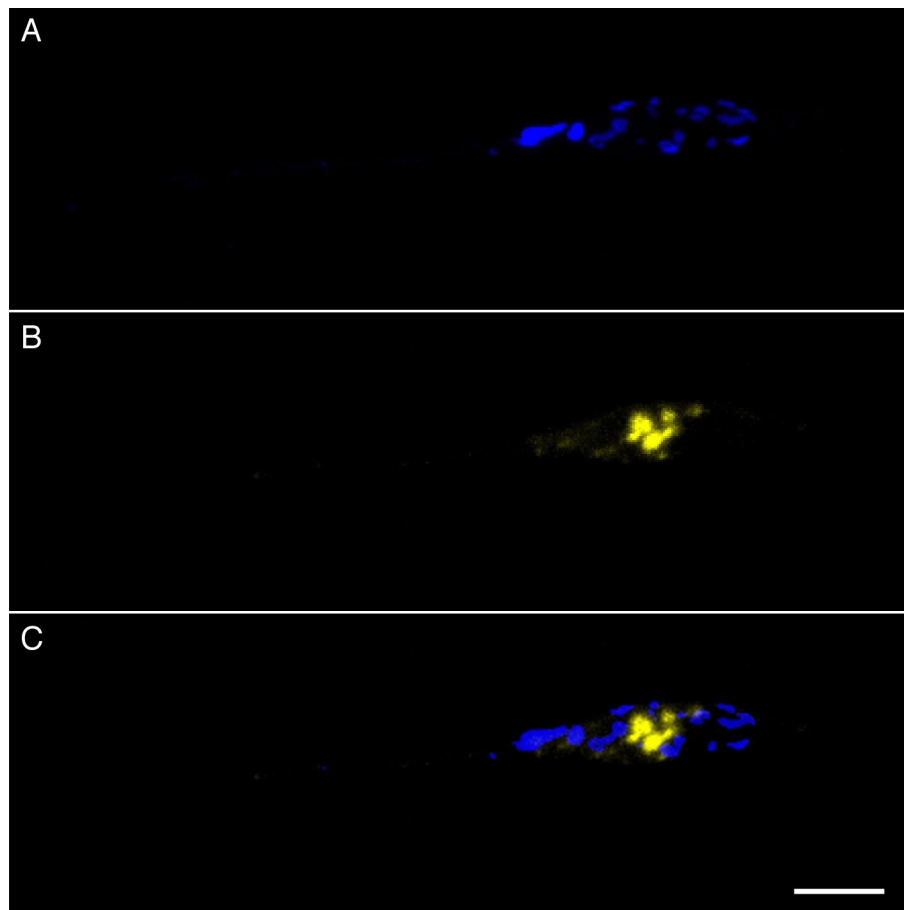


FIG 3.44. Localization of rSK2-860 with respect to the Golgi apparatus. Transient co-transfection of HEK-293 cells with rSK2-long and pEYFP-Golgi. A, Expression of rSK2-long was detected with anti-NSK2 (1/1000 dilution). B, Specific Golgi-apparatus stain, obtained by transfection of cells with a yellow fluorescent protein which is targeted to the Golgi. C, Merge of rSK2-long (A) and pEYFP-Golgi (B) images. Presented is a confocal section. Scale bar: 10 μ m

None of the previous experiments gave a clear answer as to where the rSK2-860 protein is localized. From all the pictures shown, it seemed that the α -subunits are localized close to the nucleus of the cell. To characterize better the spatial relation between rSK2-860 and the nucleus, rSK2-860 transfected cells were incubated with the primary antibodies anti-NSK2 and anti-lamin A/C. The anti-lamin A/C antibody detects the nuclear lamin which is localized at the inner side of the nuclear membrane. The primary antibodies, anti-NSK2 and anti-lamin A/C, were detected with Cy5- and Cy3-conjugated secondary antibodies, respectively. Cy3 and Cy5 were chosen to prevent cross emission when they were excited. Fig 3.45 presents the expression pattern of rSK2-860 and of the nuclear protein lamin. Although the signal rSK2-860 is very close the one of lamin, no clear co-localization of the two proteins was observed (Fig 3.45D, E, F). These data suggest that the rSK2-860 protein clusters are located in the perinuclear region.

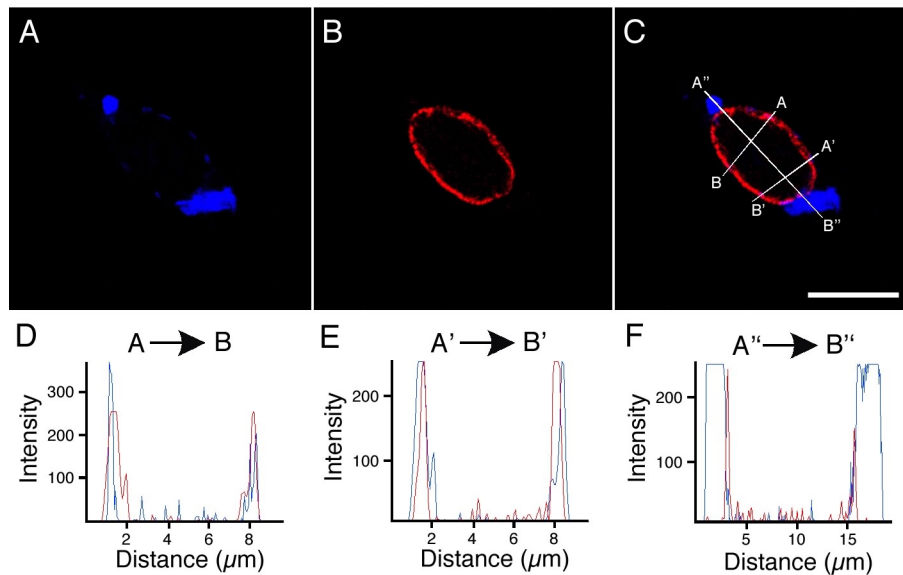


FIG 3.45. Immunostaining of rSK2-860 and lamin. HEK-293 cells were transfected with rSK2-860 and immunostaining of the α -subunits and lamin was obtained with the anti-NSK2 (1/1000) and anti-lamin A/C (1/800) antibodies. Presented is a confocal section of the cell. A, Specific expression pattern of rSK2-860. B, Immunofluorescence staining of lamin A/C. C, Overlay of A and B, no obvious overlap was detected. D, E and F, Signal intensity profiles along the lines A to B (D), A' to B' (E) and A'' to B'' (F), presented in panel C. Scale bar: 10 μm .

3.4.10 Role of the Golgi-apparatus in the trafficking of rSK2-860

At this point, an intriguing question was where and when in the protein biogenesis the rSK2-860 protein clusters were generated. Did they occur after the protein was processed in the endoplasmic reticulum (ER) or did they form after they had been modified in the Golgi-apparatus? To address this question, we decided to use Brefeldin A (BFA). Brefeldin A is known to disrupt the Golgi-apparatus and relocate Golgi-specific proteins to the ER (Lippincott-Schwartz et al., 1989, Doms et al., 1989). If our protein was targeted to the perinuclear aggregates after it had gone through the Golgi, a BFA treatment of the cells could disrupt the trafficking pathway. Disruption of the Golgi would cause the retention of the protein in the ER, giving an ER specific stain, which is characterized by a diffuse pattern of the protein in the cell.

BFA was diluted in 100% ethanol. The same concentration of ethanol was therefore used as a control on the cells expressing rSK2-860. The ethanol was applied to the cell culture medium for 60 minutes. Following the ethanol treatment the cells were washed with 1XPBS and the immunostaining was performed. As a further control, HEK-293 cells were also transfected with the Golgi marker, pEGFP-Golgi, and handled in the same way as the rSK2-long transfected cells. As shown in Fig 3.46, neither rSK2-860 nor pEGFP-Golgi expression was altered by ethanol application. pEGFP-Golgi expressed in HEK-293 showed a characteristic Golgi stain

(Fig 3.46A), while the expression of rSK2-860 resulted in the formation the typical protein clusters (Fig 3.46B).

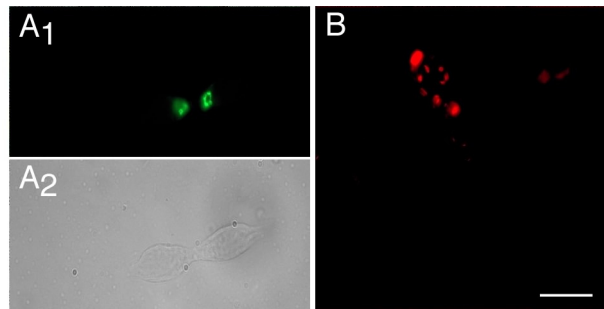


FIG 3.46. Ethanol effect on pEGFP-Golgi and rSK2-860 transiently expressed in HEK-293 cells. Before immunostaining the transfected cells were incubated for 60 min. in culture medium containing ethanol. A₁, Specific expression pattern of pEGFP-Golgi, EGFP is localized at one side of the cell. A₂ Bright field picture of the same cell as in A₁. B, Immunofluorescence of rSK2-860 detected with the anti-NSK2 antibody (1/1000 dilution). Pictures were made with a CCD camera. Scale bar: 10 μ m

However when cells transfected with pEGFP-Golgi were subjected to the BFA treatment, a redistribution of the Golgi marker occurred. The 60-minute treatment disrupted the Golgi-apparatus resulting in the re-localization of the pEGFP-Golgi to the ER (Fig 3.47A). In contrast, the same treatment did not change the expression pattern of rSK2-860 (Fig 3.47B). This result suggests that the rSK2-860 protein clusters were formed upon leaving or during the translation of the protein in the ER. However, it can not be excluded that the rSK2-860 proteins were processed through the Golgi-apparatus, and that the formed clusters remained present even after the 60-minute disruption of the Golgi.

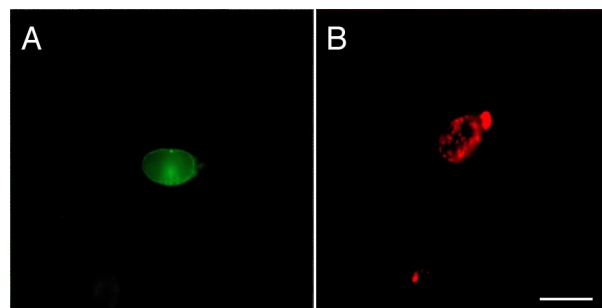


FIG 3.47. Brefeldin A effect on HEK-293 cells expressing pEYFP-Golgi and rSK2-860. Transfected cells were incubated with Brefeldin A for 1 hour, followed by immunostaining. A, Expression of pEGFP-Golgi after BFA treatment, notice the redistribution of the protein in comparison to Fig 3.46A. B, Specific staining for rSK2-860 using the anti-NSK2 antibody (1/1000 dilution). Pictures were taken with a CCD camera. Scale bar: 10 μ m

3.4.11 Does rSK2-860 code for a misfolded or inefficiently folded membrane protein?

Many misfolded and unassembled proteins inappropriately expose hydrophobic surfaces that are normally buried in the protein's interior or at the interface with other subunits (Wetzel, 1994). The exposure of misfolded proteins to the cytosol can lead to the interaction between the hydrophobic stretches and formation of aggregates. Recently, a new cellular and molecular response to the formation of aggregates of misfolded proteins have been characterized, called the aggresome response. Characteristic for this mechanism is that the aggresome formation is accompanied by the collapse of the intermediate filament protein, vimentin, to form a ring-like structure around the aggregates at the centrosome (Johnston et al., 1998).

In order to determine if the characteristic rSK2-860 clusters are aggregates of misfolded proteins, transfected cells were subjected to an anti-vimentin antibody stain. As control, HEK-293 cells were also transfected with rSK2, which forms functional channels and therefore was not expected to affect the vimentin distribution. In both cases, HEK-293 cells were transfected with 2 μ g of rSK2 or rSK2-860. After 48 hours cells were fixed with 4% paraformaldehyde, permeabilized and incubated with the primary antibodies anti-rSK2 (1/1000 dilution) and anti-vimentin (1/200 dilution). The immunofluorescence data show that HEK-293 cells expressing rSK2 did not present an altered distribution of the filamentous vimentin network (Fig 3.48). As observed in the Fig 3.48B, the intermediate filaments are clearly distributed throughout the cell. When compared to the HEK-293 cells transfected with rSK2-860, a similar stain for vimentin is observed (Fig 3.49B) while the rSK2-860 clusters are expressed in the cytoplasm (Fig 3.49A). These data show that although there is a difference in the rSK2 and rSK2-860 protein expression pattern, there is no difference observed in the vimentin expression pattern. Therefore I suggest that the rSK2-860 protein clusters are not aggregates of misfolded proteins.

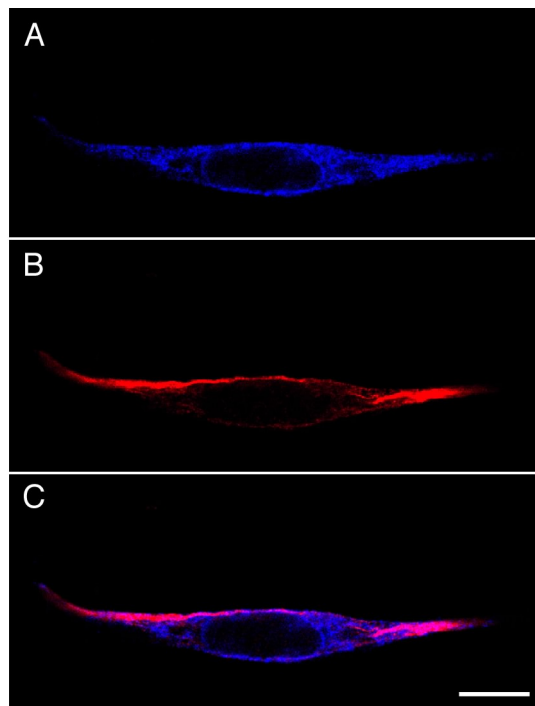


FIG 3.48. Effect of rSK2 on the intermediate filament network. HEK-293 cells expressing rSK2 α -subunits were immunostained with anti-NSK2 (1/1000) and anti-vimentin (1/200) antibodies. Presented is a confocal section of the same cell. A, Characteristic expression pattern of rSK2. B, Intermediate filament network detected with anti-vimentin, no collapse was detected. C, overlay of pictures A and B. Scale bar: 10 μ m.

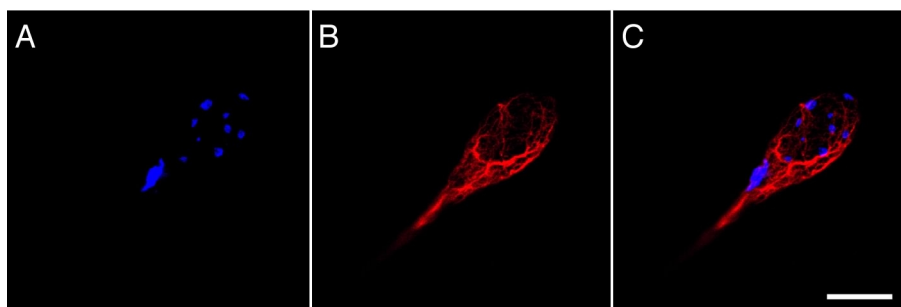


FIG 3.49. Response of the vimentin network in HEK-293 cells expressing rSK2-860. Transfected cells were double-stained for rSK2-860 (1/1000 anti-NSK2) antibody and vimentin (1/200 anti-vimentin) antibody. Shown is a confocal stack of the same cell. A, Specific immunostain for rSK2-860. B, Expression pattern of vimentin in the same cell. C, Merged picture of rSK2-860 (A) with vimentin (B). Scale bar: 10 μ m.

3.4.12 Ubiquitination, a new mechanism of protein targeting

Ubiquitination, a new mechanism for protein regulation, has been characterized (Ward et al., 1995, Staub et al., 1997, Kopito, 1997, Hershko and Ciechanover, 1998, Hedge and DiAntonio, 2002, Hicke and Dunn, 2003). Ubiquitin is a 76 amino acid protein that regulates protein transport between membrane compartments by serving as a sorting signal on protein cargo and by controlling the activity of the trafficking machinery.

Two different mechanisms for ubiquitination, mono- or poly-ubiquitination, of target proteins have been identified. Poly-ubiquitinated proteins are subjected to proteasomal degradation (Chau et al., 1989, Finley et al., 1994, Pickart, 2000), while mono-ubiquitinated proteins are not involved in proteasome degradation, but the single ubiquitin appears to act as a trafficking signal in a host of processes, including endocytosis, endosome internalization and viral budding (Hicke, 2001, Katzmann et al., 2002).

In order to determine if rSK2-860 might be subjected to ubiquitination and targeted to the proteasome by poly-ubiquitinylation or is monoubiquitinylated and targeted to the lysosome, transfected cells were double stained for rSK2-860 (anti-NSK2 antibody, 1/1000) and for ubiquitin (anti-ubiquitin antibody; FK2, 1/5000). FK2 is a monoclonal antibody which recognizes both polyubiquitinylated and monoubiquitinylated proteins, but not free ubiquitin.

For the immunofluorescence, cells were fixed using 100% cold methanol instead of the usual paraformaldehyde fixation. As control, HEK-293 cells were transfected with Hrs-EGFP (Hrs-EGFP, hepatocyte growth factor receptor substrate tagged to the green fluorescent protein was a kind gift of Dr. P. Woodman) and immunostained for ubiquitination. Expression of Hrs-EGFP in HEK-293 cells results in the formation of protein aggregates which are targeted for destruction by using the ubiquitination pathway. Fixation with methanol allowed the anti-ubiquitin antibody to detect the epitope. Fig 3.50A showed the expression pattern of the EGFP tagged Hrs protein, similar to the expression pattern reported by Bishop (Bishop et al., 2002). When the transfected cells were co-stained for the ubiquitin protein, a complete overlapping expression pattern was observed (Fig 3.50B, C). Thus, these data show that the anti-ubiquitin antibody detects ubiquitinated proteins, which will be degraded using the ubiquitine/protease pathway.

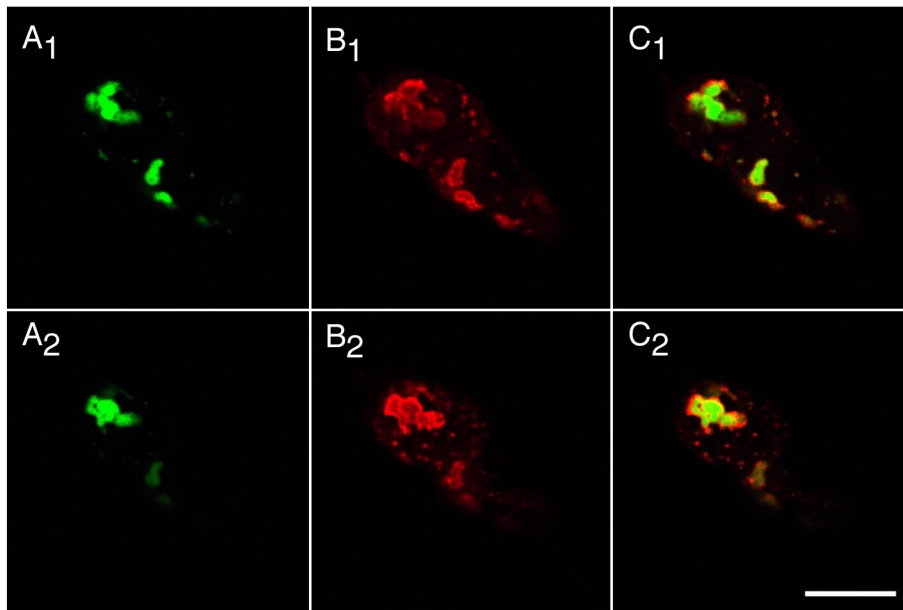


FIG. 3.50. Detection of the ubiquitinated Hrs-EGFP protein. Presented are two confocal sections (1 and 2) of the same cell. A, shows the expression pattern of the EGFP tagged Hrs protein. B, detection of ubiquitinated protein using a specific anti-ubiquitin antibody (FK2, 1/5000 dilution). C, overlay of the Hrs-EGFP stain (A) with the ubiquitin stain (B), observed is the co-localization of both proteins. Scale bar: 10 μ m.

Finally, we investigated if the rSK2-860 clusters are regulated by this ubiquitin pathway, and thus targeted to the proteasome, by incubating transiently transfected cells with the anti-ubiquitin antibody (FK2). Like for the Hrs-EGFP transfected cells, cells which were transfected with rSK2-860 were fixed with 100% methanol to allow the FK2 antibody to detect the epitope. Fig 3.51A presents the specific rSK2-860 stain using the anti-NSK2 antibody. As secondary antibody FITC was used. However when the transfected cells were co-stained for the ubiquitin protein, no complete overlap between the both proteins was observed (Fig 3.51B, C). These data suggest that the rSK2-860 protein is not targeted to the proteasome for degradation.

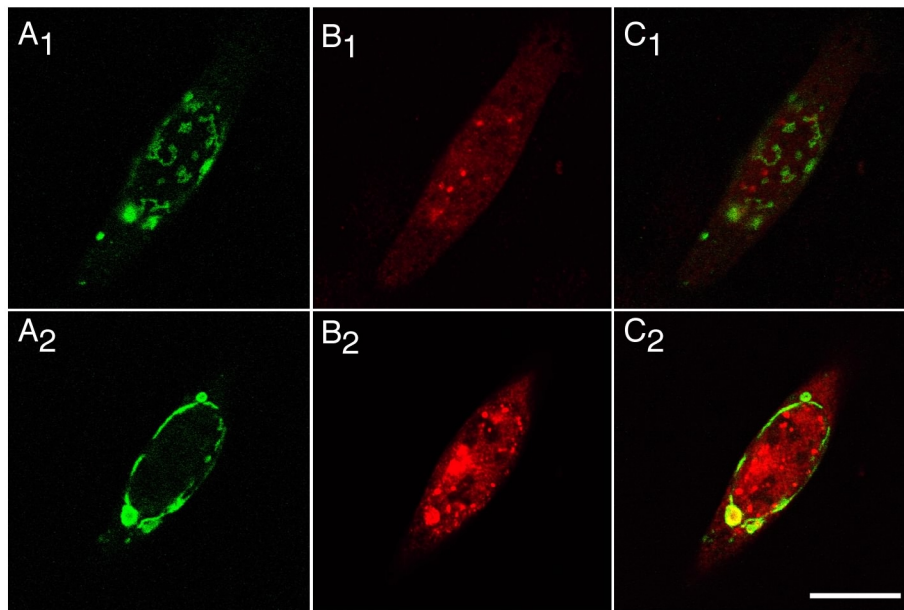


FIG. 3.51 Immunostaining of rSK2-860 and ubiquitin. Shown are two optical section of the same cell (1 and 2). A, presents the immunostain of rSK2-860 using the anti-NSK2 antibody (1/1000 dilution). B, detection of the ubiquitin protein using FK2, the anti-ubiquitin antibody (1/5000 dilution). C, Overlay of panels A and B. Scale bar: 10 μ m.

3.4.13 Conclusion

We characterized a new splice variant, rSK2-860, which encodes for a protein, which is 275 amino acids longer at its amino-terminus when compared with the originally cloned rSK2 channel. Expression in different types of expression systems resulted in the formation of protein clusters, which seems to form in the perinuclear region. Furthermore, several studies show that an 100 amino acid long sequence in the 275 amino acid longer stretch is responsible for the clustering and retention of the proteins. The studies performed with vimentin and ubiquitin suggest that these characteristic rSK2-860 protein clusters are not clusters of misfolded proteins which would be targeted to the proteasome for degradation.

4. Discussion

4.1 Tamapin: a novel SK channel toxin

Role of ion channel blockers. A proper understanding of many CNS diseases and disorders requires identification of the ion channels underlying them and knowledge of their normal physiological roles. Therefore, it is necessary to identify toxins or organic compounds which could differentiate between different types of ion channels. A number of ion channel blockers have been identified throughout the years and have shown to be useful tools to dissect the physiological role of several ion channels in the CNS (Southan et al., 2000, Marinelli et al., 2000, Pedarzani et al., 2000, Wolfart et al., 2001, Hosseini et al., 2001). The most common used blocker to make a distinction between the different members of the SK channels is apamin. Apamin is an 18 amino acid long peptide which was isolated from the venom of the bee, *Apis mellifera* (Habermann et al., 1972). In heterologous systems, it has been shown that apamin blocks SK2 channels more potently than SK3 and SK1 (see Introduction table 1). In this study, I investigated the selectivity of tamapin on the different SK channels, stably expressed in mammalian cells.

Stable expression of SK channels. In order to determine the sensitivity of tamapin for the different SK channels, I generated stable cell lines expressing the SK channels. Immunofluorescence experiments demonstrated the expression of the rSK2 or rSK3 protein in HEK-293 cells. The expression of hSK1 in cell lines could not be shown by using immunocytochemistry, since a hSK1 specific antibody is not available. Instead electrophysiological recordings were performed and confirmed the expression of hSK1 channels. Furthermore, HEK-rSK2 and HEK-rSK3 cell lines were also subjected to electrophysiological experiments. The data obtained for the HEK-rSK2 cell line was similar to the data reported by other groups (see Introduction table 1). In contrast, the data obtained for the HEK-rSK3 cell line did not match with published data, since I obtained different values for apamin as well as for dTC. Our measurements showed that rSK3 was more sensitive to apamin and dTC than in previous reports. To exclude the possibility of an exchange between the different cell lines, although immunocytochemistry confirmed the expression of only the rSK3 protein, experiments were performed on different days and similar results were obtained. However, I do not have a plausible explanation for this phenomenon, therefore more experiments should be performed.

		10		20		30
Tamapin 1	A F C N	L R R C E	L S C R S L G L L G K C I G	E E C K C V P Y		
Scyllatoxin	A F C N	L R M C Q	L S C R S L G L L G K C I G	D K C E C V K H		
PO5	T V C N	L R R C Q	L S C R S L G L L G K C I G	V K C E C V K H		

Effect of tamapin on SK channels. Tamapin is a 31 amino acid long peptide, just like scyllatoxin and PO5. All three toxins exhibit 6 cysteine residues at the same place in the sequence. It has been shown that these 6 cysteines in scyllatoxin shape the toxin backbone by forming three disulfide bridges (Chicci et al., 1988, Martins et al., 1990, Zerrouk et al., 1993, Martins et al., 1995, Calabro et al., 1997). Amino acid sequence alignment showed that tamapin shares 77% homology with scyllatoxin and 74% with PO5. Pharmacological studies on the cloned SK channels showed that tamapin had a higher sensitivity for SK2 ($IC_{50} = 24$ pM) when compared to SK1 or SK3. My experiments have also revealed that tamapin is more potent to block SK channels than scyllatoxin or PO5 (see Introduction, table 1). Several options for the higher potency of tamapin over the other toxins can be hypothesized. 1) Structure-function studies of scyllatoxin showed that, when amino acids at positions 25 (K, lysine), 27 (E, glutamate) and 30 (K, lysine) are chemically modified or mutated, there is a substantial loss of potency of scyllatoxin when applied to the muscle bands of the large intestine (taenia coli), without affecting significantly its ability to displace apamin binding. Furthermore, it was shown that the histidine at position 31 plays a very important role in the binding activity of the toxin and in the induction of contractions in taenia coli (Auguste et al., 1992). By contrast, tamapin displayed full biological activity when tested on the recombinant SK channels, in spite of the presence of amino acids with opposite charges in the positions 25, 27 and 30, and of a tyrosine in position 31. 2) At the N-terminal region, the first amino acids (positions 1 and 2) of tamapin are identical to those of scyllatoxin, but different from those of PO5. Those two residues have been shown to contribute to the higher potency of scyllatoxin on SK2 and SK3 channels when compared to PO5 (Shakkottai et al., 2001), and it is therefore likely that they might be also important determinants of the even higher potency displayed by tamapin. 3) Another noticeable difference between tamapin and previously characterized SK channel blockers is located at the level of the LRXCQ motif, conserved in PO5 and scyllatoxin (Shakkottai et al., 2001), but changed into LRRCE in tamapin. It has been proposed that the methionine at position 7 of scyllatoxin is important for the enhanced potency of this toxin compared to PO5, which contains an arginine residue in the same position, just like tamapin. However, tamapin differs significantly from the LRXCQ motif in having a negatively charged glutamate residue at position 9, there where the other SK channel blockers have a glutamine. The classical LRXCQ motif is therefore not fully conserved in

tamapin and further studies will be necessary to understand the molecular basis for the high affinity of tamapin towards SK channels, and in particular for SK2. A first step in this direction was made by Shakkottai and collaborators (2001), who placed small, positively charged amino acids in position 7 of scyllatoxin and thereby enhanced the selectivity of the mutated toxin for SK2 versus SK3. Keeping all this analysis in mind, future structure-function studies could help to understand which determinants of tamapin are involved in binding to SK channels, and might lead to mutant toxins with further improved selectivity for SK channel subtypes.

In conclusion, tamapin represents a novel, promising pharmacological tool, as it is the most potent SK2 blocker characterized so far, and it blocks SK2 channels ~ 1700 fold and ~ 70 fold more potently than SK1 and SK3 channels respectively, making it the most selective SK2 channel natural toxin characterized so far. In the future it might be useful to: 1) study the physiological role that the different SK channels play in native tissue, 2) purify SK channels from native tissues and determine their subunit composition, and 3) develop the pharmacology of SK channels in view of their possibility involvement in cognitive functions and diseases such as epilepsy.

4.2 Domain analysis of the calcium-activated potassium channel SK1 from rat brain: Functional expression and toxin sensitivity.

Expression of rSK1 in mammalian cells. Until now only two independent groups have shown the expression of rSK1 using antibodies specifically generated against the rSK1 channel α -subunit. One group showed the expression of the rSK1 protein in dissociated hippocampal pyramidal neurons using an antibody generated against the carboxy-terminus of the subunit (Bowden et al., 2001), while the second group showed the expression of the SK1 protein in rat brain (Sailer et al., 2002) using specific anti amino- and carboxy-terminal antibodies. In order to understand the functional and pharmacological properties of the rSK1 channels, we transiently transfected the rSK1 α -subunit in HEK-293 cells. To detect the expression of the rSK1 protein, we used a novel antibody generated against a unique sequence in the amino-terminus of the rat SK1 (anti-NSK1). The anti-NSK1 antibody detected the rSK1 protein distribution throughout the cell (Fig 3.16B, also immunoblot experiments confirmed the expression of rSK1 protein; data not shown, D'hoedt et al., 2004). Electrophysiological recordings of HEK-293-cells transiently transfected with rSK1 did not show K^+ -currents above background (Fig 3.19A). These data suggest that the rSK1 protein is not functionally expressed at the cell membrane, but is most probably retained. Our findings are in good agreement with the data published by Benton et al. (2003), who showed that the expression of rSK1 in HEK cells did not result in SK currents, and furthermore that immunostaining showed a signal primarily in the intracellular compartments (Benton et al., 2003). The fact that there is a higher expression of the protein intracellularly and no signal on the cell membrane could be the reason for the lack of current in cells expressing the rSK1 protein. To identify molecular determinants responsible for the lack of rSK1 functional expression, we generated chimeric subunits.

Role of amino- and carboxy- termini in the functional expression of rSK1 channels. In the last decade a growing amount of papers have been published showing the specialized functions of the amino- or carboxy-termini of ion channels. It has been shown for example that the amino-terminus in voltage gated potassium channels (K_v) contains the tetramerization domain (T1 domain). This domain was identified originally as an important site for regulating intersubunit interactions during channel assembly, such that only a restricted number of heterotetramers are made between K_v channels (Jan L.Y and Jan Y.N., 1990, Lee et al., 1994, Deal et al., 1994, Xu J et al., 1994, Shen N.V. and Pfaffinger P.J, 1995, Strang et al., 2001). However, several groups have reported the functional expression of K_v channels after deletion of this T1 domain (Lee et al., 1994, Tu et al., 1996, Kobertz W.R. and Miller C., 1999), in contrast to other reports that T1 deletion precludes channel assembly (Shen et al., 1993, Hopkins et al.,

1994, Shen N.V. and Pfaffinger P.J, 1995, Schulteis et al., 1998). The presence of the leucine zipper and dileucine motifs in the amino-terminus of SK4 channels have shown to be essential for channel assembly and trafficking to the plasma membrane (Jones et al., 2004). However, several studies have also been performed on the influence of the carboxy-terminus on SK channels expression. This resulted in the identification of 2 domains important for assembly and membrane targeting: the Ct1 domain, corresponding to the CaM-binding region of the channels (Xia et al., 1998) and the Ct2 domain, corresponding to the distal part of the carboxy-terminus containing a leucine zipper motif (Joiner et al., 1997, Joiner et al., 2001, Syme et al., 2003). Thus, in the case of the SK/IK channels it is not entirely clear which part of the channel is essential for the tetrameric assembly, and which parts might instead take part in the intracellular sorting and membrane trafficking.

The biggest difference between the rSK1 and rSK2 subunit sequences lie in their amino- and carboxy-terminal regions. According to the possibility of an amino- and/or carboxy terminus involvement in channel assembly and functional expression, we constructed several chimeric subunits in which the amino- and/or carboxy-region of rSK1 was exchanged. The first chimera rSK1_{N-C_rSK2}, in which both rSK1 amino- and carboxy-termini are exchanged by the corresponding ones of rSK2, assembled and formed functional calcium-activated potassium channels (Fig 3.18F, Fig 3.19D, Fig 3.22). Furthermore, when only the carboxy-terminus of rSK1 was replaced by the carboxy-terminus of rSK2 or hSK1, the resulting rSK1_{C_rSK2} and rSK1_{C_hSK1} assembled into functional K⁺ channels as demonstrated by the K⁺ currents elicited in the presence of calcium (Fig 3.18B, G, Fig 3.19 C, F, Fig 3.22). However, when we exchanged the amino-terminus of rSK1 by the corresponding region of rSK2 or hSK1, no current above background was detected (Fig 3.19 B, E, Fig 3.22), although the protein was expressed (Fig 3.18C). These results show that substitution of the rSK1 carboxy-terminus by rSK2 or hSK1, but not the substitution of the corresponding amino-terminus, is per se sufficient to obtain its functional expression. This suggests that the carboxy-terminus of rSK1 is responsible for the lack of functional rSK1 channel expression. It has been shown that obstruction of CaM binding to the carboxy-terminus of SK channels results in the retention of the channels in the endoplasmic reticulum. Joiner and colleagues showed that interference with the binding of CaM to IK α -subunits, by overexpressing the CaM binding domain Ct1 which then acted as a dominant negative, and therefore decreased the amount of CaM bound to the full length α -subunits, resulted in a decrease of the whole cell current and a redistribution of the IK protein from the cell membrane to the cytoplasm (Joiner et al., 2001). Furthermore, Lee and colleagues demonstrated that when the electrostatic interaction between rSK2 and CaM, at the CaMBD, was disrupted by mutating the responsible amino acids, the rSK2 protein was not expressed anymore

at the cell membrane (Lee et al., 2003). With these findings in mind, we thought that the interaction between CaM and the rSK1 α -subunit was disrupted. Therefore, the channel did not get expressed at the cell surface, and thus no current would be observed. Surprisingly, when we then exchanged the carboxy-terminus of hSK1 with the corresponding part of rSK1, functional channels were observed (Fig 3.21 B, C). This result argues against an impairment of CaM binding and gating solely due to the rSK1 carboxy terminus. By contrast, when we substituted the amino- and the carboxy-termini of hSK1 by the amino- and carboxy-termini of rSK1, functional channel expression was hindered. Thus, substitution of both amino- and carboxy-termini of rSK1 into hSK1 subunits, which normally form functional homomeric channels, hinders their functional expression, which is in good agreement with previous evidence that both amino- and carboxy-termini of SK channels are important for the SK channel assembly and tetramerization (Joiner et al., 2001, Fanger et al., 2001, Miller et al., 2001, Syme et al., 2003 Jones et al., 2004).

Even if the rSK1 carboxy-terminus is able to bind CaM and allow channel gating as revealed by the functional expression of hSK1_{CtSK1}, the role of the carboxy-terminus in assembly might explain the lack of functional expression of homomeric channels. There are several options why rSK1 does not form functional channels. First, rSK1 α -subunits do not assemble properly and as consequence there is no transport of functional homotetrameric channels to the cell membrane. As previously mentioned, there are two important domains in the carboxy-terminus of SK channels which are important for channel assembly, Ct1 and Ct2. When the primary sequence of rSK1 is compared with rSK2 or hSK1, which form functional channels, there is a big difference between the carboxy-termini of the channels. This sequence divergence might affect the proper assembly and/or transport of rSK1 channels to the cell membrane, although the leucine zipper in the Ct2 domain of rSK1 is preserved as well as the ability to bind CaM to the Ct1 domain (functional expression of hSK1_{CtSK1}). Second, membrane expression of rSK1 might require an auxiliary subunit, such as a β -subunit, which acts as a chaperone and targets the channel to the membrane. It has been reported for some Na⁺, Ca²⁺ and K_v channels, that they require a β -subunit in order to increase channel expression at the cell surface (Isom et al., 1994, Shi et al., 1996). The absence of this β -subunit in our expression system could then explain the lack of rSK1 expression. Finally, it is possible that rSK1 subunits acts as other modulatory subunits, also called “silent subunits”. This means that when the subunit is expressed on its own it will not form functional channels, as it is the case for example for K_v6.3, K_v9.3, K_v10.1, K_v11.1 (Kerschensteiner and Stocker, 1999, Ottschytch et al., 2002). However, when such a silent subunit co-assembles with another family member, it forms heteromeric channels with peculiar functional and pharmacological features. Indeed, recently it has been shown that

rSK1 is able to form functional heteromeric channels with rSK2 (Benton et al., 2003). Therefore it would not be unconceivable that such an interaction would occur under native conditions, where the different SK channel subunits are co-expressed in the same cell type (Stocker and Pedarzani, 2000, Sailer et al., 2002).

Pharmacological properties of the rSK1 core chimeras. The difference in apamin and d-tubocurarine sensitivity between SK channels has been attributed to some distinct amino acids in the pore region of the α -subunits (Ishii et al., 1997, Shakkottai et al., 2001). Until now, there was no possibility to investigate the pharmacological properties of rSK1 because it was not functionally expressed. We used our chimeras, rSK1_{N-C_rSK2}, rSK1_{CrSK2} and rSK1_{hSK1}, which formed functional channels (Fig 3.19C, D, F) and contained the core domain (pore region and transmembrane domains) of rSK1, to test the apamin and dTC sensitivity of rSK1. When we applied 100 nM apamin or 50 μ M dTC to these chimeras, no effect was observed (Fig 3.23A-C and Fig 3.24A-C). However, when apamin (10 nM) or dTC (50 μ M) were applied to the chimeras containing the hSK1 core domains, hSK1_{CrSK1} and hSK1_{NrSK1}, the currents generated by the chimeric subunits were blocked (Fig 3.23E, F and Fig 3.24E). This finding was quite surprising, as it was shown that the amino acids, responsible for the difference in sensitivity for apamin and dTC between hSK1 and rSK2, were located in the pore region (Ishii, 1997). However, when the primary amino-acid sequences between rSK1 and hSK1 were compared (Fig 3.15) there was no difference in amino acid sequence in the pore region between rSK1 and hSK1. This would suggest that there is another mechanism involved, which contributes to the drug sensitivity of SK channels. A possible explanation for this sensitivity difference is that amino-acids located outside the pore region may contribute to apamin and dTC binding. This would suggest that the determinants for apamin and dTC binding are most likely located between the S1 and S6 domains. In this region, the rSK1 and hSK1 sequences differ by 16 amino acids.

In conclusion, we showed that the rSK1 protein is synthesized but does not form functional homotetrameric channels. Furthermore, the chimeras with the amino and carboxy termini or with only the carboxy terminus substituted by hSK1 or rSK2 and containing the core rSK1 domain, formed functional channels which were not sensitive to apamin and dTC. Further experiments need to be performed in order to understand the difference in apamin and dTC sensitivity between rSK1 and hSK1 channels.

4.3 Characterization of a novel splice variant of the calcium-activated potassium channel rSK2.

Expression of rSK2-860. The functional, structural and developmental diversity of K⁺ channels is generated by several mechanisms. These include gene diversity, alternative splicing, hetero-tetramerization of α - (pore-forming) subunits, and modulation of pharmacological and gating properties via β - (non-pore-forming) subunits. Alternative splicing is very commonly found among *Drosophila melanogaster* K⁺ channel genes as well as among vertebrate K⁺ channel genes (Timpe et al., 1988, Luneau et al., 1991). Vertebrate BK (large conductance calcium- and voltage-activated potassium channel) channels undergo extensive alternative splicing (Butler et al., 1993). In contrast, alternate transcripts of the IK gene cloned from human (Ishii et al., 1997), rat (Joiner et al., 1997) and mouse (Vandorpe et al., 1998) have not been reported so far. Furthermore, a recent study revealed that the mouse SK1 gene undergoes extensive alternative splicing, resulting in various mSK1 polypeptides (Shmukler et al., 2001).

We showed the existence of a splice variant of the rSK2, called rSK2-860. A RNase protection assay showed that the transcript of this long rSK2 variant is truly existing (Dr. Stocker's personal communication). The transcript exhibits a longer 5' nucleotide sequence which encodes for a longer amino-terminal amino acid sequence. Furthermore, when we expressed the rSK-860 cDNA into different expression systems, we obtained a very distinct expression pattern (Fig 3.27, Fig 3.29 and Fig 3.31) in comparison to the original rSK2 (Fig 3.26, Fig 3.28 and Fig 3.30). These data suggest that the longer amino-terminus of rSK2-860 contains a specific sequence information that is necessary for clustering of the α -subunits in the cell cytoplasm. However, when we examined the primary sequence of the amino-terminus we could not find any specific targeting signal which could be responsible for retention and clustering of the channel subunit. Additionally, co-expression of rSK2-860 with a Golgi marker (pEYFP-Golgi) or a cell membrane marker (pEGFP-F), did not result in an overlap of both proteins. Furthermore, when rSK2-860 was co-stained with a nuclear membrane antibody (anti-lamin A/C), no co-localization was observed. However, an expression profile was made and showed that the rSK2-860 protein clusters are closely located to the nuclear membrane. These data suggest that the protein clusters are located in the perinuclear region.

Truncation and deletion studies of the amino-terminus of rSK2-860. In order to determine which segment in the amino-terminus is responsible for the formation of aggregates at the perinuclear region, we performed several truncation studies. When rSK2-829 and rSK2-795 were expressed in HEK-293 cells, the same expression pattern as with rSK2-860 was observed (Fig 3.35 and Fig 3.36). In contrast, expression of rSK2-695 resulted in a membrane expression

(Fig 3.37) and the formation of functional channels (preliminary electrophysiological data confirm the formation of functional channels activated by Ca^{2+} in the cell membrane). These data suggest that the segment which is responsible for the clustering of the rSK2-860 channel subunit is localized between amino acids 67 and 166, resulting in a hundred amino acid long stretch localized in the middle of the total 275 amino acid longer amino terminus. This finding is in good agreement with the data obtained using the different GFP-tagged amino-terminal regions. All the GFP constructs containing this area in the tagged segment resulted in formation of big clusters (Fig 3.41A₁, B₁, D₁). Furthermore, the SK2-N9 construct, which lacks this segment in the resulting tagged protein, did not result in the formation of aggregates (Fig 3.41C₁). However, one construct was in disagreement with this hypothesis: when construct SK2-N12 was expressed in HEK-293 cells, there was no formation of clusters, although the construct contained a part of the suggested 100 amino acid long stretch. Two possible explanations for this result could be: 1) Although the protein contains 50% of the segment putatively responsible for the clustering, it could be that the signal necessary for clustering is hindered or embedded by the tertiary structure of the GFP-tagged protein; 2) The protein contains the part of the segment which does not include the specific signal for cluster formation. Consequently, the GFP-tagged protein is not forming clusters and shows the diffuse GFP pattern. Therefore, future experiments, such as tagging the proposed 100 amino acid long segment with a GFP-tag, or generating more truncated proteins between rSK2-794 and rSK2-695 in order to narrow down the region responsible for rSK2-860 protein clusters, might give us a better view on the region responsible for cluster formation or reveal a new signal sequence responsible for the retention of the rSK2-860 subunit in the cytoplasm.

Function of rSK2-860. In the past years, researchers have shown that protein clusters in the cell cytoplasm is a response of the cell to misfolded proteins, such as the mutations in $\text{K}_v1.1$ resulting in the formation of protein aggregates and results in a neurological disorder (Manganas et al., 2001). A common feature for protein aggregation is the co-localisation with ubiquitin, which is a signal for the cell to degrade the protein via the proteasome pathway (Ward, 1995, Hicke L, 1997, Hicke and Dunn, 2003, Aguilar and Wendland, 2003, Pickart, 2004). However, when we transfected HEK-293 cells with rSK2-860 or with the originally cloned rSK2 subunits, no co-localisation between the channel proteins and the ubiquitin protein was observed (Fig 3.51). This result suggests that the rSK2-860 gene products are not misfolded protein aggregates targeted to the proteasome for degradation. A similar result was obtained when rSK2-860 aggregates were tested for the formation of aggresomes by co-staining with vimentin. Also in this case, there was no co-localisation of the vimentin protein and the rSK2-860 protein (Fig 3.49).

The following hypothesis could be formulated for the function of the rSK-860 protein clusters. Experiments showed that the rSK2-860 protein was able to interact with the original rSK2 protein (Fig 3.42), and kept it partially “trapped” in the clusters. These data shows that the co-expression of rSK2-860 downregulates the surface expression of the original rSK2 protein in the cell membrane. Therefore, we can assume that the rSK2-860 protein could behave as a dominant negative subunit when it is co-expressed with the original rSK2 protein. If this interaction would also occur *in vivo*, then it could have physiological consequences. As mentioned (see Introduction 1.4), SK channels are contributing to the I_{AHP} in several neurons. Until now it was assumed that the I_{AHP} current, when measured in brain slices or primary cell culture, is the result of the total SK channel pool expressed at the cell membrane of the neuron. However, if, as shown in our experiments, rSK2-860 also interacts with rSK2 *in vivo*, and thus acts as a dominant negative subunit which suppresses a big part of the I_{AHP} current, the observed I_{AHP} current is only the result of a partial expression of the SK channels at the cell membrane of the neuron. Thus, this could have a significant impact on the firing pattern in neurons when this rSK2-860/rSK2 complexes are released and targeted to the membrane, while the firing pattern of neurons is controlled by the I_{AHP} . It has been shown that the firing frequency of neurons can be changed when the I_{AHP} is influenced (Vergara et al., 1998, Pedarzani et al., 2001, Faber et al., 2003). Several mechanisms could be used to target the rSK2-860/rSK2 complexes to the membrane: 1) The complex could be targeted to the membrane after the activation of a secondary pathway. It has been shown that Kv2.1 channels are clustered in the somata and dendrites of cultured neurons. However, when the neurons were subjected to a glutamate stimulation, a relocation of the clusters to the surface of the neuron was observed. The glutamate stimulation induced a Ca^{2+} influx in the cell, which activated the Ca^{2+} -dependent phosphatase, calcineurin. Therefore, dephosphorylation of Kv2.1 resulted in the relocation of the channel to the membrane (Misonou et al., 2004). Similar mechanisms, which activate secondary pathways, such as kinases, proteases or as shown here, phosphatases could be necessary to relocate the complex to the membrane. 2) The clusters need an additional β -subunit to be transported to the cell surface. It has been shown that expression in cells of Kv1.2 results in a perinuclear staining. However, when Kv1.2 is co-expressed with the β -subunit, Kv β 2, the channel is targeted to the membrane (Shi et al., 1996). Therefore, it might be possible that rSK2-860 clusters are relocated to the surface upon interaction with a β -subunit, which has not been identified yet. Future experiments, such as yeast-two hybrid screens could reveal the existence of a β -subunit which could be the chaperone for rSK2-860 channels. Furthermore, we will investigate how this protein acts in native systems such as in neurons in culture.

In conclusion, we found a new splice variant of the rSK2 channel, which displays a very distinct expression pattern in comparison with the originally cloned rSK2 channel. Furthermore, we partially narrowed down the region responsible for the clustering of the α -subunit of rSK2-860. We hypothesize a possible physiological role for this α -subunit.

Abbreviations

A	Ampere
AHP	Afterhyperpolarization
bp	basepairs
CaM	calmodulin
CaMBD	calmodulin binding domain
CHO	Chinese hamster ovary cells
COS	African green monkey kidney cells
CTX	charybdotoxin
dTC	d-tubocurarine
EBIO	1-ethyl-2-benzimidazolinone
EC ₅₀	half maximal excitatory concentration
EF hands	calcium binding domains
EGTA	Ethylenglycol-bis(β-aminoethylether-)-N,N,N',N'-Tetra acetic acid
ER	endoplasmatic reticulum
g	gram
HEK	human embryonic kidney cells
HEPES	N-2-Hydroxyethylpiperazine-N'-2ethane-sulfonic acid
hSK1 (K _{Ca} 2.1)	small-conductance calcium-activated potassium channel from human
IC ₅₀	half maximal inhibitory concentration
I _{AHP}	afterhyperpolarization current
K _{Ca}	calcium-activated potassium channel
K _V	voltage-gated potassium channel
l	liter
M	molar
mAHP	medium afterhyperpolarization
min	minutes
PCR	polymerase chain reaction
RT	room temperature
rSK1 (K _{Ca} 2.1)	small-conductance calcium-activated potassium channel from rat
rSK2 (K _{Ca} 2.2)	small-conductance calcium-activated potassium channel from rat
rSK3 (K _{Ca} 2.3)	small-conductance calcium-activated potassium channel from rat
s	seconds
S	Siemens

sAHP	slow afterhyperpolarization
sI_{AHP}	slow afterhyperpolarization current
V	volt
V_m	membrane potential

Appendix

Amino acid sequences of the cloned SK channels

1.1. hSK1

MNSHSYNGSV	GRPLGSGPGA	LGRDPPDPEA	GHPPQPPHSP	GLQVVAKSE	50
PARSPGSPR	GPODQDDDE	DDEEDEAGRQ	RASGKPSNVG	HRLGHRRALF	100
EKRKRLSDYA	LIFGMFGIVV	MVTETELSWG	VYTKESLYSF	ALKCLISLST	150
ATLLGLVVLV	HAREIQLFMV	DNGADDWRIA	MTCERVFLIS	LELAVCATHP	200
VPGHYRFTWT	ARLAFTYAPS	VAEADVDVLL	SIPMFLRLYL	LGRVMLLHSH	250
IFTDASSRSI	GALNKITFNT	RFVMTLMTI	CPGIVLLVFS	ISSWIIAAWT	300
VRVCERYHDK	QEVTSNFLGA	MWLISITFLS	IGYGMVPHT	YCGKGVCLLT	350
GIMGAGCTAL	VVAVVARKLE	LTKAEKHVHN	FMMDIQLTKR	VKNAAANVLR	400
ETWLIYKHTR	LVKKPDQARV	RKHQRKFLQA	IHQAKLRSV	KIEQKGLNDQ	450
ANTLTDLAKT	QTVMYDLVSE	LHAQHEELEA	RLATLESRLD	ALGASLQALP	500
GLIAQAIRPP	PPPLPPRPGP	GPODQAARSS	PCRWTVPAPS	DCG	543

1.2. rSK1

MSSRSHNGSV	GRPLGSGPGF	LGWEPVDPEA	GRPRQPTQGP	GLQMMAKGQP	50
AGLSPSGPRG	HSQAQEEEE	EEDEDPRGSG	KPPTVSHRLG	HRRALFEKPK	100
RLSDYALIFG	MFGIVVMVTE	TELSWGVYTK	ESLCSFALKC	LISLSTVILL	150
GLVILYHARE	IQLFLVDNGA	DDWRIAMIWE	RVSLISLELA	VCAIHPVPGH	200
YRFTWTARLA	FSLVPSAAEA	DVDVLLSIPM	FLRLYLLARV	MLLHSRIFTD	250
ASSRSIGALN	RVTFNIRFVT	KILMTICPGT	VLLVFSISSW	IVAAWIVRVC	300
ERYHDKQEV	SNFLGAMWLI	SITFLSIGYG	DMVPHTYCGK	GVCLLTGIMG	350
AGCTALVVAV	VARKLELTKA	EKHVHNFMD	TQLTKRVKNA	AANVLRRETWL	400
IYKHTRLVKK	PDQSRVRKHQ	RKFLQAIHQA	QKLRTVKIEQ	GKVNDQANTL	450
ADLAKAQSTIA	YEVVSELQAQ	QEELEARLAA	LESRLDVLGA	SLQALPSLIA	500
QAICPLPPPWW	PGPSHLITAA	QSPQSHWLP	TASDCG		536

1.3. rSK2

MSSCRYNGGV	MRPLSNLSSS	RRNLHEMDSE	AQPLQPPASV	VGGGGGASSP	50
SAAAAASSSA	PEIVVSKPEH	NNSNNLALYG	TGGGGSTGGG	GGGGGGGGGS	100
GHGSSSGTKS	SKKKNQNIY	KLGHRRALFE	KRKRLSDYAL	IFGMFGIVVM	150
VIETELSWG	YDKASLYSLA	LKCLISLSTI	ILLGLIIVYH	AREIQLFMVD	200
NGADDWRIAM	TYERIFFICL	EILVCAIHPI	PGNYTFIWTIA	RLAFSYAPST	250
TTADVDIILS	IPMFLRLYLI	ARVMLLHSHL	FTDASSRSIG	ALNKINFNTR	300
FVMKTLMTIC	PGTVLLVFSI	SLWIIAAWTV	RACERYHDQ	DVTSNFLGAM	350
WLISITFLSI	GYGDMVPNTY	CGKGVCLLTG	IMGAGCTALV	VAVVARKLEL	400

TKAEKHVHNF	MMDTQLTKRV	KNAAANVLRE	TWLIYKNTKL	VKKIDHAKVR	450
KHQRKFLQAI	HQLRSVKMEQ	RKLNDQANTL	VDLAKTQNM	YDMISDLNER	500
SEDFEKRIVT	LETKLETLIG	SIHALPGLIS	QTIRQQQDF	IETQMENYDK	550
HVTYNAERSR	SSSRRRRSS	TAPPTSSESS			580

1.4. rSK3

MDTSGHFHDS	GVGDLDEDPK	CPCPSSGDEQ	QQQQQPPPPS	APPAVPOQPP	50
GPLLQOPPPQ	LQOQOQOQOQ	QOQOQOQOQO	APLHPLPQLA	QLQSOLVHPG	100
LLHSSPTAFR	APNSANSTAI	LHPSSRQGSQ	LNLNDHLLGH	SPSSTATSGP	150
GGGSRHRQAS	PLVHRRDSNP	FTEIAMSSCK	YSGGVMKPLS	RLSASRRNLI	200
EAEPEGQPLQ	LFSPSNPPEI	IISREDNHA	HQTLHHPNA	THNHQAGTT	250
AGSTTFPKAN	KRKNQNIQYK	LGHRRALFEK	RKRLSDYALI	FGMFGIVVMV	300
IETELSWGLY	SKDSMFSLAL	KCLISLSTII	LLGLIAYHT	REVQLFVIDN	350
GADDWRIAMT	YERILYISLE	MLVCAIHPIP	GEYKFFWTAR	LAFSYTPSRA	400
EADVDIILSI	PMFLRLYLIA	RVMLLHSKLF	TDASSRSIGA	LNKINFNTRF	450
VMKTLMTICP	GTVLLVFSIS	LWIIAAWIVR	VCERYHDQOD	VTSNFLGAMW	500
LISITFLSIG	YGDMVPHTYC	GKGVCLLTGI	MGAGCTALVV	AVVARKLELT	550
KAEKHVHNF	MDTQLTKRIK	NAAANVLRET	WLIYKHTKLL	KKIDHAKVRK	600
HQRKFLQAIH	QLRGVKMEQR	KLSDQANTLV	DLSKMQNVMY	DLITELNDRS	650
EDLEKQIGSL	ESKLEHLTAS	FNSLPLLIAD	TLRQQQQQLL	TAFVEARGIS	700
VAVGTSHAPP	SDSPIGISST	SFPTPYTSSS	SC		732

Amino acid sequence alignments

2.1. Alignment of hSK1, rSK2 and rSK3 protein sequences

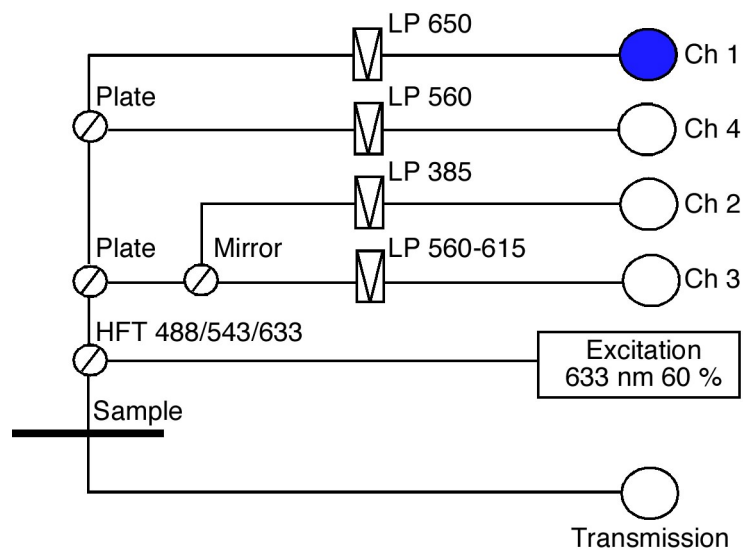
hSK1	MNSHS-YNGSVGRPLGSSG-----GALGRDPPDPEAGHPPQPPHSPGLQVVAKSEPARPSPGSPR	60	
rSK2	MSSC-RYNGGVMRPLSN-----LSSRRNLHEMDSEAQ-	32	
rSK3	MDTSGHFHDSGVGDLDEDPKCPSPSSGDEQ0000QPPPPSAPPVAPQPPGPLLQPPQLQ00000000	70	
hSK1	GQPQDQDDDE-----	70	
rSK2	-----PLQP-----PASVVGGGGGASSPSAAAAASSAPEIVVSKPEHNNNSN-NLA--LYGT	81	
rSK3	0000000000APLHPLPQLAQLQSQLVHPGLLHSSPTAFRAPNSANSTAILHPSRQGSQLNLDHLLGH	140	
hSK1	-----DDEEDEAGRQRASG-----	84	
rSK2	GGGGSTGGGGGGG-----GGG-----	98	
rSK3	SPSSTATSGPGGSRHRQASPLVHRSDSNPFTEIAMSSCKYSGGVMKPLSRLSASRRNLIEAPEGOPLQ	210	
hSK1	-----KPSNVGHR LGHRRALFEK	102	
rSK2	-----GSGHGSSSGTKSSKKKQNIQYK LGHRRALFEK	131	
rSK3	LFSPSNPPEIISSREDNHAHQTLHHPNATHNHQHAGTTAGSTTFPKANKRKNQNIQYK LGHRRALFEK	280	
	S1	S2	
hSK1	RKRLSDYALIFGMFGIVVMVITETELSWGVTIKESLYSALKCLISLSTAILLGLVWLYHAREIQLFMVDN	172	
rSK2	RKRLSDYALIFGMFGIVVMVITETELSWGAYDKASLYSALKCLISLSTAILLGLIIVYHAREIQLFMVDN	201	
rSK3	RKRLSDYALIFGMFGIVVMVITETELSWGYSKDSVFSALKCLISLSTAILLGLIAYHAREIQLFVIDN	350	
	S3	S4	
hSK1	GADDWRIAMTCERVFLISLEAVCAIHPVPGHYRFTWTARLAFIYAPSVAEADVDVLSIPMFLRLYL LG	242	
rSK2	GADDWRIAMTYERITFFILEILLVCAIHPVPGNYRFTWTARLAFSYAPSTTTADVDIISIPMFLRLYL IA	271	
rSK3	GADDWRIAMTYERILYISLEMLVCAIHPVPGEYRFTWTARLAFSYTPSRAEADVDIISIPMFLRLYL IA	420	
	S5		
hSK1	RVMLLHSKLFTDASSRSIGALNKIIFNTRFVMKTLMTICPGTVLLVFSISLWIIAAWTVRCERYHDQDE	312	
rSK2	RVMLLHSKLFTDASSRSIGALNKIIFNTRFVMKTLMTICPGTVLLVFSISLWIIAAWTVRACERYHDQDD	341	
rSK3	RVMLLHSKLFTDASSRSIGALNKIIFNTRFVMKTLMTICPGTVLLVFSISLWIIAAWTVRCERYHDQDD	490	
	P-region	S6	
hSK1	VTSNFLGAMWLLISITFLSTGYGDMVPHYCYCGKGVCLLTGIMGAGCTALVVAVVARKLELTKAEKHVHNF	382	
rSK2	VTSNFLGAMWLLISITFLSTGYGDMVPHNYCYCGKGVCLLTGIMGAGCTALVVAVVARKLELTKAEKHVHNF	411	
rSK3	VTSNFLGAMWLLISITFLSTGYGDMVPHYCYCGKGVCLLTGIMGAGCTALVVAVVARKLELTKAEKHVHNF	560	
hSK1	MDTQLTKRDKNAANANVLRETWLIYKHTLWKKPDQARVRKHQRKFLQAIHQAKLRSVKTEQKLNLDQAN	452	
rSK2	MDTQLTKRDKNAANANVLRETWLIYKNTLWKKIDAKVRKHQRKFLQAIHQ---LRSVKTEQRKLNLDQAN	478	
rSK3	MDTQLTKRDKNAANANVLRETWLIYKHTLWKKIDAKVRKHQRKFLQAIHQ---LRGKVEQRKLNLDQAN	627	
hSK1	TLVDLAKTQTVMYDLVSELAHQHELEEARLATLESRLDALGASLQALPGLIAQAIRPPPPPL-----	514	
rSK2	TLVDLAKIQNIYDMISDLNERSDFEKRIVLETKLETIGSIHALPGLISQTIROQQRDFIETQMENY	548	
rSK3	TLVDLSKIQNVMYDLITEINDRSEDLKQIGSLESKLEHTASNSLPLEIADTLR0000LLTAFVEAR	697	
hSK1	-----PPRPGPGPDQAAARSSPCRWTPVAPSDCG	543	
rSK2	DKHVTYNAERSRSSRRRRSSSTAPPT---SSSS	580	
rSK3	GISVAVGTSHAPPSDSPIGISSSFPTPYTSSSSC	732	

Black boxes correspond with the amino acids which differ between the three aligned sequences. The yellow boxes (S1-S6) present the 6 transmembrane domains, and the green corresponds with the pore region (P-region), in the α -subunit. AS observed from this alignment, there is a high difference between the amino- and carboxy-termini of the subunits.

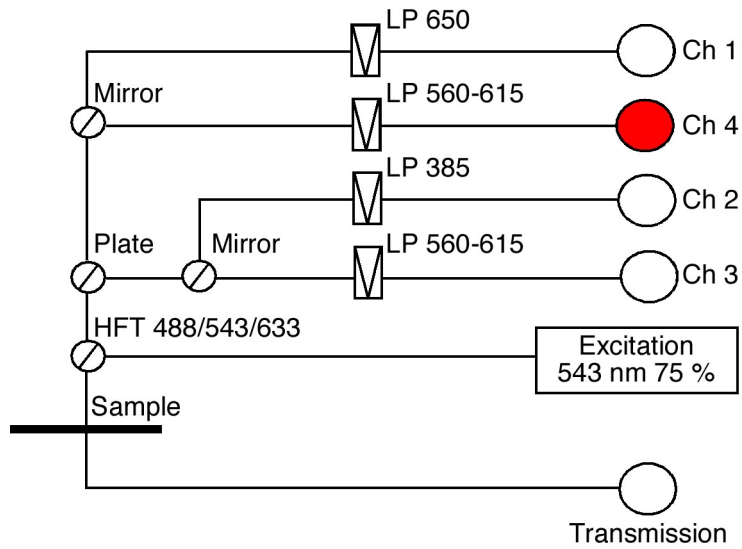
Configuration for the LSM software of the confocal microscope.

In order to detect fluorescent signals using a confocal microscope (LSM 510), several scan modules had to be programmed, as shown below. For colocalization experiments, pictures were obtained in the multitrack mode. In this mode, 2 different fluorescence signals can be detected, used modes were GFP/Cy3, YFP/Cy5 and Cy3/Cy5. Samples with Cy5 were excited using a HeNe laser 633 nm, those with Cy3 were excited with a HeNe laser 543 nm. To detect signals from samples containing EGFP or EYFP, they had to be excited with an Ar laser with wavelength 458, 477, 488 and 514 nm. To avoid cross-talk between different secondary antibodies, the right filter sets had to be put in place. HFT and NFT are dichroic mirrors, HFT separates excitation (laser) and emission light (fluorescence), while NFT effects spectral division of fluorescence light (e.g. NFT 545: reflects light of $\lambda < 545$ nm and transmits light of $\lambda > 545$ nm). Furthermore, LP (long pass) and BP (band pass) filters were also incorporated in the fluorescence light path.

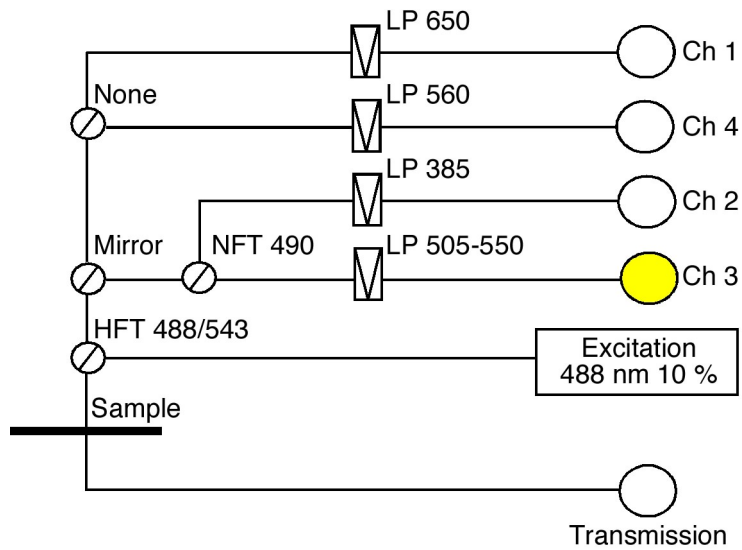
Settings for detection of the Cy5 secondary antibody:



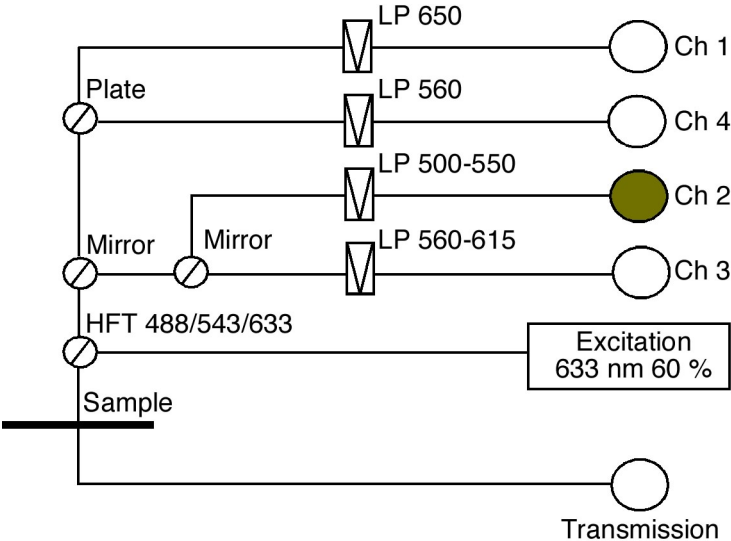
Settings for the detection of the Cy3 secondary antibody:



Settings for the detection of the EYFP tagged proteins.



Settings for EGFP tagged proteins, or for the secondary antibody FITC



Reference table:

Adelman J.P., Shen K.Z., Kavanaugh M.P., Warren R.A., Wu Y.N., Lagrutta A., Bond C.T., North R.A., Calcium-activated potassium channels expressed from cloned complementary DNAs, 1992, *Neuron*, 9, 209-16

Adrian R.H., Rectification in muscle membrane, 1969, *Prog. Biophys. Mol. Biol.*, 19, 340-369

Aguilar R.C. and Wendland B., Ubiquitin: not just for proteasomes anymore, 2003, *Curr. Opin. Cell Biol.*, 184-190

Alves-Rodriguez A., Gregori L., Figueiredo-Pereira M.E., Ubiquitin, cellular inclusions and their role in neurodegeneration, 1998, *Trends Neurosci.*, 21, 516-20

Atkinson N.S., Robertson G.A. and Ganetzky B., A component of calcium-activated potassium channels encoded by the *Drosophila slo* locus, 1991, *Science*, 253, 551-555

Auguste P., Hugues M., Grave B., Gesquiere J.C., Maes P., Tartar A., Romey G., Schweitz H., Lazdunski M., Leiurotoxin I (Scyllatoxin), a peptide ligand for Ca^{2+} -activated K^+ channels, 1990, *JBC*, 265, 4753-4759

Auguste P., Hugues M., Mourre C., Moinier D., Tartar A., Lazdunski M., Scyllatoxin, a blocker of Ca^{2+} -activated K^+ channels: Structure-function relationship and brain localization of the binding sites, 1992, *Biochem.*, 31, 648-654

Bakke O., Dobberstein B., MHC class II-associated invariant chain contains a sorting signal for endosomal compartments, 1990, *Cell*, 63, 707-16

Barhanin J., Lesage F., Guillemare E., Fink M., Lazdunski M., Romey G., K(V)LQT1 and *IsK* (*minK*) proteins associate to form the *I(Ks)* cardiac potassium current, 1996, *Nature*, 384, 78-80

Benton D.C.H., Monaghan A.S., Hosseini R., Bahia P.K., Haylett D.G. and Moss G.W., Small conductance Ca^{2+} -activated K^+ channels formed by the expression of rat SK1 and SK2 genes in HEK 293 cells, 2003, *J. Physiol.*, 553.1, 13-19

Bishop N., Horman A., Woodman P., Mammalian class E vps proteins recognize ubiquitin and act in the removal of endosomal protein-ubiquitin conjugates, 2002, *J. Cell Biol.*, 157, 91-101

Boettger M.K., Till S., Chen M.X., Anand U., Otto W.R., Plumpton C., Trezise D.J., Tate S.N., Bountra K., Coward K., Birch R. and Anand P., Calcium-activated potassium channel SK1- and IK1-like immunoreactivity in injured human sensory neurons and its regulation by neurotrophic factors, 2002, *Brain*, 125, 252-263

Bond C.T., Pessia M., Xia X.M., Lagrutta A., Kavanaugh M.P., Adelman J.P., Cloning and expression of a family of inward rectifier potassium channels, 1994, *Receptors Channels*, 2, 186-91

- Boussif O., Lezoualc'h F., Zanta M.A., Mergny M.D., Scherman D., Demeneix B., Behr J.P., A versatile vector for gene and oligonucleotide transfer into cells in culture and in vivo: polyethylenimine, 1995, PNAS, 92, 7297-301
- Bowden S.E.H., Fletcher S., Loane D.J. and Marrion N.V., Somatic colocalization of rat SK1 and D class (Ca_v 1.2) L-type calcium channels in rat CA1 hippocampal pyramidal neurons, 2001, J. Neurosci., 21, RC175 1-6
- Bredt D.S., Wang T.L., Cohen N.A., Guggino W.B., Snyder S.H., Cloning and expression of two brain-specific inwardly rectifying potassium channels, 1995, PNAS, 92, 6753-7
- Bruening-Wright A., Schumacher M.A., Adelman J.P. and Maylie J., Localization of the activation gate for small conductance Ca^{2+} -activated K^+ channels, 2002, J. Neurosci., 22, 6499-6506
- Calabro V., Sabatier J.M., Blanc E., Lecomte C., Van Rietschoten J. and Darbon H., Differential involvement of disulfide bridges on the folding of a scorpion toxin, 1997, J. Peptide Res., 50, 39-47
- Cao Y., Dreixler J.C., Roizen J.D., Roberts M.T., Houamed K.M., Modulation of recombinant small-conductance $Ca(2+)$ -activated $K(+)$ channels by the muscle relaxant chlorzoxazone and structurally related compounds, 2001, J. Pharmacol. Exp. Ther., 296, 683-9
- Cao Y.J., Dreixler J.C., Couey J.J., Houamed K.M., Modulation of recombinant and native neuronal SK channels by the neuroprotective drug riluzole, 2002, Eur. J. Pharmacol., 449, 47-54
- Capener C.E., Kim H.J., Arinaminpathy Y. and Sanson M.S.P., Ion channels: structural bioinformatics and modeling, 2002, Hum. Mol. Gen., 11, 2425-2433
- Castle N.A. and Strong P.N., Identification of two toxins from scorpion (*Leiurus quinquestriatus*) venom which block distinct classes of calcium-activated potassium channel, 1986, FEBS Lett., 209, 117-21
- Castle N.A., London D.O., Creech C., Fajloun Z., Stocker J.W. and Sabatier J.-M., Maurotoxin: A potent inhibitor of intermediate conductance Ca^{2+} -activated potassium channels, 2003, Mol. Pharmacol., 63, 409-418
- Castellino R.C., Morales M.J., Strauss H.C., Rasmusson R.L., Time- and voltage-dependent modulation of a $Kv1.4$ channel by a beta-subunit (Kv beta 3) cloned from ferret ventricle, 1995, Am. J. Physiol., 269, H385-91
- Chen C. and Okayama H., High efficiency transformation of mammalian cells by plasmid DNA, 1987, Mol. Cell. Biol., 7, 2745-275
- Chicchi G.G., Gimenez-Gallego G., Ber E., Garcia M.L., Winkquist R., Cascieri M.A., Purification and characterization of an unique, potent inhibitor of apamin binding from *Leiurus quinquestriatus* hebraeus venom, 1988, JBC, 263, 10192-10197
- Cui J., Mandel G., DiFrancesco D., Kline R.P., Pennefather P., Datyner N.B., Haspel H.C., Cohen I.S., Expression and characterization of a canine hippocampal inwardly rectifying K^+ current in *Xenopus* oocytes, 1992, J. Physiol., 457, 229-46

- Dale T.J., Cryan J.E., Chen M.X., Trezise D.J., Partial apamin sensitivity of human small conductance Ca^{2+} -activated K^+ channels stably expressed in Chinese hamster ovary cells, 2002, *Naunyn-Schmiedeberg's Arch. Pharmacol.*, 366, 470-477
- Deal K.K., Lovinger D.M., Tamkun M.M., The brain Kv1.1 potassium channel: in vitro and in vivo studies on subunit assembly and posttranslational processing, 1994, *J. Neurosci.*, 14, 1666-76
- Desai R., Peretz A., Idelson H., Lazarovici P. and Attali B., Ca^{2+} -activated K^+ channels in human Leukemic Jurkat T cells, 2000, *JBC*, 275, 39954-39963
- Devor D.C., Singh A.K., Frizzell R.A., Bridges R.J., Modulation of Cl^- secretion by benzimidazolones. I. Direct activation of a Ca^{2+} -dependent K^+ channel, 1996, *Am. J. Physiol.*, 271, 775-84
- D'hoedt D., Hirzel K., Pedarzani P. and Stocker M., Domain analysis of the Calcium-activated potassium channel SK1 from rat brain, 2004, *JBC*, 279, 12088-12092
- Doms R.W., Russ G., Yewdell J.W., Brefeldin A redistributes resident and itinerant Golgi proteins to the endoplasmic reticulum, 1989, *J. Cell Biol.*, 109, 61-72
- Dreixler J.C., Bian J.-T., Cao Y.-J., Roberts M.T., Roizen J.D., Houamed K. M., Block of rat brain recombinant SK channels by tricyclic antidepressants and related compounds, 2000, *Eur. J. Pharm.*, 401, 1-7
- Dunn P.M., Dequalinium, a selective blocker of the slow afterhyperpolarization in rat sympathetic neurons in culture, 1994, *Eur. J. Pharm.*, 252, 189-194
- Dunn P.M., UCL 1684: a potent blocker of Ca^{2+} -activated K^+ channels in rat adrenal chromaffin cells in culture, 1999, *Eur. J. Pharm.*, 368, 119-123
- Doyle A.D., Cabral J.M., Pfuetzner R.A., Kuo A., Gulbis J.M., Cohen S.L., Chai B.T., MacKinnon R., The structure of the potassium channel: Molecular basis of K^+ conduction and selectivity, 1998, *Science*, 280, 69-77
- Duprat F., Lesage F., Fink M., Reyes R., Heurteaux C., Lazdunski M., TASK, a human background K^+ channel to sense external pH variations near physiological pH, 1997, *EMBO*, 16, 5464-71
- Fanger C.M., Ghanshani S., Logsdon N.J., Rauer H., Kalman K., Zhou J., Beckingham K., Chandy K.G., Cahalan M.D., Aiyar J., 1999, *JBC*, 274, 5746-54
- Fanger C.M., Rauer H., Neben A.L., Miller M.J., Rauer H., Wulff H., Rosa J.C., Ganellin C.R., Chandy K.G. and Cahalan M.D., Calcium-activated potassium channels sustain calcium signaling in the T Lymphocytes, 2001, *JBC*, 276, 12249-12256
- Fink M., Duprat F., Lesage F., Reyes R., Romey G., Heurteaux C., Lazdunski M., Cloning, functional expression and brain localization of a novel unconventional outward rectifier K^+ channel, 1996, *EMBO*, 15, 6854-62

- Fink M., Duprat F., Lesage F., Heurteaux C., Romey G., Barhanin J., Lazdunski M., A new K⁺ channel beta subunit to specifically enhance Kv2.2 (CDRK) expression, 1996, *JBC*, 271, 26341-8
- Galvez A., Gimenez-Gallego G., Reuben J.P., Roy-Contancin L., Feigenbaum P., Kaczorowski G.J., Garcia M.L., Purification and characterization of a unique, potent, peptidyl probe for the high conductance calcium-activated potassium channel from venom of the scorpion *Buthus tamulus*, 1990, *JBC*, 265, 11083-90
- Gao X., Huang L., A novel cationic liposome reagent for efficient transfection of mammalian cells, 1991, *Biochem. Biophys. Res. Commun.*, 179, 280-5
- Grunnet M., Jespersen T., Angelo K., Frokjaer-Jensen C., Klaerke D.A., Olesen S.P., Jensen B.S., Pharmacological modulation of SK3 channels, 2001, *Neuropharm.*, 40, 879-887
- Grunnet M., Jensen B.S., Olesen S.P., Klaerke D.A., Apamin interacts with all subtypes of cloned small-conductance Ca²⁺-activated K⁺ channels, 2001, *Pflug. Arch.*, 441, 544-550
- Habermann E., Bee and wasp venoms, 1972, *Science*, 177, 314-322
- Habermann E. and Fischer K., Bee venom neurotoxin (apamin): iodine labeling and characterization of binding sites, 1979, *Eur. J. Biochem.*, 94, 355-64
- Hamill O.P., Marty A., Neher E., Sakmann B., Sigworth F.J., Improved patch-clamp techniques for high-resolution current recording from cells and cell-free membrane patches, 1981, *Plügers Arch.*, 392, 85-100
- Heginbotham L., Lu Z., Abramson T., and MacKinnon R, A functional connection between the pores of distantly related ion channels as revealed by mutant K⁺ channels, 1992, *Science*, 258, 1152-5
- Heginbotham L., Lu Z., Abramson T., and MacKinnon R, Mutations in the K⁺ channel signature sequence, 1994, 1061-1067
- Heinemann S., Rettig J., Scott V., Parcej D.N., Lorra C., Dolly J., Pongs O., The inactivation behaviour of voltage-gated K-channels may be determined by association of alpha- and beta-subunits, 1994, *J. Physiol. Paris*, 88, 173-80
- Hicke L., Ubiquitin-dependent internalization and down-regulation of plasma membrane proteins, 1997, *FASEB*, 11, 1215-26
- Hicke L. and Dunn R., Regulation of membrane protein transport by ubiquitin and ubiquitin-binding proteins, 2003, *Annu. Rev. Cell Dev. Biol.*, 19, 141-72
- Hirschberg B., Maylie J., Adelman J.P. and Marrion N.V., gating of recombinant small-conductance Ca-activated K⁺ channels by calcium, 1998, *J. Gen. Physiol.*, 111, 565-581
- Hopkins W.F., Demas V., Tempel B.L., Both N- and C- terminal regions contribute to the assembly and functional expression of homo- and heteromultimeric voltage-gated K⁺ channels, 1994, *J. Neurosci.*, 14, 1385-93

Hosseini R., Benton D.C., Dunn P.M., Jenkinson D.H., Moss G.W., SK3 is an important component of K⁺ channels mediating the afterhyperpolarization in cultured rat SCG neurons, 2001, *J. Physiol.*, 535, 323-34

Ishii T.M., Maylie J. and Adelman J.P., Determinants of apamin and d-Tubocurarine block in SK potassium channels, 1997, *JBC*, 272, 23195-23200

Ishii T.M., Silvia C., Hirschberg B., Bond C.T., Adelman J.P., Maylie J., A human intermediate conductance calcium-activated potassium channel, 1997, *PNAS*, 94, 11651-11656

Isom L.L., De Jongh K.S., Catterall W.A., Auxiliary subunits of voltage-gated ion channels, 1994, *Neuron*, 12, 1183-94

Jan L.Y., Jan Y.N., How might the diversity of potassium channels be generated?, 1990, *Trends Neurosci.*, 13, 415-9

Jana NR, Nulina N, Recent advances in understanding the pathogenesis of polyglutamine diseases: involvement of molecular chaperones and ubiquitin-proteasome pathway, 2003, *J. Chem. Neuroanat.*, 26, 95-101

Jensen B.S., Strobaek D., Christophersen P., Jorgensen T.D., Hansen C., Silaharoglu A., Olesen S.P., Ahring P.K., Characterization of the cloned human intermediate-conductance Ca²⁺-activated K⁺ channel, 1998, *Am. J. Physiol.*, 275, C848-56

Jiang B., Sun X., Wang R., Endogenous Kv channels in human embryonic kidney (HEK-293) cells, 2002, *Mol., Cell Biochem.*, 238, 69-79

Johnston J.A., Ward C.L., Kopito R.R., Aggresomes: a cellular response to misfolded proteins, 1998, *J. Cell Biol.*, 143, 1883-1898

Joiner W.J., Wang L.Y., Tang M.D., Kaczmarek L., hSK4, A member of a novel subfamily of calcium-activated potassium channels, 1997, *PNAS*, 94, 11013-11018

Joiner W.J., Khanna R., Schlichter L.C., Kaczmarek L.K., Calmodulin regulates assembly and trafficking of SK4/IK1 Ca²⁺-activated K⁺ channels, 2001, 276, 37980-5

Jones H.M., Hamilton K.L., Papworth G.D., Syme C.A., Watkins S.C., Bradbury N.A. and Devor D.C., Role of the NH₂ terminus in the assembly and trafficking of the intermediate conductance Ca²⁺-activated K⁺ channel hIK1, 2004, *JBC*, 279, 15531-15540

Ju M., Stevens L., Leadbitter E. and Wray D., The roles of N- and C-terminal determinants in the activation of the Kv2.1 potassium channel, 2003, *JBC*, 278, 12769-12778

Kaczorowski G.J., Knaus H.G., Leonard R.J., McManus O.B., Garcia M.L., High-conductance calcium-activated potassium channels; structure, pharmacology, and function, 1996, *J. Bioenerg. Biomembr.*, 28, 255-67

- Kaczorowski G.J. and Garcia M.L., Pharmacology of voltage-gated and calcium-activated potassium channels, 1999, *Curr. Opin. Chem. Biol.*, 3, 448-458
- Keen J.E., Khawaled R., Farrens D.L., Neelands T., Rivard A., Bond C.T., Janowsky A., Fakler B., Adelman J.P. and Maylie J., Domains responsible for constitutive and Ca²⁺-dependent interactions between calmodulin and small-conductance Ca²⁺-activated potassium channels, 1999, *J. Neurosci.*, 19, 8830-8838
- Kerschensteiner D, Stocker M., Heteromeric assembly of Kv2.1 with Kv9.3: effect on the state dependence of inactivation, 1999, 77, 248-57
- Ketchum K.A., Joiner W.J., Sellers A.J., Kaczmarek L.K., Goldstein S.A., A new family of outwardly rectifying potassium channel proteins with two pore domains in tandem, 1995, *Nature*, 376, 690-5
- Khawaled R., Bruening-Wright, Adelman J.P., Maylie J., Bicuculline block of the small-conductance calcium-activated potassium channels, 1999, *Eur. J. Physiol.*, 438, 314-321
- Kim S., Nollen E.A.A., Kitagawa K., Bindokas V.P. and Morimoto R.I., Polyglutamine protein aggregates are dynamic, 2002, *Nat. Cell Biol.*, 4, 826-831
- Kobertz W.R. and Miller C., K⁺ channels lacking the 'tetramerization' domain: implications for pore structure, 1999, *Nat. Struct. Biol.*, 6, 1122-1125
- Kohler M., Hirschberg B., Bond C.T., Kinzie J.M., Marrion N.V., Maylie J., Adelman J.P., Small conductance, calcium activated potassium channels from mammalian brain, 1996, *Science* 273, 1709-1714
- Kopito R.R., ER quality control: the cytoplasmic connection, 1997, *Cell*, 88, 427-430
- Lee T.E., Philipson L.H., Kuznetsov A., Nelson D.J., Structural determinant for assembly of mammalian K⁺ channels, 1994, *Biophys. J.*, 66, 667-73
- Lee A., Zhou H., Scheuer T., Catterall W.A., Molecular determinants of Ca(2+)/calmodulin-dependent regulation of Ca(v)2.1 channels, 2003, *PNAS*, 100, 16059-64
- Lee W.-S., Ngo-Anh T. J., Bruening-Wright A., Maylie J., Adelman J.P., Small conductance Ca²⁺-activated K⁺ channels and calmodulin, 2003, *JBC*, 278, 25940-25946
- Linial M., Proline clustering in proteins from synaptic vesicles, 1994, *Neuroreport*, 5, 2009-15
- Lippincott-Schwartz J., Yuan L.C., Bonifacino J.S., Klausner R.D., Rapid redistribution of Golgi proteins into the ER in cells treated with brefeldin A: evidence for membrane cycling from Golgi to ER, 1989, *Cell*, 56, 801-13
- Logsdon N.J., Kang J., Togo J.A., Christian E.P., Aiyar J., A novel gene, hKCa4, encodes the calcium-activated potassium channels, 1997, *JBC*, 272, 32723-32726
- MacKinnon R., Determination of the subunit stoichiometry of Shaker potassium channel inactivation, 1991, *Nature*, 350, 232-235

MacKinnon R., New insights into the structure and function of potassium channels, 1991, *Curr. Opin. Neurobiol.*, 1, 14-19

Madison D.V., Nicoll R.A., Noradrenaline blocks accommodation of pyramidal cell discharge in the hippocampus, 1982, *Nature*, 299, 636-8

Madison D.V., Nicoll R.A., Control of the repetitive discharge of rat CA 1 pyramidal neurones in vitro, 1984, *J. Physiol.*, 354, 319-31

Maylie J., Bond C.T., Herson P.S., Lee W.S., Adelman J.P., Small conductance Ca^{2+} -activated K^{+} channels and calmodulin, 2003, *J. Physiol.*, 554.2, 255-261

Margeta-Mitrovic M., Jan Y.N. and Jan L.Y., A trafficking checkpoint controls $GABA_B$ receptor heterodimerization, 2000, *Neuron*, 97-106

Marinelli S., Bernardi G., Giacomini P., Mercuri N.B., Pharmacological identification of the K^{+} currents mediating the hypoglycemic hyperpolarization of rat midbrain dopaminergic neurons, 2000, *Neuropharmacology*, 39, 1021-8

Marty A., Blocking of large unitary calcium-dependent potassium currents by internal sodium ions, 1983, *Pflugers Arch.*, 396, 179-81

Martins J.C., Zhang W., Tartar A., Lazdunski M., Borremans F.A., Solution conformation of leiurotoxin I (scyllatoxin) by 1H nuclear magnetic resonance, 1990, *FEBS Lett.*, 260, 249-253

Martins J.C., Van de Ven F.J., Borremans F.A., Determination of the three-dimensional solution structure of scyllatoxin by 1H nuclear magnetic resonance, 1995, *J. Mol. Biol.*, 1995, 253, 590-603

McManus O.B., Helms L.M., Pallanck L., Ganetzky B., Swanson R., Leonard R.J., Functional role of the beta subunit of high conductance calcium-activated potassium channels, 1995, *Neuron*, 14, 645-50

Meech R.W., Calcium-dependent potassium activation in nervous tissue, 1978, *Annu. Rev. Biophys. Bioeng.*, 7, 1-18

Messier C., Mourre C., Bontempi B., Sif J., Lazdunski M., Destrade C., Effect of apamin, a toxin that inhibits Ca^{2+} -dependent K^{+} channels, on learning and memory processes, 1991, *Brain Res.*, 551, 322-6

Michikawa T., Hamanaka H., Otsu H., Yamamoto A., Miyawaki A., Furuichi T., Tashiro Y., Mikoshiba K., Transmembrane topology and sites of N-glycosylation of inositol 1,4,5-trisphosphate receptor, 1994, *JBC*, 269, 9184-9

Miller M.J., Rauer H., Tomita H., Rauer H., Gargus J.J., Gutman G.A., Cahalan M.D., Chandy K.G., Nuclear localization and dominant-negative suppression by a mutant SKCa3 N-terminal channel fragment identified in a patient with schizophrenia, 2001, *JBC*, 276, 27753-6

Misonou H., Mohapatra D.P., Park E.W., Leung V., Zhen D., Misonou K., Anderson A.E., Trimmer J.S., Regulation of ion channel localization and phosphorylation by neuronal activity, 2004, *Nat. Neurosci.*, Jun 13 [Epub ahead of print]

Morales M.J., Castellino R.C., Crews A.L., Rasmusson R.L., Strauss H.C., A novel beta subunit increases rate of inactivation of specific voltage-gated potassium channel alpha subunits, 1995, *JBC*, 270, 6272-7

Munro S., Pelham H.R., A C-terminal signal prevents secretion of luminal ER proteins, 1987, *Cell*, 13, 899-907

Nagaya N., Papazian D.M., Potassium channel alpha and beta subunits assemble in the endoplasmic reticulum, 1997, *JBC*, 272, 3022-7

Neher E., Sakmann B., Single-channel currents recorded from membrane of denervated frog muscle fibres, 1976, *Nature*, 260, 799-802

Ottschytch N., Raes A., Van Hoorick D., Snyders D.J., Obligatory heterotetramerization of three previously uncharacterized Kv channel alpha-subunits identified in the human genome, 2002, *PNAS*, 99, 7986-91

Pedarzani P., Kulik A., Muller M., Ballanyi K., Stocker M., Molecular determinants of Ca^{2+} - dependent K^{+} channel function in rat dorsal vagal neurons, 2000, *J. Physiol.*, 527, 283-90

Pedarzani P., Mosbacher J., Rivard A., Cingolani L.A., Oliver D., Stocker M., Adelman J.P., Fakler B., Control of electrical activity in central neurons by modulating the gating of small conductance Ca^{2+} -activated K^{+} channels, 2001, *JBC*, 276, 9762-9

Pedersen K.A., Schroder R.L., Skaaning-Jensen B., Strobaek D., Olesen S.P., Christophersen P., Activation of the human intermediate-conductance Ca^{2+} -activated K^{+} channel by 1-ethyl-2-benzimidazolinone is strongly Ca^{2+} -dependent, 1999, *Biochim. Biophys. Acta*, 1420, 231-40

Perier F., Coulter K.L., Radeke C.M., Vandenberg C.A., Expression of an inwardly rectifying potassium channel in *Xenopus* oocytes, 1992, *J. Neurochem.*, 59, 1971-4

Pickart C.M., Back to the future with ubiquitin, 2004, *cell*, 116, 181-190

Rettig J., Heinemann S., Wunder F., Lorra C., Parcej D., Dolly J., Pongs O., Inactivation properties of voltage-gated K^{+} channels altered by presence of beta-subunit, 1994, *Nature*, 369, 289-294

Rochat H., Kharrat R., Sabatier J.M., Mansuelle P., Crest M., Martin-Eauclaire m.F., Sampieri F., Oughideni R., Mabrouk K., Jacquet G., Van Rietschoten J. and Ayeb M.E., Maurotoxin, a four disulfide bridges scorpion toxin acting on K^{+} channels, 1998, *Toxicon*, 36, 1609-1611

Romey G., Hugues M., Schmid-Antomarchi H. and Lazdunski M., Apamin: a specific toxin to study a class of Ca^{2+} -dependent K^{+} channels, 1984, *J. Physiol.*, 79, 259-264

Sah P., $Ca(2+)$ -activated K^{+} currents in neurones: types, physiological roles and modulation, 1996, *Trends Neurosci.*, 19, 150-4

- Sailer C.A., Hu H., Kaufmann W.A., Trieb M., Schwarzer C., Storm J.F. and Knaus H.G., Regional differences in distribution and functional expression of small-conductance Ca^{2+} -activated K^+ channels in rat brain, 2002, *J. Neurosci.*, 22, 9698-9707
- Sanguinetti M.C., Curran M.E., Zou A., Shen J., Spector P.S., Atkinson D.L., Keating M.T., Coassembly of K(V)LQT1 and minK (IsK) proteins to form cardiac I(Ks) potassium channel, 1996, *Nature*, 384, 80-83
- Schulteis C.T., Nagaya N., Papazian D.M., Subunit folding and assembly steps are interspersed during Shaker potassium channels biogenesis, 1998, *JBC*, 273, 26210-7
- Schumacher M.A., Rivard A.F., Bachinger H.P., Adelman J.P., Structure of the gating domain of a Ca^{2+} -activated K^+ channel complex with Ca^{2+} /calmodulin, 2001, *Nature*, 410, 1120-1124
- Schutze M.P., Peterson P.A. and Jackson M.R., An N-terminal double-arginine motif maintains type II membrane proteins in the endoplasmic reticulum, 1994, *EMBO*, 13, 1696-1705
- Shah M. and Haylett D.G., The pharmacology of hSK1 Ca^{2+} -activated K^+ channels expressed in mammalian cell lines, 2000, *Br. J. Pharmacol.*, 129, 627-30
- Shakkottai V.G., Regaya I., Wulff H., Fajloun Z., Tomita H., Fathallah M., Cahalan M.D., Gargus J.J., Sabatier J.-M. and Chandy K.G., Design and characterization of highly selective peptide inhibitor of the small conductance calcium-activated K^+ channel, *SkCa2*, 2001, *JBC*, 276, 43145-43151
- Shen N.V., Chen X., Boyer M.M., Pfaffinger P.J., Deletion analysis of K^+ channel assembly, 1993, *Neuron*, 11, 67-76
- Shen N.V., Pfaffinger P.J., Molecular recognition and assembly sequences involved in the subfamily-specific assembly of voltage-gated K^+ channel subunit proteins, 1995, *Neuron*, 14, 625-33
- Shi G., Nakahira K., Hammond S., Rhodes K.J., Schechter L.E., Trimmer J.S., Beta subunits promote K^+ channel surface expression through effects early in biosynthesis, 1996, *Neuron*, 16, 843-52
- Shmukler B.E., Bond C.T., Wilhelm S., Bruening-Wright A., Maylie J., Adelman J.P., Alper S.L., Structure and complex transcription pattern of the mouse SK1 K_{Ca} channel gene, *KCNN1*, 2001, *Bio. et Bio. Acta*, 1518, 36-46
- Snyders D.J., Structure and function of cardiac potassium channels, 1999, *Cardio. Res.*, 42, 377-390
- Southan A.P., Robertson B., Electrophysiological characterization of voltage-gated K^+ currents in cerebellar basket and purkinje cells: Kv1 and Kv3 channel subfamilies are present in basket cell nerve terminals, 2000, *J. Neurosci.*, 20, 114-122

- Staub O., Abriel H., Plant P., Ishikawa T., Kanelis V., Saleki R., Horisberger J.D., Schild L., Rotin D., Regulation of the epithelial Na⁺ channel by Nedd4 and ubiquitination, 2000, *Kidney Int.*, 57, 809-15
- Stocker M., Krause M., Pedarzani P., An apamin-sensitive Ca²⁺-activated K⁺ current in hippocampal pyramidal neurons, 1999, *PNAS*, 96, 4662-4667
- Stocker M. and Pedarzani P., Differential distribution of three Ca²⁺-activated K⁺ channel subunits, SK1, SK2, and SK3 in the adult rat central nervous system, 2000, *MCN*, 15, 476-493
- Strang C., Cushman S.J., eRubeis D., Peterson D., Pfaffinger P.J., A central role for the T1 domain in voltage-gated potassium channel formation and function, 2001, *JBC*, 276, 28493-28502
- Strobaek D., Jorgensen T.D., Christophersen P., Ahring P.K. and Olesen S.P., Pharmacological characterization of small-conductance Ca²⁺-activated K⁺ channels stably expressed in HEk 293 cells, 2000, *Br. J. Pharm.*, 129, 991-999
- Strong P.N., Potassium channel toxins, 1990, *Pharmac. Ther.*, 46, 137-162
- Strong P.N., Clark G.S., Armugam A., De-Allie F.A., Joseph J.S., Yemul V., Deshpande J.M., Kamat R., Gadre S.V., Gopalakrishnakone P., Kini R.M., Owen D.G., Jeyaseelan K., Tamulustoxin: a novel potassium channel blocker from the venom of the Indian red scorpion *Mesobuthus tamulus*, 2001, *Arch. Biochem. Biophys.*, 385, 138-144
- Syme C.A., Gerlach A.C., Singh A.K., Devor D.C., Pharmacological activation of cloned intermediate- and small-conductance Ca(2+)-activated K(+) channels, 2000, *Am. J. Physiol. Cell Physiol.*, 278, C570-81
- Syme C.A., Hamilton K.L., Jones H.M., Gerlach A.C., Giltinan L., Papworth G.D., Watkins S.C., Bradbury N.A., Devor D.C., Trafficking of the Ca²⁺-activated K⁺ channel, hIK1, is dependent upon a C-terminal leucine zipper, 2003, *JBC*, 278, 8476-8486
- Tagawa K., Hoshino M., Okuda T., Ueda H., Hayashi H., Engemann S., Okado H., Ichikawa M., Wanker E.E., Okazawa H., Distinct aggregation and cell death patterns among different types of primary neurons induced by mutant huntingtin protein, 2004, *J. Neurochem.*, 89, 974-87
- Takumi T., Ishii T., Horio Y., Morishige K., Takahashi N., Yamada M., Yamashita T., Kiyama H., Sohmiya K., Naknshi S., A novel ATP-dependent inward rectifier potassium channel expressed predominantly in glial cells, 1995, *JBC*, 270, 16339-46
- Tempel B.L., D.M. Papazian, T.L. Schwarz, Y.N. Jan and L.Y. Jan, Sequence of a probable potassium channel component encoded at Shaker locus of *Drosophila*, 1987 *Science*, 237, 770-775
- Terstappen G.C., Pula G., Carignani C., Chen M.X., Roncarati R., Pharmacological characterization of the human small conductance calcium-activated potassium channel hSK3 reveals sensitivity to tricyclic antidepressants and antipsychotic phenothiazines, 2001, *Neuropharm.*, 40, 772-783

- Terstappen G.C., Pellacani A., Aldegheri L., Graiani F., Carignani C., Pula G., Virginio C., The antidepressant fluoxetine blocks the human small conductance calcium-activated potassium channels SK1, SK2 and SK3, 2003, *Neurosci. Lett.*, 346, 85-88
- Trimmer J.S., Regulation of ion channel expression by cytoplasmic subunits, 1998, *Curr. Opin. Neurobiol.*, 8, 370-4
- Trowbridge I.S., Endocytosis and signals for internalization, 1991, *Curr. Opin. Cell Biol.*, 3, 634-41
- Tseng-Crank J., Foster C.D., Krause J.D., Mertz R., Godinot N., DiChiara T.J., Reinhart P.H., Cloning, expression, and distribution of functionally distinct Ca²⁺-activated K⁺ channel isoforms from rat brain, 1994, 13, 1315-30
- Van Vliet C., Thomas E.C., Merino-Trigo A., Teasdale R.D., Gleeson P.A., Intracellular sorting and transport of proteins, 2003, *Prog. in Bioph. and Mol. Biol.*, 83, 1-45
- Vandorpe D.H., Shmukler B.E., Jiang L., Lim B., Maylie J., Adelman J.P., de Franceschi L., Cappellini M.D., Brugnara C., Alper S.L., cDNA cloning and functional characterization of the mouse Ca²⁺-gated K⁺ channel, mK1. Roles in regulatory volume decrease and erythroid differentiation, 1998, *JBC.*, 273, 21542-53
- Varadan R., Assfalg M., Haririnia A., Raasi S., Pickart C. and Fushman D., Solution conformation of Lys63-linked di-ubiquitin chain provides clues to functional diversity of polyubiquitin signaling, 2004, *JBC*, 279, 7055-7063
- Villalobos C., Shakkottai V.G., Chandy K.G., Michelhaugh S.K., Andrade R., SKCa channels mediate the medium but not the slow calcium-activated afterhyperpolarization in cortical neurons, 2004, *J. Neurosci.*, 24, 3537-42
- Ward C.L., Omura S., Kopito R.R., Degradation of CFTR by the ubiquitin-protease pathway, 1995, *Cell*, 83, 121-7
- Wetzel R., Mutations and off-pathway aggregation of proteins, 1994, *Trends Biotechnol.*, 12, 193-198
- Wilcox C.A., Redding K., Wright R., Fuller R.S., Mutation of a tyrosine localization signal in the cytosolic tail of yeast Kex2 protease disrupts Golgi retention and results in default transport to the vacuole, 1992, *Mol. Cell Biol.*, 3, 1353-71
- Wissman R., Bild W., Neumann H., Rivard A., Klocker N., Weitz D., Schulte U., Adelman J., Bentrop D. and Fakler B., A helical region in the C-terminus of small-conductance Ca²⁺-activated K⁺ channels controls assembly with Apo-calmodulin, 2002, *JBC*, 277, 4558-4564
- Wolfart J., Neuhoff H., Franz O., Roeper J., Differential expression of the small-conductance, calcium-activated potassium channel SK3 is critical for pacemaker control in dopaminergic midbrain neurons, 2001, *J. Neurosci.*, 21, 3443-56
- Wood M.W., VanDongen H.M.A. and VanDongen A.M.J., Structural conservation of ion conduction pathways in K channels and glutamate receptors, 1995, *PNAS*, 4882-4886

Xia X.M., Fakler B., Rivard A., Wayman G., Johnson-Pais T., Keen J.E., Ishii T., Hirschberg B., Bond C.T., Lutsenko S., Maylie J. and Adelman J.P., Mechanism of calcium gating in small-conductance calcium-activated potassium channels, 1998, *Nature*, 395, 503-507

Xu J., Yu W., Jan Y.N., Jan L.Y. and Li M., Assembly of voltage-gated potassium channels, 1995, *JBC*, 270, 24761-24768

Zerangue N., Jan Y.N. and Jan L.Y., An artificial tetramerization domain restores efficient assembly of functional Shaker channels lacking T1, 2000, *PNAS*, 97, 3591-3595

Zerrouk H., Mansuelle P., Benslimane A., Rochat H., and Martin Eauclaire M.F., Characterization of a new Leiurotoxin I-like scorpion toxin PO₅ from *Androctonus mauretanicus mauretanicus*, 1993, *Febs Lett.*, 320, 189-192

Zhang B.M., Kohli V., Adachi R., Lopez J.A., Udden M.M. and Sullivan R., Calmodulin binding to the C-terminus of the small-conductance Ca²⁺-activated K⁺ channel hSK1 is affected by alternative splicing, 2001, 40, 3189-3195

Acknowledgements

I would like to acknowledge all the friends I worked with in the Department of Molecular Biology of Neuronal Signals at the Max-Planck Institute for Experimental Medicine in Gottingen.

In particular, I wish to thank Professor Walter Stühmer for giving me the opportunity to work at the Max-Planck Institute, and for his invaluable support throughout the course of my Ph.D.

I would like to thank Dr. Paola Pedarzani and Dr. Martin Stocker for their support, input and guidance. I also like to thank them for giving me the opportunity to come to London and continue my Ph.D. course at the University College of London.

I want to show my appreciation to my supervisor Professor Thomas Carell, in the Department of Organic Chemistry at the Ludwig-Maximilians-University.

I am very grateful to my colleagues Dr. Klaus Hirzel, Teresa Ferraro, Dr. Andreas Nolting, Dr. Federica Giovannini, Dr. Antonny Czarnecki, Raffaella Bosurgi, Dr. Derek Costello, Ruth Taylor and Dr. Lorenzo Cingolani, for their friendship and support throughout my Ph.D. course. We shared some difficult but many nice moments which I will always remember.

I would like to thank my Belgian friends, Alain Labro, Dr. Adam Raes and Professor Dr. Dirk Snyders at the University of Antwerp, who taught me the patch-clamp technique and who always welcomed me, and gave me advice when I visited my homeland.

Finally, I would like to thank my parents, brother and sisters for continuous support.

Curriculum Vitae

Dieter D'hoedt

Brusselsestraat 290, bus 10, 3000 Leuven, Belgium

☎ ++ 32 (0)16 345 724 (lab), ++32 (0)16 22 11 07 (home)

Email: Dieter.DHoedt@med.kuleuven.ac.be

Date of birth: 6 August 1977

Nationality: Belgian

University Education:

02/2005 – present: Post-doctoral position funded by Human Frontier, at the Catholic University of Leuven (KUL), Faculty of Medicine, Department of Physiology under the supervision of Prof. Dr. Bernd Nilius

02/2003 – 01/2005: PhD project on the molecular composition and pharmacological properties of calcium-activated potassium channels (SK channels) in the rat central nervous system, under the supervision of Prof. Dr. Thomas Carell at the University of Marburg.

11/2001 – 01/2005: Visiting student at University College London, Department of Physiology and Wellcome Laboratory for Molecular Pharmacology under the supervision of Drs. Paola Pedarzani and Martin Stocker.

07/2000 – 11/2001: PhD project on the molecular composition and pharmacological properties of calcium-activated potassium channels (SK channels) in the rat central nervous system at the Department of Molecular Biology of Neuronal Signals directed by Prof. Walter Stühmer at the Max-Planck Institute for Experimental Medicine in Göttingen, Germany.

06/2000: Final thesis on “Probing Mink/K_vLQT1 interactions using Mink/Mirp1 chimeras” at the Department of Molecular Biology, Pharmacology and Physiology directed by Prof. Dirk J. Snyders.

1998-2000: Degree in Biochemistry at the University of Antwerp (UIA).

1995-1998: Degree in Chemistry at the University of Antwerp (RUCA);

Publications:

Papers in Peer Reviewed Journals

Owsianik G., D'hoedt D*, Voets T. and Nilius B
Structure-function relationship of the TRP channel superfamily.
Rev. Physiol. Biochem. Pharmacol., 2006, 156:61-90

* *Shared first authorship*

Cuajungco M.P., Grimm C., Oshima K., D'hoedt D., Nilius B., Mensenkamp A.R., Bindels R., Plomann M. and Heller S.

PACSINs bind to the TRPV4 cation channel. PACSIN3 modulates the subcellular localization of TRPV4.
Journal of Biological Chemistry, 2006, 281(27), 18753-62

P. Pedarzani , D. D'hoedt *, K. B. Doorty, J. D. F. Wadsworth, J. S. Joseph, K. Jeyaseelan, R. M. Kini, S. V. Gadre, S. M. Sapatnekar, M. Stocker and P. N. Strong.

Tamapin, a venom peptide from the Indian Red Scorpion (*Mesobuthus tamulus*) that targets small conductance Ca²⁺-activated K⁺ channels and afterhyperpolarization currents in central neurons.
Journal of Biological Chemistry, 2002, 277(48), 46101-9

* *Shared first authorship*

D. D'hoedt , K. Hirzel *, P. Pedarzani and M. Stocker

Domain analysis of the calcium-activated potassium channel SK1 from rat brain: Functional expression and toxin sensitivity.

Journal of Biological Chemistry, 2004, 279(13):12088-92

* *Shared first authorship*

M. Stocker , K. Hirzel , D. D'hoedt and P. Pedarzani

Matching molecules to function: Neuronal Ca²⁺-activated K⁺ channels and afterhyperpolarizations.
Toxicon. 2004 Jun 15, 43(8):933-49.

J. Scuvée-Moreau, A. Boland, A. Graulich, L. Van Overmeire, D. D'hoedt, F. Graulich-Lorge, E. Thomas, A. Abras, M. Stocker, J. F. Liégeois, V. Seutin

Electrophysiological characterization of the SK channel blockers methyl-laundanosine and methyl-noscapine in the cell lines and rat brain slices.

British Journal of Pharmacology, 2004, 143(6), 753-64

Published Communications:

A.L. Raes, D. D'hoedt, N. Ottschytsch, A. J. Labro & D. J. Snyders, 2001.

Probing mink/kvlqt1 interactions using mink/mirp1 chimeras.

Biophysical Journal 80(1): A213

D. D'hoedt, K. B. Doorty, K. Jeyaseelan, J. D. F. Wadsworth, M. Stocker, P. Pedarzani & P. N. Strong, 2001.

Tamapin: a new peptide toxin from the Indian red scorpion targeting SK channels and AHP currents in central neurons.

31st Annual Meeting of the Society for Neuroscience, San Diego, California, USA, November 10-15, 2001. Society for

Neuroscience Abstracts 27(1): 1003.

T. Ferraro, K. Hirzel, D. D'hoedt, D. Kerschensteiner, M. Stocker.

MOLECULAR AND FUNCTIONAL CHARACTERIZATION OF RAT $K_{CA22-860}$, A NEW SK2 CHANNEL

SUBUNIT VARIANT Program No. 376.12. *2005 Abstract Viewer/Itinerary Planner*. Washington, DC: Society for

Neuroscience, 2005

Unpublished Communications:

A.L. Raes, D. D'hoedt, N. Ottschytsch, A. J. Labro & D. J. Snyders, 2001.

Probing mink/kvlqt1 interactions using mink/mirp1 chimeras.

24th Meeting of the European Group working on Cardiac Cellular Electrophysiology.